Towards Flow Propagation Modeling with System Dynamics?

Application on the ring of Brussels

by

H.A.G. Benaich

to obtain the degree of Master of Science
at the Delft University of Technology,
to be defended publicly on Friday October 30, 2015 at 1:00 PM.

Student number:	4316371	
Project duration:	February 27, 2015 – October 2, 2015	
Thesis committee:	Prof. dr. ir. A. Verbraeck,	TU Delft, chairman
	Dr. E. Pruyt,	TU Delft, daily supervisor
	Dr. J. A. Annema,	TU Delft, second supervisor
	Ir. G. De Ceuster,	TM Leuven, external supervisor

An electronic version of this thesis is available at http://repository.tudelft.nl/.

TU Delft

Preface

Writing this thesis was certainly one of the hardest challenges I have accomplished so far. Before starting to develop the results and findings of my thesis, I would like to dedicate some words to the persons without whom I could have not achieve this work.

The first persons I would like to thank is my graduation committee without whom I could have not led this project to its end. My first words are for Dr. Erik Pruyt, thanks to whom I could come up with this topic when I started to look for a thesis topic. His support all along my work on the thesis greatly helped me to build the model presented thereafter and to present it at the 33rd International Conference of hte System Dynamics Society in Boston this summer.

The second committee member I would like to thank a lot is Ir. Griet De Ceuster, from Transport and Mobility (TM) Leuven, who gave me the opportunity to carry out my project as an associate researcher within TM Leuven. Her feedback really helped me to progress throughout my work there.

My last words go to Prof. dr. ir. Alexander Verbraeck and Dr. Jan Anne Annema, respectively committee chairman and second supervisor, for their availability and help. Their regular feedback really helped me to write and reflect on my thesis work.

Second, I would like to thank all the academic personnel that have helped me to lead my project in the optimal conditions. I would like to thank first Drs. C.A. Hoek, International Officer of the faculty of Technology, Polciy and Management (TPM) at the Delft University of Technology, for her regular guidance while I was working on my thesis out of Delft.

Besides this, I am grateful to the International Office of the TU Delft and the secretary of the Policy Analysis department of the TPM faculty at the TU Delft, for their financial support during my project for my stay in Leuven as well as my trip to Boston to present my project at the International Conference of the System Dynamics Society.

I would like to show my gratitude to Dr. Victor Knoop, traffic researcher at the faculty of Civil Engineering of the TU Delft, for helping me to draw the last conclusions about my model outcomes.

My final words for academic persons are aimed to Prof. dr. Stef Proost, from the Economcs-Energy, Transport and Environment faculty of the Katholieke Universiteit Leuven, and Dr. ir. Chris Tampère, from the faculty of Traffic and Infrastructure of the Katholieke Universiteit Leuven. Their insights were very valuable when it came to reflect on my findings and think about the added value of the method I used for developing my model.

The following acknowledgements are dedicated to the TM Leuven staff, with whom I spent five enriching months from March to July. I am very grateful to all of them for their help in transportation modeling, thanks to which I could mark out the scope of my project and be steered in the good direction for my research.

Besides their help, I would like to thank them for their availability and their expertise during my research. Their help was very valuable throughout my stay there. Their knowlegde and opinion was of great help to guide me through my research and to draw appropriate conclusions about my work.

I would like to acknowledge them not only for their contribution to this thesis, but also for all the activities we participated together. Arriving in a new city is never easy. The way they welcomed me and really helped me to thrive out during my stay.

My final words are for my family, my partner Anne-Sophie and all my friends that I have met so far. I am very grateful to them for their support and their help not only during my thesis, but all along my studies in Delft. I would like to cheerfully thank you another time for everything that you have brought to me. This thesis is also yours.

Hugo Benaich
Delft, October 2015

Summary

Caused by the soar of car ownership and economic growth, traffic congestion has become a major issue. In developing countries—Europe, North America and China—it affects not only the traveling time, but also leads to higher levels of noise and air pollution and productivity losses. In developed countries—Asia and South America—congestion is a major hindrance to their growth. In order to avoid or mitigate it, transportation modeling is of importance for policy-makers so as to design effective solutions. Among decision tools available for policy-makers, four-step model is perhaps the most outstanding and widespread paradigm. The objective of such models is to assign on a network trips between different areas for a given planning period based on the travel costs. However, they require substantial amounts of data to be run, and yield static equilibrium conditions. In reality, conditions may widely differ from it. Besides planning, models can be used for simulating flow propagation through a network. Initially, this type of model was developed to understand propagation and congestion dynamics. When it comes to policy analysis, they may be of interest to check the actual effects of policy on traffic.

System Dynamics (SD) is a relevant tool to cope with transportation related issues since it allows to relate the behavior of a system to its structure and the other way round. Planning models using SD can be found in literature. However, flow modeling in SD cannot easily address for the spatial character of propagation. In order to tackle this, a cell-based approach can be implemented, the Cell-Transmission Model (CTM). Developed by Daganzo, this approach turns traffic into a purely dynamic phenomenon. Flow propagates then from cell to cell, its rate depending on the occupancy and characteristics of receiving and emitting cells. It is then possible to create elementary building blocks thanks to which complex networks can be developed. The first objective of this research is hence to determine the extent to which SD can be used for reproducing flow propagation. The second research objective of the thesis is thereby to determine the added value of using SD for flow propagation. Indeed, the CTM has already been modeled and studied with other pieces of software, such as Matlab.

In order to answer these two questions, a practical case about the northern section of the Great Ring of Brussels R0 is to be carried out. Brussels indeed faces dire congestion around its ring ways, caused not only by commuters, but also by transit traffic. Among the different arterials where congestion is the starkest, the R0 section between Strombeek-Bever and Zaventem is one of the most crucial for the nationwide Belgian network. This section is thereby modeled by means of elementary building blocks based on the CTM. The resulting model is then tested for different traffic conditions: light traffic, temporary bottleneck (infrastructure-caused congestion) and heavy traffic—demand-caused congestion. The flows propagating through the model are actually composed by sub-flows between chosen origins and destinations.

The analysis of the model outcomes exhibits a proper temporal behavior of the model. The propagation of flows and of shock waves generated by hindrances are well replicated. Plots representing cell outflow with respect to its occupancy indicate a correct behavior. The values taken are the one predicted by the macroscopic fundamental diagram of the CTM. Sensitivity and uncertainty analyses show that potential policy leverages are the capacity, the demand level and shock wave speed. A deeper study of the model behavior for greater variations of this last parameter highlights the key importance of this parameter for model behavior. Finally, a basic policy analysis of a capacity increase reveals that adding extra capacity to a road yields interesting results when the capacity is evenly allocated between the two roads merging. At a methodological level, it can then be concluded that SD is a promising approach to reproduce flow propagation.

The added value of SD does not only come from this. Existing models yield the same results. The genuine contribution of SD can be described in three points. First, it is an method adapted for the analysis of complex systems, the behavior of which cannot be described by isolating its different subsystems. Second, SD is a purely dynamic method and easily allows temporal dynamics such as delays

or learning. Third, uncertainty can conveniently be coped with thanks to SD-based approach. Parameters with key role in dynamics and high uncertainty can be included and used for developing broader scenarios. In order to illustrate these three advantages, two conceptual models aiming at improving the current model are proposed and described.

Based on all these arguments, the use of SD for traffic-flow modeling sounds noticeably appealing. However, this study should be considered as a first investigation and is therefore incomplete. Indeed, many improvements have been brought to the seminal CTM, on which the model has been built. Besides this first point, it can be pointed out that the model is not computationally efficient. This method is not suitable if too long networks must be modeled. Furthermore, the allocation process is unstable, which means that the quality of the outcomes may be challenged. Finally, the current version of the model can assess a small range of policies only. The added value of SD based on the current research seems then narrow. This does not mean that SD should be discarded for modeling traffic though. The most up-to-date software developments are actually more promising when it comes to exploratory modeling and model building. This research is however a first step; further investigations still need to be carried out.

Contents

1 Introduction **1**

2 Network Building Blocks **5**
2.1 Theoretical Background . . . 5
2.1.1 Lighthill-Whitham-Richards Model . . . 5
2.1.2 Cell-Transmission Model . . . 8
2.2 Software Opportunities . . . 11
2.3 Basic Structures . . . 12
2.4 Complex Structures . . . 14

3 Case Study: The Ring of Brussels **17**
3.1 Case Introduction . . . 17
3.2 Case Description . . . 19
3.3 Model Structure . . . 20
3.4 Behavior . . . 23
3.4.1 Free Flow Conditions . . . 24
3.4.2 Congested Conditions . . . 26
3.5 Influence of Uncertainty . . . 36
3.6 Policy Analysis . . . 40
3.7 Reflection on the Model . . . 42

4 Discussion **47**

5 Conclusion **53**

A Overview of Models used in Transportation Issues **57**
A.1 Planning Models . . . 57
A.1.1 Land-use Models . . . 58
A.1.2 Trip- and Activity-Based Models . . . 58
A.1.3 Economic Models . . . 61
A.2 Flow Propagation Models . . . 62
A.3 Use of System Dynamics in Transportation-related Issues . . . 64

B Model Data **65**

C Mathematical demonstrations **71**

Bibliography **73**

1

Introduction

Traffic congestion is an issue that has been soaring since the boom of car manufacturing and ownership. It can be described as the slowing down of traffic flows caused by the accumulation of vehicles on a road. This translates the fact that this road cannot bear the actual number of vehicles currently driving on it. It is possible to visualize traffic as a market for trips. On the one hand, transport infrastructure is designed for enabling a given number of vehicles to run during a given time period. This room, defined as the infrastructure capacity, not only depends on road features such as the number of lanes, the number of travel directions—one-way or two-ways—the speed limitation. It is also dependent on external parameters such as the weather or the wear. On the other hand, individuals travel for various purposes, such as work, education or leisure. Those who have decided to travel with private vehicles generate a transport demand. Congestion occurs when travel demand has reached or has overshot available travel supply [27]. This may be caused either by an excessive demand or by a disturbance on infrastructure.

The most tangible impact of congestion on human activities is the increase in travel time. Because of congestion, traffic tends to flow at slower speed and therefore vehicle drivers need more time to reach their destination. In the analysis of its annual scorecards issued for 2013, INRIX [43] points out the increase of congestion in Europe and United States in the aftermath of the Great Depression. A person living in one of the ten most congested cities in the United States wastes each year 47 hours on average in traffic jams. The actual values vary between 40 and 64 hours. In Europe, drivers tend to waste 64 hours in congestion on average, the actual wasted time varying between 52 and 83 hours. In extreme cases, gridlock may take place: traffic becomes still and may remain in this state for minutes or even hours [94]. A second-order consequence of congestion is a waste of productivity: drivers either spend important amounts of time into traffic jams waiting for the situation to alleviate or may try to avoid peak hours either by postponing or bring forward their departure. In Belgium, the most recent daily cost of congestion is estimated to 600,000 € and can rise up to 3 million € in case of dense traffic [53]. A rough estimation of the yearly cost of congestion in Belgium yields the value of 135 million €. In a developing country such as Pakistan, these costs are even higher: the cost of congestion for the sole city of Karachi is roughly equal to $ 690 million [2].

Besides this, congestion causes the increase of negative externalities in the environment. Vehicles emit gases and noise that other users or persons must deal with. A car engine tends to consume more fuel at low-speed regimes and through this increases air pollution [27]. Moreover, as Ross et al. [75] point out, noise pollution is correlated to traffic level: dense traffic flows tend to generate more noise. Both pollution and noise have negative effects on human activities: too high levels undermine the quality of life and may lead to respiratory diseases for people leaving nearby dense roadways. As a consequence, the congestion costs presented in the previous paragraph should take into account the indirect costs induced as well. An example of such costs is healthcare expenditure to treat respiratory diseases in areas facing a high level of pollution. Finally, congestion negatively impacts commercial exchanges. Freight traffic stuck in congestion leads to higher transportation costs because it includes driver's wage, which increases together with the time spent on traffic. Besides this cost, fees to compen-

sate the client in case of delayed delivery may be charged as well Le Soir [53]. As all these examples show, congestion is bound to become a burden for societies.

A well-suited example of city where congestion is critical is Brussels. Because of its central location in Belgium, the Brussels external ring R0 collects not only commuting traffic from and to the city of Brussels, but also national and international traffic. In 2012, about 7 millions of vehicles traveled along the R0 for both commuting and transit [13]. The picture 1.1 illustrate observed traffic levels on Brussels main ways during an evening peak. Brown and red hues stand for intense traffic loads. Dark red indicates highly congested sections. On average, commuters based in Brussels spent on average 76.1 hours in traffic jams over the last 12 months. Only London-based commuters spend more time—almost 90 hours [43]. This substantial traffic actually affects the air quality around the city: the level of particulates is beyond the acceptable limits defined by the EU [42].

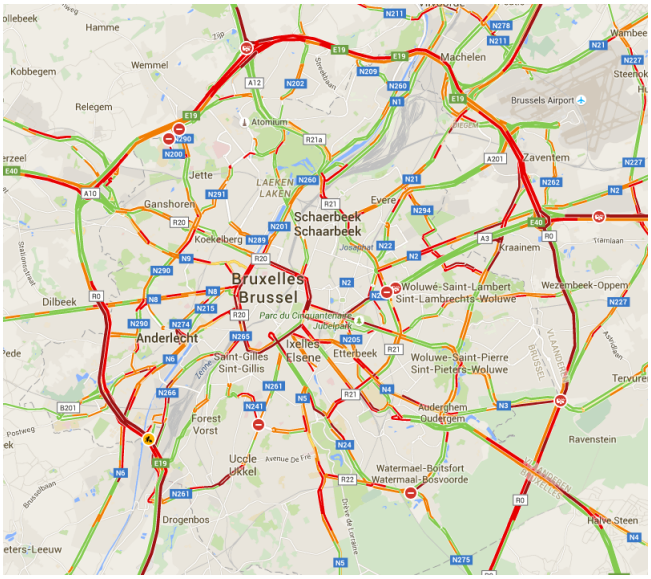


Figure 1.1: Observed traffic level around Brussels during an evening peak (source: Google Maps).

Transportation systems may be extremely complex. It involves multiple actors or groups of actors whose objective or point of view may greatly differ and creates dilemmas. For instance, basic users tend to prefer networks that minimize their travel time whereas infrastructure managers seek for cost-minimizing networks. It may feature several transportation subsystems the management of which is ruled by different stakeholders. Problems that arise in a transportation system then tend to be wicked [74]. No consensus is guaranteed about the nature of the problem, and any attempt to solve it is irreversible. Because of this multi-actor setting and the complexity of the issue, models can be used to help a decision-maker to develop solutions for transportation systems. For wicked problems, well-calibrated quantitative models may be insufficient, albeit powerful, to test different policy options. They should be completed with qualitative models, thank to which the issue to be solved can be conceptualized. Several modeling techniques are common to deal with transportation issues: four-step framework, agent-based models and system dynamics (SD).

A first field where transportation models are applied is transportation planning, that is monitoring of existing system in order to sustain it and develop it. In order to do so, forecasts and policy analysis need to be carried out in order to determine what should be implemented in order to ensure the sustainability of the transportation system. There exist a high number of models, that can be sorted with respect to their focus: land-use, traffic load on the network, financial costs of congestion, and so on. The objective of these models is to assess how different policy instruments affects the system equilibrium. Planning models are therefore useful for designing optimal policies, given a focus and a list of objectives. One of the widespread transportation models, the four-step model (FSM), falls into this category of models. A model of this kind aims at determining the traffic load generated by different areas on the transportation network of interest. Its inputs are network characteristics and socio-economic data of the different

areas. The traffic loads are determined in four steps: three steps to compute the transportation demand from data of the different zones, and one step to assign it on the network according to specific requirements—for instance, with respect to the shortest path independently of actual traffic conditions. However, these models are data-intensive and, according to Maerivoet [59], remain based on a static assignment: temporal effects are not always accounted for, in spite of recent developments of dynamic techniques. As a consequence, outcomes of the models may mismatch actual observations in congested areas.

Besides planning issues, transportation models can be developed for reproducing traffic propagation so as to get insights about the underlying mechanism. Hoogendoorn & Bovy [40] list a thorough overview of the different analytical models existing as well as several characteristics to distinguish them. They are usually sorted with respect to the modeling scale, which goes from macroscopic to microscopic. Macroscopic models are based on hydrodynamics: a flow of vehicles is represented as a continuum wherein no individual unit can be mapped. The smaller the scale becomes, the more detailed the model will be: vehicles can be individually identified and can reproduce a wide range of behaviors. In general, flow propagation models are of interest when dynamic effects of congestion have to be accounted for in a larger model. The models are thereby employed to simulate the loading of a network. In practice, flow propagation models are continuous analytical models made of several partial differential equations (PDE). So as to ease their implementation, numerical schemes are derived from it. These are usually build and run with MATLAB [6; 54; 65; 78]. However, a pure computational environment may not be suitable for policy analysis related to traffic.

Instead, System Dynamics (SD) modeling may be an interesting alternative. SD is a modeling paradigm developed in the 1960s bay Jay Forrester and applied to the investigation of industrial dynamics Forrester [29]. The objective of SD is to expand system learning by relating the structure of a model to its behavior [71; 79]. In other words, the way a system behaves is caused by its underlying structure, and the other way round. Stock-flow structure and feedback are key notions in SD. By the former is meant that information, material or objects in a system accumulates in so-called stocks. A dam is a plain example of a stock-flow system. Whichever its purpose—irrigation or power production—the structure holds water flows arriving upstream of it so that it can accumulate and creates a reservoir. In order to avoid its overflowing, water can flow out of the dam at a variable rate. A schematic SD model of a dam is presented in the figure 1.2.

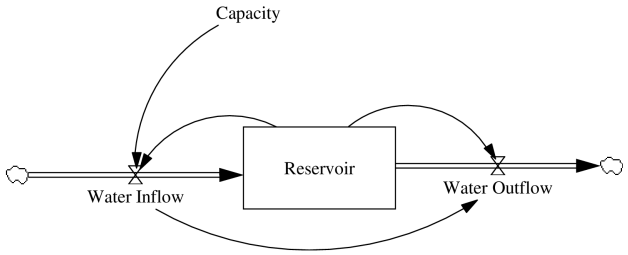


Figure 1.2: Stock-flow structure of a dam.

Coupled to feedback, the role of stocks is crucial in SD. The feedback loops that the structure of a model presents indeed determines its behavior. For instance, a reinforcing structure can lead to an exponential growth of the system over time. As Sterman [79] explains, the accumulation of information or material inside a stock creates memory effect on which decisions are based. However, in the meanwhile, a stock decouples its inflow from its outflow and thereby creates delays that contribute to the apparition of disequilibrium dynamics. In SD, the dynamic behavior of a system matters more than its numerical exactness. As a consequence, systems tend to be represented at a macroscopic level, so that broad system boundaries can be chosen: SD is then a holistic method and thereby leads to a better understanding of it [1; 80]. Such approach is therefore suitable to cope with wicked problems, such as the ones occurring on transportation systems.

Even though interesting, SD faces important limitations [1, p. 23]: “Spatial aspects and distribution

effects are not easily accounted for." Flow propagation characteristics are actually dependent on flow position in space. Numerical approximations of macroscopic flow models discretize the space, but the resulting schemes do not show out a stock-flow structure. Instead, there exist models wherein the spatial dimension of traffic propagation becomes an implicit parameter. The seminal model of this type is known as the Cell Transmission Model (CTM) and was developed by Daganzo [16]. The principle of this model is to divide a road network into cells of finite size. This internalizes then the spatial dimension of traffic propagation. The current occupancy of a cell depends on its inflow and outflow, the latter being equal to the inflow of the next cell downstream. Since the cells are fixed, only the cell inflows needs to be computed; the model gotten is hence purely dynamic and can may be then modeled by means of SD. Moreover, the most recent version of SD software feature tools and functions that enable the modeler to develop even more complex systems.

In this thesis, two different objectives are to be investigated. The first is to determine the extent to which flow propagation can be modeled by means of the most recent SD techniques. The second is to discuss about the potential advantages of using SD rather than usual methods such as four-step models. All along the thesis, the chosen approach has shown promising results; however its relevance over other methods should be strongly motivated. To illustrate both points, a model of the R0 ring road of Brussels is to be built and a basic traffic policy are to be investigated. The thesis is structured as follows. The chapter 2 is introducing the methodological background that was adopted in this thesis. Keys concepts are thereby presented and described. In the chapter 3, a model of a small section of Brussels ring road R0 is built and thoroughly described. The fourth chapter deals with the potential added value of this method. The chapter 5 closes the research by listing the limitations of the chosen method, concluding about the interest of this method and further works that have to be done.

2

Network Building Blocks

2.1. Theoretical Background

This first chapter aims at introducing the theory and the concepts that are necessary to understand this thesis. The first section introduces the cornerstone of the model, the LWR model, and a numerical scheme related to it, the CTM. The second section presents the software opportunities that were used for creating the model. The two last sections deals with the building blocks of the model. They are introduced in two-steps: first, elementary blocks and second, advanced blocks.

2.1.1. Lighthill-Whitham-Richards Model

Traffic modeling is a recent subject initiated in the 1930s, by the works of Greenshields. This seminal research aimed at measuring traffic characteristics and relations between them, based on observations and he made by means of cameras [50]. In 1952, Wardrop started to develop a theoretical approach which would be used as an input for policy analysis related to traffic. Similarly to Greenshields, his work consisted of deriving relationships between traffic characteristics based on observations. Both of these works mainly rely on statistical treatment of data acquired. The extent to which these results are valid may then be limited.

In 1955, Lighthill & Whitham introduced a totally different approach for traffic modeling, based on fluid dynamics, which is adapted for large-scale problems such as [56, p. 319] “the distribution of traffic along long, crowded routes” [56, p. 319]. In this approach, a flow of vehicles is then considered as a continuum where vehicles cannot be individually mapped from each other. This way of representing traffic, known as macroscopic [40] requires a few number of variables to describe a traffic flow:

- The flow density, noted $k(x,t)$ and expressed in vehicles per unit of length—usually in km. It describes the spatial distribution of the flow on the network;
- The flow intensity[1], noted $q(x,t)$ and expressed in vehicles per unit of time—often hour. It describes the spatial evolution of the flow over time;
- The flow speed, noted $v(x,t)$ and expressed in a distance per unit of time—usually km/h. It quantifies the rate at which traffic proceeds through the network.

Since the focus of macroscopic models is made on the global behavior of the flow rather than on the local one, SD may be a suitable modeling approach for it [79; 80].

The first macroscopic model, developed by Lighthill and Whitham in 1955, and expanded by Roberts in 1956, is known as the LWR model. It consists of three equations relating these three traffic variables with respect to prior findings and conservation rules. This seminal model was later expanded by including new rules. In [40], two enhancements of the LWR model are introduced: Payne models, where

[1] Usually referred as flow in the literature. However, due to its definition, the author has decided to use the notion of intensity instead.

the speed is described by means of another differential equation, and Helbing model, where the velocity variance is ruled by another specific PDE. In Costeseque & Lebacque [15], the LWR model is presented as a general second-order model (GSOM) for traffic for which there is no specific driver attribute such as (2014) “driver aggressiveness, the driver destination or the vehicle class”. It stems from this development that the seminal LWR model is the cornerstone of macroscopic traffic flow models and is therefore deemed appropriate as a starting point for investigations.

The first of the three equations of the LWR model, known as the fundamental relation or *continuity equation* [41], relates the three traffic variables:

$$q(x,t) = k(x,t) \cdot v(x,t) \tag{2.1}$$

This equation is actually one of the findings of Greenshields and Wardrop researches, and always holds true when the speed used for computation is the space-mean speed. In Wardrop [93] and Hoogendoorn & Knoop [41], this speed is defined as the average speed of vehicles between two time instants. It can be measured by tracking specific vehicles on aerial pictures [86] or SPECS[2] or by retrieving data from navigation systems for instance. However, as Hoogendoorn & Knoop [41] outlines, some applications tend to use time-mean speeds, that is the instantaneous speed of a vehicles measured by speed cameras. The relation 2.1 is then only valid when the speed is constant. From this point on, speed always refers to space-mean speed. As a consequence of this equation, **only two of the three traffic variables are actually required to describe a traffic flow**. The third being gotten by computing their product or their ratio. This is hence helpful to estimate the flow density k, the measure of which can be only gotten by aerial measurements.

The second equation is known as the equation of the *fundamental diagram*:

$$\forall x,t \; ; \; q\,(x,t) \equiv q\,(k\,(x,t)) \tag{2.2}$$

In other words, there always exists a relation between the flow intensity and density. Since the three equations are related, the fundamental relation can also be expressed as a relation between the flow intensity and the flow speed:

$$\forall x,t \; ; \; v\,(x,t) \equiv v\,(k\,(x,t)) \tag{2.3}$$

Greenshields was the first to observe and derive such relation between two variables. In his work, the speed is found to be a linear function of the traffic density. As a consequence thereof, the relation between the density and the intensity is parabolic. The figure 2.1 , taken from Gordon & Tighe [35], presents the three macroscopic fundamental diagrams (MFD) yielded by Greenshields’ relationship.

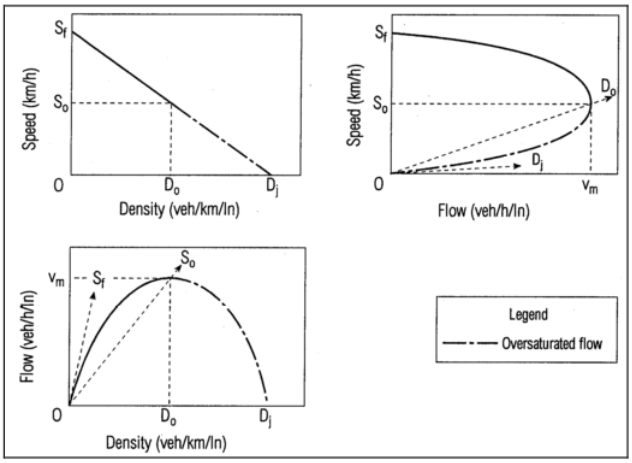


Figure 2.1: Greenshields’ Fundamental Diagrams (source: [35])

From the figure 2.1, 3 parameters can be defined:

[2]Known as ‘Trajectcontrole’ in the Netherlands and Belgium, or ‘radar tronçon’ in France.

- The road capacity q_m, noted C thereafter, which is equal to the maximal intensity the road can bear;
- The jam density D_j, noted k_j thereafter, defined as the density from which traffic becomes still;
- The free flow speed S_f, noted v_0 thereafter, stands for the maximal speed at which flow can proceed on the road.

Besides these, two critical quantities for the speed and the density, respectively noted S_0 and D_0 in the figure, and v_C and k_C in this thesis, can be observed. These values are optima: when the flow has a density equal to k_C, it proceeds at v_C. The rate of vehicles crossing the section is equal to the road capacity. For higher values of k, the flow characteristics start to decay: speed and intensity decreases until k_j is reached: the flow becomes still and gridlock occurs. This relation is idealistic though. Indeed, fundamental diagrams based on actual observations tend to exhibit an asymmetric, triangular-shaped relation [20; 72]:

- For a density below its critical value, the flow intensity increases at a rate equal to the free flow speed.
- For a density higher than its critical value, the flow intensity decreases at a slower rate, in absolute value, than the free flow speed.

The latter point can be explained by the sudden changes of the density, speed and intensity. In the LWR model, this results in the creation of shock waves that propagates backwards through the traffic flow. The speed at which these waves propagate, noted w, is estimated as follows:

$$w = \frac{\Delta q}{\Delta k} \tag{2.4}$$

to wit the ratio of the variation in flow intensity versus its variation in flow density. However, the shock wave velocity is in general not equal to the free flow speed, which explains a lower value for the downward slope. Daganzo [16][][p. 19] shows that

> the wave speed discrepancy [does not] change the time when approaching vehicles would pass a bottleneck and, hence, [does not] influence the resulting vehicle delay.

In other words, the shock wave speed can then be assumed as constant. In this thesis, this assumption is to be later questioned.

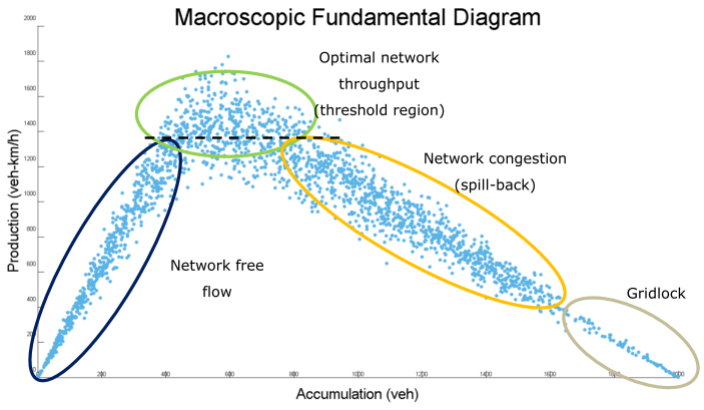


Figure 2.2: Triangualar-shaped Fundamental Diagram (source: [20]

The last equation is a PDE that is known as the flow conservation equation:

$$\frac{\partial q}{\partial x} + \frac{\partial k}{\partial t} = 0 \tag{2.5}$$

It can be described as follows: “any small change of the density over time locally leads to a small opposite variation of the flow intensity”. Let be a small road section of length ∂x. The equation 2.5 can be written as follows:

$$\frac{\partial k}{\partial t} \cdot \partial x = q\,(x) - q\,(x + \partial x)$$

The quantity $\partial k \cdot \partial x$ is equal to the number of vehicles contained in the section previously defined. As a consequence, the number of vehicles inside this small section of length ∂x is equal to the balance of its inflow and outflow. A last point that can be raised regarding this equation is the spatial character of traffic propagation. In Abbas [1], such effects are difficult to integrate into a SD model and therefore may need to be adapted to ensure proper modeling of flow propagation.

2.1.2. Cell-Transmission Model

SD is a powerful approach to deal with purely dynamic phenomena [79], such as congestion. However, as underlined at the end of previous subsection 2.1.1, it is not convenient for addressing spatial effects. A potential solution to cope with that is to build up a numerical model by discretizing the space—in the case of a road network, space consists of the roadways. The traffic variables are then computed for specific points of space. These numeric schemes can be of two kinds: bivariate or univariate. For the former category, the flow propagation across time and space is computed from values of density and intensity [31; 45] whereas only one variable is computed for the latter one. In that case, the density, as well as the spatial dependency of traffic is actually internalized in the notion of cell wherein vehicles flow and can stop. Traffic propagation then becomes a purely dynamic model. It can be properly reproduced by means of a SD model. The most known approach for univariate numerical models is the Cell-Transmission Model (CTM), developed by Daganzo [16] and which has been proven to be a numerical model approximating the LWR model [59].

The cornerstone of this method is a simple equation of transition: $N_i(\mathbf{t}) = N_{i+1}(\mathbf{t+1})$. Let be a vehicle flow proceeding at a given speed in a sole predefined direction through a network, and the time step at which the model is computed. In light traffic conditions, the traffic flow proceeds at the free flow speed. A cell is then defined as a small section of road the length of which, noted L, is equal to the distance cleared by a vehicle tripping at the free flow speed v_0 during one time step δt:

$$L = v_0 \cdot \delta t \tag{2.6}$$

This means that in free flow conditions, the vehicles that are located within a cell i can be found in the next cell $i + 1$ after one time step, which is stipulated by the equation of transition. The core objective of this model is to determine, for every time step, the occupancy of each cell of the network. It is hence not a flow propagation model *per se*. The CTM was twofold introduced by Daganzo: the first part [16] introducing the global concept of the CTM, and the second [17] expanding the structure in order to enable the building of complex networks with merging or diverging roads.

Let be a cell i, the length of which L_i checking the equation 2.6 and containing $n_i(t)$ vehicles at time step t. Since it has a finite size, it can only contain up to $N_i(t)$. The size is actually equal to the length of the cell L_i times the jam density k_j. Moreover, only up to $Q_i(t)$ can flow into the cell, regardless of the available space inside it, that is to say the capacity of the cell $C_i(t)$ times the time step δt. The number of vehicles flowing in the cell i after one time step, noted $y_i(t)$, is then equal to the minimal value of these quantities:

- The number of vehicles currently in cell $i - 1$, noted $n_{i-1}(t)$;
- The ’capacity flow’, that is the maximal number of vehicles that can flow into cell i, noted $Q_i(t)$;
- The available room for new vehicles, that is the difference between the size of the cell and its current occupancy, noted $N_i(t) - n_i(t)$.

In other words:

$$y_i(t) = \min\left(n_{i-1}\,(t)\,, Q_i\,(t)\,, N_i\,(t) - n_i\,(t)\right) \tag{2.7}$$

Similarly to the LWR model, the variation of the number of vehicles within the cell i between two time steps is equal to the net flow of vehicles, that is:

$$n_i\,(t+\delta t) = n_i\,(t) + y_i\,(t) - y_{i+1}\,(t) \tag{2.8}$$

Even though straightforward, this formula does not account for the case where two consecutive cells have different capacities—for instance when a new lane is added on a motorway. In Daganzo [17], this situation is dealt with by adding the capacity of the cell located upstream within the min operator in the equation 2.7, that is $Q_{i-1}\,(t)$:

$$y_i(t) = \min\left(n_{i-1}\,(t)\,, Q_{i-1}\,(t)\,, Q_i\,(t)\,, N_i\,(t) - n_i\,(t)\right)$$

These terms can be gathered by pairs with respect to their subscripts, the equation thereby becomes:

$$y_i(t) = \min\left(\min\left(n_{i-1}\,(t)\,, Q_{i-1}\,(t)\right), \min\left(Q_i\,(t)\,, N_i\,(t) - n_i\,(t)\right)\right) \tag{2.9}$$

The first quantity, $\min\left(n_{i-1}\,(t)\,, Q_{i-1}\,(t)\right)$ is actually equal to the flow that can be sent at time instant t by the cell $i-1$. It is noted as S_{i-1} thereafter. The second quantity, $\min\left(Q_i\,(t)\,, N_i\,(t) - n_i\,(t)\right)$, is, on the other hand, equal to the flow that the cell i can receive at time t. However, in this expression, traffic shock waves are assumed to propagate at a speed equal to the free flow speed v_0. As explained in the sub-section 2.1.1, this speed, noted w is often slower. A corrective term equal to w/v_0 should be introduced in the second quantity to take this discrepancy into account: $\min\left(Q_i\,(t)\,, \frac{w}{v_0}\,(N_i\,(t) - n_i\,(t))\right)$ This second quantity is noted R_i from this point on. The previous equation then becomes:

$$y_i(t) = \min\left(R_i(t), S_{i-1}(t)\right) \tag{2.10}$$

As Daganzo [17, p. 85][3] outlines, this equation introduces the notion of causality:

> During time periods when $S_{Bk} < R_{Ek}$, the flow on link k is dictated by upstream traffic conditions—as would be predicted from the forward-moving characteristics of the LWR model. Conversely, when $S_{Bk} > R_{Ek}$, flow is dictated by downstream conditions and backward-moving characteristics.

This definition of the cell inflow has consequences on its behavior. In the figure 2.3, taken from Daganzo [16], is displayed the theoretical MFD of a cell inflow. It consists of a bounded triangular MFD where three different domains can be distinguished:

1. a first domain $[0, k_A]$, matching low densities, where the flow intensity increases in relation to its density. It is actually equal to the flow that the outbound cell can send. For densities belonging to this domain, the flow propagates in free flow conditions. Because of the equation 2.1, the slope is equal to the free flow speed.
2. a second domain $[k_A, k_B]$ where the flow intensity is equal to the cell capacity. Since the flow intensity remains steady whatever the amount of vehicles entering the cell, queuing appears.
3. a third domain $[k_B, k_j]$, for high densities, where the flow intensity decreases in relation to its density, matches the congested regime. In this domain, the flow intensity is equal to the flow the inbound cell can receive. Because of the equation 2.4, the slope of this curve is equal to the shock wave speed.

In the case where the capacity of the receiving cell differs from the receiving cell, the value for the cell capacity is equal to the minimal value between both cell capacities.

To enable the modeling of more complex networks where roads intersect, two new cells are introduced by Daganzo [17]: a merge cell, and a diverge cell. The former is a cell where two roads or carriageways are combined to a single one, such as an on-ramp on a motorway. The flow entering the merge cell depends on the flow it can receive and of the flow that can be sent by both cells upstream. Based on this, two cases can be distinguished:

[3] In this quotation, Bk and Rk respectively stand for $i-1$ and i.

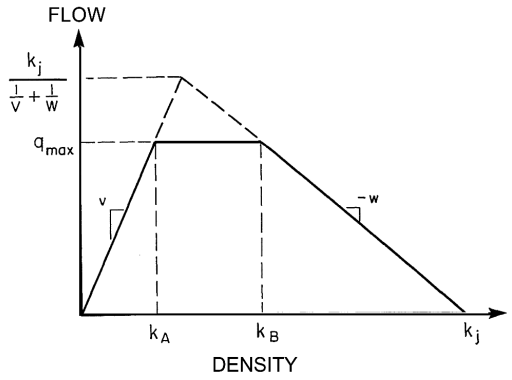


Figure 2.3: Theoretical MFD associated to the CTM [16]

- The sum of the two flows that can be sent by the cells upstream is smaller than the flow that can be received by the cell. In this case, both flows arriving at the merge can proceed into it.
- The sum of the two flows that can be sent by the cells upstream is higher than the flow that can be received by the cell. In that case, the flow entering into the the merge is made of a combination of vehicles from each flow, the proportion of which depends on the priority of one flow over the other one.

This notion of priority actually tends to estimate the proportion of each flow into the merge outflow, as well as the extent to which a flow can crowd out another flow that must yield at the merge. This crowding out is defined as a third causality regime, defined as 'mixed' by Daganzo [17, p.85]: "[The] flow is dictated by conditions upstream for one approach and downstream for the other." Corthout [14] presents different methods of estimating the priority of each road.

The diverge cell is a cell where a carriage is split into two smaller roads, such as a motorway off-ramp. The diverge outflow depends on the total flow leaving it, the flow each of the road cells downstream can receive and the proportion of vehicles 'turning'—for instance, leaving the motorway in the case of the off-ramp. This proportion can be either fixed or variable. In the latter case, a FIFO discipline must be added into the model, in order to prevent the flows that have recently arrived at the diverge to leave it before older elements that have been queuing for a longer time. The proportion of turns must be included because it actually translates the fact that queues appear if a too high proportion of a flow actually takes a road that cannot receive it. The figure 2.4 presents a schematic view of these three different elements.

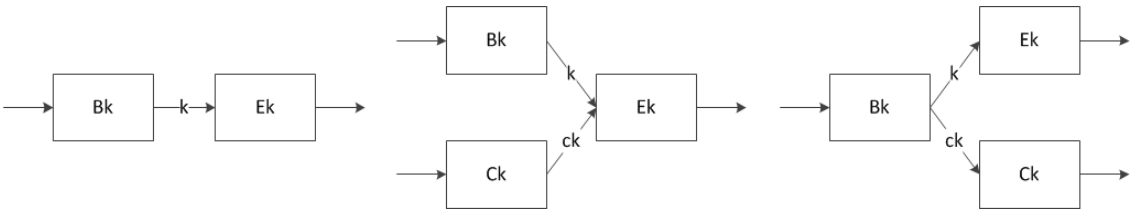


Figure 2.4: The three types of cells defined by Daganzo [17]. From left to right: a road cell, a merge cell and a diverge cell. The notations are the one defined by Daganzo.

All the elements that have been introduced so far are useful for building complex motorway networks with complete interchanges. Indeed, three flows are barely merge into a single flow at an interchange. Instead, slower flows are first merged together before being merged with the fastest flow. Doing so limits the number of points where traffic shock waves can be created owing to a too high difference in speed between both inflowing flows. In order to model the flows of vehicles, two sub-models are introduced by Daganzo. The first is a source sub-model, which consists of a first cell containing an infinite number of vehicles and flowing into a second cell of infinite size and of finite capacity. Thanks to this second cell, it is possible to hold vehicles into the system and release them at a rate equal to

its capacity. The second is a sink model, which is actually made of a single cell of infinite size where vehicles ‘stack up’ while leaving the network.

2.2. Software Opportunities

Computational power has been exponentially increasing for decades, enabling even faster running of even more complex models in an even clearer working environment. All these improvements helped the thriving of SD software such VENSIM, the sixth release of which has been chosen to develop the models presented in this thesis. Launched in the 1990s, this software have been continuously improving. Among these improvements can be listed a more user-friendly interface, a more accessible model building, improved computational features and functions or the possibility to communicate with external spreadsheets or databases [88]. In the previous section, it has been shown that the notion of cell enables to build a SD model for traffic modeling. In this section, VENSIM features that are relevant for the model are summarized from the VENSIM help and the Vensim website (2015).

In Pruyt [71], SD is defined as a modeling technique aiming at representing continuous variations over time. However, some models may require the inclusion of time-discrete functions, such as the arrival of items that have been placed on a conveyor. In order to enable this, VENSIM features some discrete functions that can be easily introduced in a model. Among these functions, one is crucial in this thesis: the function QUEUE FIFO, which is actually an enhanced stock function. In Sterman [79], a stock is defined as an accumulation of objects or information that varies under the effects of flows. These can either bring new material- to the stock–inflows—or empty it—outflows. Stocks are the memory of a system and play a key role in the system dynamics. The QUEUE FIFO function not only integrates the flows bound to the stock, but also works as a time stamp by tracking the arrival time of inflowing material. Queuing performances can be retrieved by means of dedicated functions that estimate the average and the maximal values of the material inside the stock. Such data may be of interest to implement a FIFO discipline inside a model: oldest vehicles can be allocated to available capacity first.

A second feature of interest for this thesis is the subscript feature, which enables a soft replication of a structure. Suppose that a model consists of several identical sub-structures, for instance the simple model presented in the figure 2.5 reproducing the demographic dynamics of a country. If the global model aims at estimating the population dynamics in the Benelux, then this structure can be replicated three times, once for every country, as the figure 2.6 displays. However, this method quickly becomes tedious if the global model is about the Eurozone (17 countries) or the European Union (28 countries). An alternative method then involves the subscripting of the initial structure by a variable ‘country’ listing all the countries that have to be modeled. In the case of the Benelux, ‘country’ is equal to the set [BE, NL, LX]. Subscripting the structure 2.5 is equivalent to the model 2.6, but only one stock-flow structure is physically modeled. The extension of the model is thereby easier: the only variable that has to be updated is ‘country’. In the case of the Eurozone, it becomes equal to the set [BE, NL, LX, FR, DE...] and the model physically features a single stock-flow structure. The use of subscripts is introduced in the sections 2.3 and 2.4.

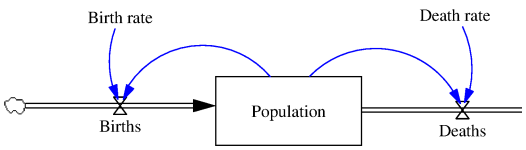


Figure 2.5: Basic demographic model of a country.

Finally, some words are to be given regarding the design of macros in VENSIM. Similarly to Excel, a macro is a user-defined function working as a specific procedure and can be seen as the equivalent feature of subscripts for function. Macros are appealing tools in the case where subscripts cannot be used for structure replication and that a complex equation must be written anew. Even though they

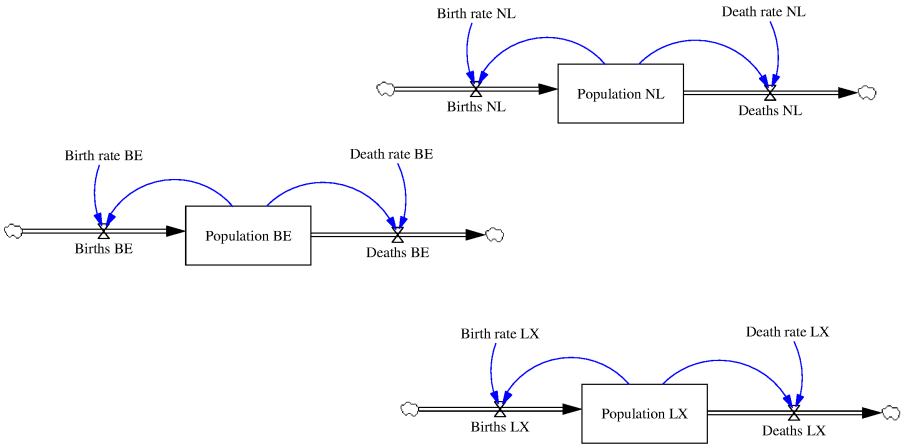


Figure 2.6: Naive replication of the demographic model of a country for the Benelux.

are by essence unique and designed for a highly-specific case, some macros that were deemed worth enough have been gradually implemented as default functions in VENSIM releases, such as the ALLOCATION BY PRIORITY procedure. This function was developed to cope with the allocation of a scarce resource over several suppliers, each of which requesting a different quantity and benefiting from a different attractiveness. A last parameter named 'width', is defined as the gap in attractiveness that ensures a first-come-first serve allocation. For low values compared to the values of the attractiveness, the allocation tends to respect this logic. For higher values instead, allocation tends to be more equitable. Again, the concrete use of this function is to be developed in the sections 2.3 and 2.4.

2.3. Basic Structures

It has been shown so far that SD is theoretically a suitable method for traffic flow modeling, and that the most recent software developments enable easier model building. In this section are to be designed the three road elements introduced by Daganzo [17] and represented in figure 2.4. Their behavior is to be described in the chapter 3.

Before building a structure by means of the piece of software chosen, some changes have to be brought to the equations introduced in the section 2.1.2. The objective of these changes is to highlight stock-flow structures, which are a cornerstone of SD models. Because of its accumulative character, a stock can decouple its outflow from the inflow and thereby creates, inertia, delays and disequilibrium into the system [79]. Such structure can be derived from the equation 2.8. Indeed, this equation can be written as follows:

$$n_i\,(t+\delta t) - n_i\,(t) = y_i(t) - y_{i+1}(t)$$

By assuming small variations of time:

$$n_i\,(t+\delta t) = n_i\,(t) + \delta t \cdot \frac{dn_i}{dt}$$

Thus

$$\frac{dn_i}{dt} = \frac{y_i(t)}{\delta t} - \frac{y_{i+1}(t)}{\delta t}$$

Let the quantity $y_i/\delta t$ be written as q_i, this latter equation finally becomes:

$$\frac{dn_i}{dt} = q_i - q_{i+1} \tag{2.11}$$

This equation is a typical equation of a stock named n_i accumulating material conveyed by the inflow q_i and emptied by the outflow q_{i+1}. Road cells are therefore to be modeled as stocks through which a flow of vehicles proceeds. The newly defined variable $q_i(t)$ actually represents the inflow intensity in vehicles per unit of time entering into the cell i.

Introducing the variable q_i has consequences on the equation 2.9. Indeed, the quantity Q_i has been defined as the capacity flow by Daganzo [16], that is the maximal flow that can enter or leave a cell during one time step. It is therefore equal to $C_i \cdot \delta t$ and the equation 2.9 then becomes:

$$y_i(t) = \min\left(\min\left(n_{i-1}(t), C_{i-1}(t)\cdot\delta t\right), \min\left(C_i(t)\cdot\delta t, \frac{w}{v_0}\left(N_i(t) - n_i(t)\right)\right)\right)$$

Since the time step δt is positive, this equation becomes:

$$q_i(t) = \min\left(\min\left(\frac{n_{i-1}(t)}{\delta t}, C_{i-1}(t)\right), \min\left(C_i(t), \frac{w}{v_0}\cdot\frac{N_i(t) - n_i(t)}{\delta t}\right)\right)$$

Let s_i (resp. r_i) be defined as $S_i/\delta t$ (resp. $R_i/\delta t$), that are the flow intensity that can be sent (resp. received) by the cell i at time t. The previous equation then becomes:

$$q_i(t) = \min\left(s_i(t), r_{i-1}(t)\right) \tag{2.12}$$

The figure 2.7 presents the layout of a road cell and of the different auxiliaries that have been introduced so far.

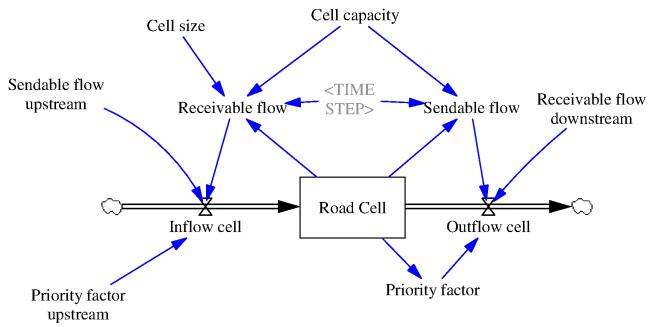
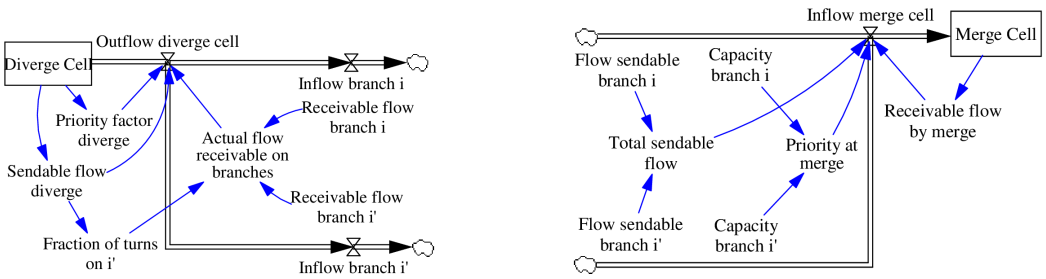


Figure 2.7: VENSIM model for a road cell built from Daganzo's CTM.

However, the flow equation 2.12 has a limited extent. Indeed, it holds true only if one single flow is modeled or when several flows the sum of which is lower than the flow that can be received by the cell. Moreover, the model should be able to feature a first-in, first-out (FIFO) logic: the first vehicles that leave a cell must be the ones that have entered into it first. Not doing so would enable multiple violations of FIFO property: vehicles conveyed by a flow that has arrived the earliest may get capacity allocated in place of vehicles have been queuing for a longer time. This situation, known as Smeed's paradox [59], should be prevented from occurring. A first intuitive and straightforward method consists in allocating the available capacity to each outbound flow with respect to their relative share inside the cell. This method, presented by Carey et al. [10] as a FIFO level 1 rule, leads to a slightly more realistic allocation, but still allows FIFO violations. Instead, they propose two allocation algorithms to ensure a FIFO discipline for a cell or a small sequence of cells—respectively described as level 2 and 3. These actually stem from an algorithm detailed by Daganzo [17] to cope with variable. In order to include the FIFO discipline into the model, an alternative method based on software features has been chosen: the equations 2.11 and 2.12 are upgraded with the ALLOCATE BY PRIORITY and QUEUE FIFO introduced in the section 2.2. Since the latter function works as a 'time stamp', it is then possible to retrieve, for every flow, information about queuing to use it as a priority factor for outbound flow. Such structure



(a) Diverge Cell. (b) Merge Cell.

Figure 2.8: VENSIM models for merge and diverge cells

is quite similar to the FIFO level 2: it “ensures that traffic exits from each cell in the same time order as it entered the cell” [10, p. 116].

Daganzo [16] introduces sources and sinks as cells, one characteristic of which is assumed to be infinite so that the flow that can be sent/received take a specific value. These structures can be made even simpler. For instance, the sink cell of infinite size can be merely replaced by a variable standing for the capacity of the outbound link. Its value can change in order to include congestion generated by traffic out of the system boundaries. Similarly, a variable is a more efficient way of generating traffic flows than a cell that contains an infinite number of vehicles. Replacing these cells by variables leads to a model with a lower complexity and is therefore relevant for models featuring a high number of sources. On the other hand, the second cell of the source, of infinite size, cannot be removed. Indeed, this cell actually holds vehicle flows generated by the source into the system, and therefore prevents them from disappearing once the sources stop emitting vehicles. Similarly to a normal cell, the QUEUE FIFO and ALLOCATE BY PRIORITY are implemented to release the vehicle flows with respect to their arrival time in the system.

Regarding the merge and diverge cells, this allocation structure must be slightly adapted. For a diverge cell, the flow that can be received downstream actually depends on the fractions of vehicles taking each outbound branch. Given a branch noted i or i', the fraction of flow that is to enter it β_i or $\beta_{i'}$ is equal to the the fraction of the outbound flow addressed to it versus the total outbound flow. The receiving capacity r_{Dns} to which the flow sent by the merge is assessed, is defined as the smallest ratio of the flow that the cell can receive over the fraction of flow entering it:

$$r_{Dns} = \min\left(\frac{r_i}{\beta_i}, \frac{r_{i'}}{\beta_{i'}}\right) \tag{2.13}$$

This is then used to compute the outflow of the merge cell first, and the inflow of both cells downstream of it. For a merge cell, the allocation process is totally different: the available capacity of the merge cell must be allocated with respect of the priority of each inbound branch. In Daganzo [17], this priority of a branch i or i' over the other one is introduced as a constants p_i and $p_{i'}$ that tally up to 1. A branch having a priority of 1 has absolute priority of the other one. In Corthout [14], priority factor of a branch can be computed as the ratio of one of its characteristic variable over the sum of the same characteristic of both cells upstream. This characteristic can be either the capacity—which has been empirically corroborated—or the total flow sent to the merge. In this thesis, the priority factor at a merge is defined from the capacity of each inbound branch i or i' and is defined as follows for the branch i:

$$P_{M,i} = \frac{C_i}{C_i + C_{i'}} \tag{2.14}$$

2.4. Complex Structures

The CTM-based structures that have been introduced so far are actually sufficient to design complex road networks. Generally speaking, a network actually consists of a set of nodes or vertices connected

by edges or links. In the case of a road network, the nodes match intersections—whatever grade-separated or not— while links are made of a cell or a sequence of cells. In order to ease the model developing, two template models are to be developed: one for links whose length exceeds 1 cell and that is to be named corridor thereafter, and a 3-way interchange from which a motorway emerges.

The road cell structure is, despite its simplicity, not suitable as is for long road sections. The longer the section, the more cells and auxiliaries are required: modeling becomes quickly tedious. Let be a motorway section made of two separate one-way carriageways whose length is equal to 20 km. By assuming a cell length of 250 m, each carriageway is made of 80 cells, thus 160 cells are required to represent this complete section. A way of facilitating the replication of a given structure is subscript feature of VENSIM introduced in the section 2.2. Fallah-Fini et al. [26] have shown that subscripting can be used for introducing smaller-scale dynamics inside a stock. In the case of a road network, subscripts can be implemented in order to compress a sequence of cells into a single stock. If so, merely a new variable needs to be added to the model: the inflow of a cell i, noted q_i. This reduces then the maximal number of equations ruling the road section behavior to 3: one for the first cell, one for the last cell and one for all the cells in-between.

A road interchange is a piece of infrastructure where at least two motorways cross each other at a different level in order to enable a high throughput of vehicles in it. Vehicles may take another direction by means of ramps or flyover that binds two carriageways. Various types of interchange exist. They are usually sorted with regard to their shape, such as clover-leaf, stack, turbine, trumpet and so on. However, the shape is not the most crucial feature of an interchange; the number of ways crossing at it is of greater importance. Based on this, two categories can be distinguished, three-way and four-way. Since vehicles can flow in different directions, the composition of the flow leaving one of the carriageway may change across time. Let be a flow crossing a road cell or a corridor. As these elements feature only one inflow and one outflow, the flow composition remains the same. In order to make it change, merge and diverge cells must be added to enable variations in intensity and composition of the flow. The number of merge and diverge cells required for each type of interchange differs: a three-way interchange requires three merges and diverges while a four-way features either 8 or 12—clover-leaf interchange with a bypass—of each. In order to keep the merge and diverge equation simple, similar topology rules as the one described by Daganzo [17] are introduced: a merge or diverge cell cannot be directly connected to another merge/diverge cell; at least one cell must lay between them. The figure 2.9 presents the basic stock-flow—without auxiliaries—structure of a three-way interchange.

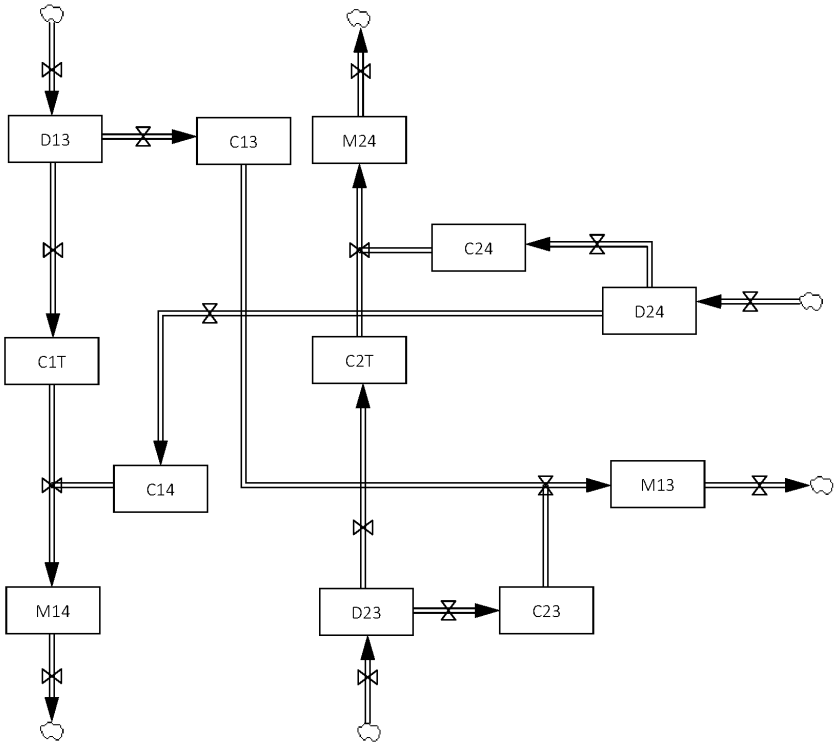


Figure 2.9: Cell layout of a three-way interchange. The stock names are the ones used in the model developed in the section 3.

3

Case Study: The Ring of Brussels

In the previous chapter, the CTM was introduced and deemed adapted to model complex road elements such as an interchange. The current chapter then deals with a simple case study to test the model: the Great Ring of Brussels R0, where congestion is the direst in Western Europe. In the a first time, more detailed about the case and relevant contextual information are provided. In a second time, the elements of interest for the model are described. Finally, the model is presented in two times: first its structure, then its behavior. Finally, a simple transport policy is tested by means of the model.

3.1. Case Introduction

Capital of Belgium and headquarters of Belgian and European institutions, Brussels is the second European city where congestion is the direst, the first being London. INRIX [43] estimates at 76 hours the time spent per year by a driver in traffic jams. This figure stands out with the same measure for drivers based in Paris for instance. Indeed, the urban area of Paris is around 7 times more inhabited[1] than Brussels one, but the time spent per by a Parisian driver is equal to 48 hours. The traffic situation in Brussels can hence be deemed singular.

Similarly to other European capitals, Brussels presents several ring roads in order to limit the vehicle inflow into the city center. According to the Belgian naming system, there are four different ringways where congestion occurs on a very regular basis:

- The R20, or 'Small Ring', is the innermost one. It surrounds the city of Brussels and crosses local and nationwide (N-network) arterials at graded and some signalized intersections. Its northwestern corner vertex is connected to the western part of the E40.
- The R21, or 'Medium Ring', surrounds the eastern side of the R20 at a distance of 3 km and is an arterial for the cities located around Brussels. Similarly to the R20, intersections with other arterials are either graded or signalized. The A12, the eastern part of the E40 and the E411 are directly bound to it.
- The R22, or 'Woluwe Dale', located east of the R21 at a distance of 3 km from it, is a major arterial connecting farthest suburbs North and East of Brussels to the R0 and the the R21.
- The R0, or 'Great Ring', is the outermost one. It lies at a distance varying between 10 km and 20 km from the city of Brussels. Most of the structuring Belgian motorways are bound to it by means of graded interchanges only.

The figure 3.1 shows the different ringways as well as the three European routes around Brussels.

The worrying levels of congestion observed on the rings can be related to the current utilization of existing infrastructure. In their 2012 report, the Conseil Economique et Social[2] (2012) of the Brussels-Capital Region provide figures outlining a sustained growth of traffic levels since 1985. At that time, the

[1] the region Ile-de-France is actually more populated than Belgium!
[2] In French, Economic and Social Council.



Figure 3.1: Road configuration around Brussels. Road names are indicated on it. The R22 is the thinnest grey line. The E40 is the thick green line.

busiest section of the R0 had to bear a vehicle load equal to 85,000 vehicles per day. 20 years later, the vehicle intensity on the same section had almost doubled: the vehicle load was equal to 168,000 vehicles per day. In 2008, the highest load actually observed is equal to 149,000 vehicles per day, but the highest value interpolated yields a load of 171,500 vehicles per day. Current infrastructure cannot support such high levels of traffic and therefore tends to be saturated. In the morning peak for instance, the saturation percentage reaches on the busiest section 118 % of the conventional capacity of a road section, equal to 2,000 vehicles per hour and per lane. Besides this, many sections have a saturation rate above the congestion threshold of 75 % of the same conventional capacity. In INRIX [43], similar data can be found for main connecting roads of Brussels.

In order to cope with congestion, mobility plans for Brussels have been developed for 20 years. The key objective of these plans is to optimize the use of existing infrastructure by developing or improving a multi-modal transportation system. The development of transport infrastructure is slower than the growth of demand and hence suffer from time inconsistency. Moreover, the capacity of infrastructure under construction may not be sufficient once it has been achieved. Instead, optimizing the use of current infrastructure by developing a multi-modal system may be an interesting alternative to extension. For this purpose, the region of Brussels-Capital developed a framework for models aiming at multi-modal mobility named IRIS Bruxelles Mobilité [9]; Région de Bruxelles-Capitale & ASBL [73]. The two most recent version of this plan and the name of the model stemming from it is IRIS 2; the new version IRIS 3 being currently under development. The IRIS 2 model is a four-step model based on data from 2001, re-calibrated on a regular basis, for an area centered around Brussels, with a radius of about 30 km. Transport policies are tested during the morning peak, for a region including not only the Brussels-capital region, but also major cities such as Mechelen or Leuven.

However, a 4-step model may not be adapted to forecast traffic for managing daily operations, for instance when a temporary building site is located on a street. Indeed, there may be a substantial number of sites to coordinate in order to avoid stark traffic congestion De Schrijver [22]. To help the Brussels Mobility Center to manage all the existing working sites, Transport & Mobility Leuven developed in 2011 a tool named IRMA. Based on a macroscopic traffic flow model and on real-time observation, the IRMA model estimates the actual impact of these sites on traffic flows and provide short-run forecasts of the traffic—between 15 and 30 minutes. Based on these, substitution routes can be provided to drivers. Besides the IRIS plans, the ring of Brussels is also included into the Flemish Brabant model developed by the Vlaams Verkeerscentrum[3]. Indeed, an important part of the ringway R0 is located

[3] In Dutch: Flemish Traffic Center

Table 3.1: European Roads going along the ring R0

European Road Number	Main Belgian Cities	Main European Cities
E19	Mons Antwerp, Mechelen	Paris, Rotterdam Amsterdam
E40	Ghent, Bruges Leuven, Liège	Calais, Dover Aachen, Cologne
E411	Namur	Luxembourg

in the Flemish region, and more exactly in the Flemish Brabant. Similarly to the IRIS 2 model, the objective of this model is to improve and supervise the mobility of inhabitants of the Flemish Brabant by monitoring actual situation and testing potential policies. Like IRIS 2, the methodology is based on the 4-step paradigm. 5 modes are taken into account: car driver; car passenger, public transport, bicycle and pedestrians. The calibration year is 2009 [55].

In Vermeersch [89], the strength of congestion around Brussels can be seen as a stark imbalance between the transportation demand and existing infrastructure. Indeed, Belgian workers often leave far from the urban areas and therefore need to commute by car to go to work. The preference for car stems from issues met by public transport—delays, saturation of existing offer—and the high ratio of company cars currently in circulation. Two reasons explain this large number of company vehicles. On the one hand, it offers tax cuts to companies that tend to offer not only a vehicle to workers, but also fuel subsidies. As a result thereof, car drivers tend to travel more [58] and thereby generate a higher level of demand. Regarding the transport supply side, the ring roads around Brussels, and especially the R0, can be seen as nationwide roundabout for structuring motorways and highways, some of them belonging to the European Route Network. The table 3.1 lists them, as well as the main Belgian and foreign cities they connect and go along Brussels. It can then be seen that the northern section of the R0 belongs to two European roads, the E19 and E40. This section tends to concentrate not only commuters, but also regional, national or even international transit. Existing infrastructure may be insufficient to bear the total demand, congestion is hence more likely to occur there.

In this thesis, the focus has been made on the section of the R0 located between the interchanges of Strombeek-Bever and Zaventem. As the previous paragraphs have highlighted, this section is of importance for regional, national and international traffic. Besides this, the R0 ring crosses other motorways at graded interchanges: conflicts at intersections that leaving or entering traffic generates are sent off to another level, ensuring a high free flow speed for passing-by flow [64]. Furthermore, the modeling approach for vehicle flow is macroscopic: vehicles cannot be individually mapped, their interactions at at-grade intersections cannot be properly modeled. Instead, macroscopic scale is more suited for "the distribution of traffic along long, crowded roads" [56, p. 318] such as motorways. The figure 3.2 displays the actual configuration of the section of interest.

3.2. Case Description

The section of interest presented in the figure 3.2 can be divided into 5 elements: three interchanges— Strombeek-Bever, Machelen and Zaventem— and two road sections, each connecting two interchanges. The first interchange, Strombeek-Bever, is the intersection between the R0 and the A12 connecting directly Brussels to Antwerp. It is a four-directional interchange: a driver arriving at it can choose between three different directions. The two other interchanges, Machelen and Zaventem, are regular three-directional and four-directional interchanges respectively. The road section connecting Strombeek-Bever to Machelen is 5.5 kilometer-long. It can actually be divided into two distinct sub-sections: a first section where the speed limitation is equal to 120 km/h, and a second section, matching the Vilvoorde Viaduct, where the speed limitation is lowered to 90 km/h. In the model, this separation has been done by creating two links, for which free flow speed, as well as the capacity, are constant for all the cells belonging to it. The second section, binding Machelen to Zaventem, actually consists of a single cell of 250 m. All the relevant data regarding all these elements is presented in the appendix B.



Figure 3.2: The section of road that is to be studied and modeled in this thesis. Interchanges are indicated by stars. The color of the road links indicate their speed limit: Dark green: 120 km/h; light green: 90 km/h

Table 3.2: Network characteristics of the different cities chosen for the OD pairs.

City	International Importance	National Importance	European Routes
Brussels	x		E19, E40, E411
Antwerp	x		E17, E19, E34
Leuven		x	E40, E314
Ghent		x	E17, E40
Mons		x	E19

Regarding the transportation demand, assumptions had to be made because no data about actual flows was available. In order to ensure that the model can be run and tested, five routes have been designed. Their origin and destination were chosen with respect to two criteria: their importance at a national or international level; and their proximity to the European route network. Five cities were then chosen: Brussels, Antwerp, Ghent, Leuven and Mons. The table 3.2 presents how they fit with each of these criteria. Based on these cities, five pairs of cities were made, which yields in total 10 different pairs of origin and destination:

- Brussels-Antwerp via the A12 (through Strombeek-Bever),
- Brussels-Antwerp via the E19 (through Zaventem and Machelen),
- Mons-Antwerp, that is the Belgian section of the E19,
- Ghent-Leuven, that is a part of the Flemish section of the E40,
- Ghent-Brussels via the A12 and E40 (through Strombeek-Bever).

This choice of OD pairs has a consequence on the model for the section of interest. Indeed, a basic assignment of each route on it brings out that some of the flyovers of Strombeek-Bever and Zaventem are not taken by any flows. As underlined in the subsection 2.1.2, the CTM is originally a model that computes the occupancy of road cells over time. If these branches remain in the model, their occupancy will be updated at every time step, even though it remains equal to 0 all along the simulation. The complexity of the model therefore increases, as well as the computational time. In order to reduce the model complexity, all unused links are removed from the model while merge and diverge cells they would connect in a complete model are turned into simple road cells that can be used for model monitoring for instance. The simplification of the interchange Zaventem is presented in the appendix B.

3.3. Model Structure

As described in the previous sections, the model consists of three corridors, three interchanges, two of which are simplified (Strombeek-Bever and Zaventem), 6 sources and 6 sinks, for a total of 184 road

cells. Besides the different elements introduced in chapter 2 some outputs have been added in order to monitor the propagation in more usual units:

- The expected travel time through a cell $t_{tr,i}$, expressed in minutes, which is defined as the ratio of the cell occupancy divided by its total outflow: $t_{tr,i} = \frac{n_i}{q_{out,i}}$. This formula is actually derived from the equation 2.1. The travel time gotten can be then tallied up in order to get the travel time over a corridor or an OD pair. Real-time travel times are often communicated by authorities to drivers by means of light boards or radio bulletins. This is actually one of the performance indicators defined by Daganzo [16]
- The jam length, which is equal to the total length of the network on which the flow intensity is at least equal to 80 % of the capacity value [13]. The real-time nationwide jam length on the main road network—motorways, Brussels ring ways and European routes—is used in Belgium as an indicator of traffic situation.

In order to identify and copy the cells ans their structure easily, a naming scheme was adopted for the different cells constituting each interchange. The figure 3.3 presents the monitoring structure for a corridor.

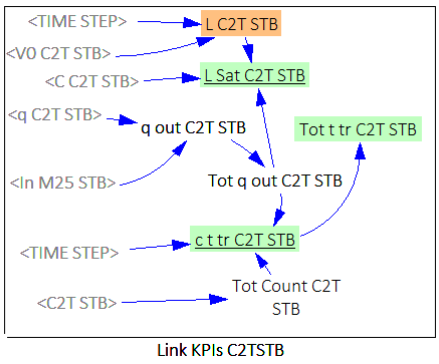


Figure 3.3: Key performance indicators tracking the flow performances through a corridor. The meaning of the variable names can be found in Appendix B.

The figures 3.4 and 3.5 present two details of the model. The former figure presents a branch of the interchange Strombeek-Bever with most of the elements presented in the sections 2.3 and 2.4, to wit one queue, one sink, one diverge cell named D16 STB, one merge cell M26 STB and two corridors C1T STB and C2C STB. The queue and the sink are deemed external to the network of interest and are hence represented in red. Cells characteristics and parameters present an orange background while model outputs are indicated with a green background. In the latter figure is shown the structure of a two-directional road corridor. Since a road cell and thereby a corridor is unidirectional, a network link should feature two identical structures for each carriageway. Since the model is based on a ring road, a carriageway can be mapped with respect to the flow direction, that is to say clockwise—for the inner one—or counter-clockwise—the outer one.

The global model only requires three parameters, the first of which being the time step δt of the model, equal to 0.125 minutes, or 7.5 seconds. This time step is actually a trade-off between reality and computational efficiency. Since the time step affects the recommended cell length, the number of cells of the model depends on its value. High time steps guarantee the computational efficiency of the model, but results in a too coarse network and the distances between modeling elements may greatly differ from the actual distances. Any value for the time step greater than 15 seconds can be then considered as too coarse for this application. On the other hand, low time steps yields a finer model, at the cost of a higher complexity. The time steps proposed by VENSIM δt_n can be written as $\delta t_n = 2^{-n}$, the number of cells therefore exponentially increases when the time step decreases. Moreover, vehicles need some time to adjust their behavior with respect to current traffic conditions. By assuming an average driver reaction time of 1 second plus a safety margin of another second, any

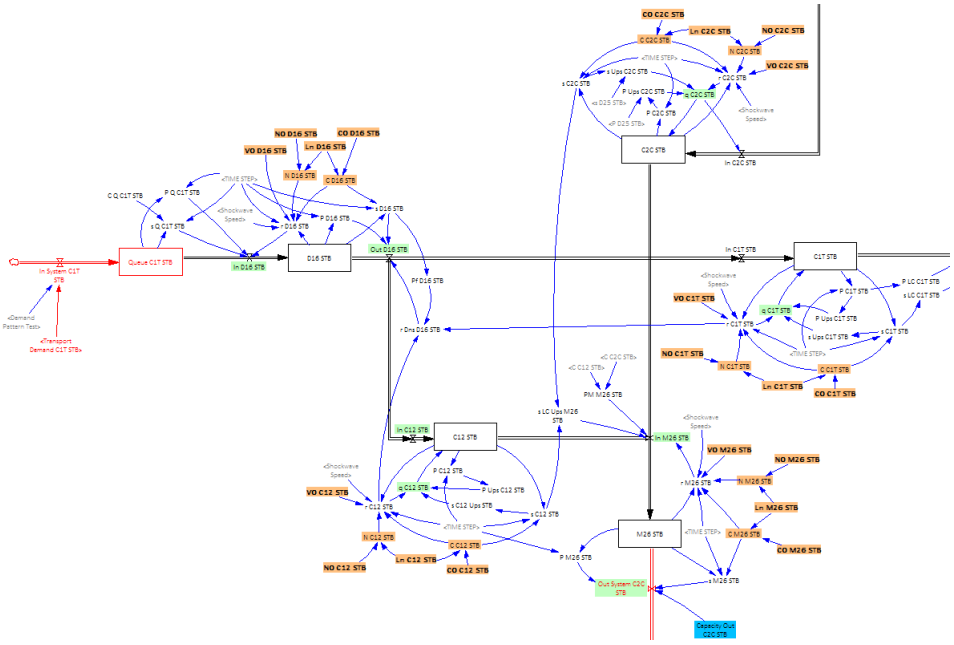


Figure 3.4: Detail of an interchange of the model. The parameters and characteristics of each stock are given in the appendix B.

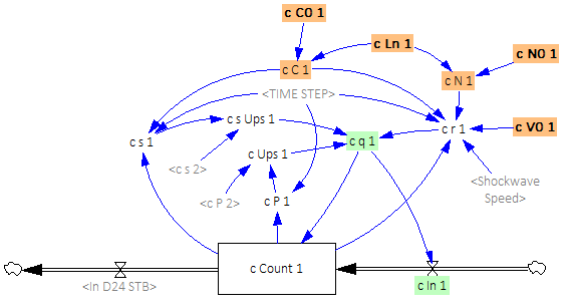


Figure 3.5: Representation of one carriageway of a motorway section.

time step below the value of two second can be deemed irrelevant for the model. Three time steps—expressed in minutes—are then possible for the model: 0.25, 0.125 and 0.0625. The second value represents then an acceptable trade-off for the model. In the appendix B are given some values of cell length with respect to their free flow speed.

The second model parameter is the jam density k_j, equal to 150 vehicles per kilometer per lane. This value is actually the upper bound of the usual range for jam densities, its lower bound being equal to 56 vehicles per kilometer per lane [97]. Even though the value of 56 vehicles per kilometer per lane is recommended by the Highway Capacity Manual [85], higher densities were actually observed. Furthermore, the jam density is equal to the inverse of the spatial headway of the flow, that is to say the distance between the front bumpers of two consecutive vehicles. By assuming the length of a vehicle equal to 4 meters, a jam density of 56 vehicles per kilometer means that the available space between two vehicles is about 14 meters. For a density value of 150 vehicles per kilometer, this inter-vehicle distance is equal to 2 meters. Such value is hence deemed more realistic when stark congestion takes place. Similarly to the time step, the jam density is a key parameter for the cells: in Daganzo [16], the size of the cell N is defined as the product of the jam density times the cell length. In other words:

$$N = k_j \cdot v_0 \cdot \delta t$$

The last parameter is the shock wave speed w and describes the speed at which traffic perturbations are carried backward. In the section 2.1.2, its value has been assumed to be constant. A traffic

perturbation results from a sudden change of the flow characteristics at its leading edge, caused either by the infrastructure—for instance a road bottleneck—or by other flows, in the case where a faster flow makes up a slower one. As the equation 2.4 presented in the chapter 2 outlines, this speed actually depends on the variation in density and the variation in intensity. The shock wave speed is an important parameter of the CTM since it determines the rate at which flow intensity diminishes as it becomes denser. In this thesis, a shock wave speed of 18 km/h (or 0.3 km/min) speed taken from a validation report [25] has been chosen to run the model. This value complies with the condition $w < v_0$ presented by Daganzo. Since no other value could be found in existing literature, uncertainty tests about this parameters are to be carried out thereafter.

3.4. Behavior

Now that the model has been built and parameters properly set up, it can be run in order to see how it reproduces the propagation of traffic flows. The model behavior is to be discussed for three different traffic situations: light traffic conditions, congestion caused by infrastructure, and congestion caused by traffic level. In order to generate these behaviors, the model is run with two distinct demand profiles:

- A first profile reproducing light traffic conditions. It features a progressive loading of the network, a short plateau and a progressive unloading. The maximal demand level, matching the plateau, is equal to 30 vehicles per minutes. This profile is used for generating the model behavior for free flow and congestion caused by infrastructure. The graph of this pattern is labeled with 1 in the figure 3.6.
- A second profile generating dense traffic conditions. The traffic pattern is qualitatively similar—to wit progressive loading and unloading separated by a short plateau. On the other hand, the profile presents a higher peak equal to 80 vehicles per minute, and is more spread over time. The graph of this pattern is labeled with 2 in the figure 3.6.

Because of the equation 2.5, the flow propagation through the network is implicitly delayed and thereby introduces time shift between flows. As a consequence, these profiles can be used to check whether FIFO is respected as well.

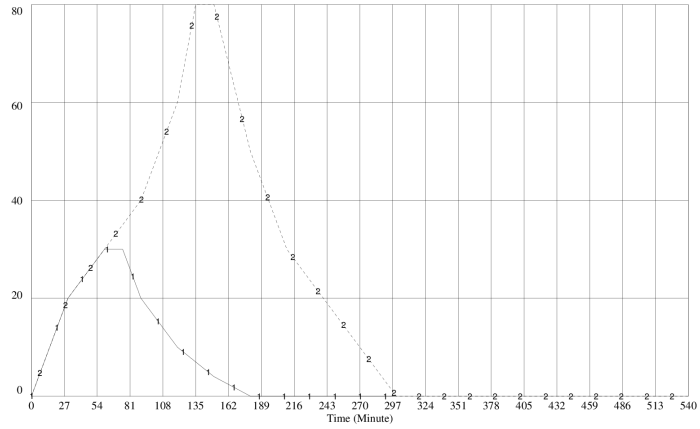


Figure 3.6: Temporal pattern demand of traffic flows entering the system. The plain curve labeled with 1 represent light traffic conditions. The dashed curve labeled with 2 represent heavy traffic conditions.

All the graphs that are to be presented in the subsections thereafter are, if no further mention is added, cumulative graphs. Let $f(t)$ be a variable of the model; a cumulative graph of $f(t)$ represents the evolution of the function $F(t) = \int_0^t f(\tau)\,\mathrm{d}\tau$. The derivative of this cumulative function at a certain point yields the value of the original function at the same point. Applied to a cell inflow (resp. outflow), the cumulative function gives the total number of vehicles that have entered (resp. left) the cell at a given time moment. These plots can hence be seen as vehicle counters. Daganzo [16] explains that cumulative flows are convenient to analyze the model behavior, since changes in the plot shape can

be interpreted in terms of behavior. However, the cumulative curves he describes are represented with respect to the distance expressed in cells. In this section, cumulative plots are displayed with respect to the time. In spite of their difference, such plots remain convenient to analyze the model behavior.

On the one hand, the slope of a plot is equal to the considered flow, by definition of the cumulative graph. The considered flow can hence be retrieved from its cumulative plot. On the other hand, it is possible to check if the allocation process is well respected. In the case of regular or diverge cell, the allocation is based on the FIFO rule.

Since no individual vehicles can be mapped, the FIFO rule can be deemed respected if the cumulative graphs of the inflow and outflow of a given cell only intersects when the network is not loaded yet or has unloaded. Any intersection means that that more vehicles have left a cell than it has entered, and therefore brings out a FIFO violation. In the case of a merge cell, the allocation of available capacity differs, since it is based on the notion of priority at the intersection. In that case, curves may intersect. The crowding out of the yielding flow can be materialized by a slowing down of the cumulative count of the cell outflow owing to the fact that fewer vehicles can leave the ramp. Because of the queue that appears and starts to spill back, the ramp outflow may become more intense compared to its expected intensity when the room for vehicles from the ramp starts to increase again. As a consequence, a stiffer evolution is expected once crowding out no longer takes place.

3.4.1. Free Flow Conditions

The free flow conditions are simulated thanks to the first demand profile. The resulting vehicle density throughout the network is then relatively low, and the total flow crossing a cell never exceeds its capacity. Besides this, yielding vehicles at merges are not crowded out by the main flow. According to the MFD associated with a road cell, it can be expected that the flow clearing a cell increases in relation to its current occupancy.

From a disaggregated point of view, the values of OD flows connecting any pair of cell are always positive or equal to 0: the flows hence proceed in the correct direction. As a consequence, the total flow between any pair of cells, equal to the sum of all the OD flows between these same cells, is always positive and equal to 0. In complement to this, the total outflow never exceeds the capacity value of the cell it enters. Regarding the number of vehicles per cell, similar observations can be made for aggregated and disaggregated variables. Because the QUEUE FIFO function was used for computing the cell occupancy,its value must remain positive or nil. If it takes negative values the cell occupancy should not become negative, else warnings are emitted by VENSIM. A careful analysis of warnings about negative values signaled during the run showed out that their magnitude is around 10^{-15}. These values may result from computation rounding and can then be estimated as insignificant. Besides this, the total count of vehicles inside a cell never exceeds its size.

Regarding qualitative propagation, interesting results can be derived from the outputs. The figure 3.7 presents the cumulative inflow—plain line, labeled with 1—and outflow—dashed line, labeled with 2—of a single OD flow crossing a corridor. It can be observed that the vehicle counts between the inlet and the outlet are parallel and shifted by the free flow travel time of this corridor. The same time shift can be observed if the plotted flow is the aggregated one. More generally, a similar propagation pattern can be observed for any corridor, whatever its length, whichever the flow considered—aggregated or not. This means that the flow propagation is driven by changes occurring upstream of it. The model hence reproduces properly the ‘forward’ causality regime defined by Daganzo [17].

A plausible temporal behavior is not sufficient to validate the model. A second point to check is whether the vehicle flows leave a cell by respecting a FIFO rule. As explained as the beginning of the sub-section 3.4.1, the different OD flows generated are endogenously delayed while proceeding through the network. This means that these delays must be observed while checking the disaggregated outflow of a merge, where the aggregated flow composition can change. The figure 3.8 presents the cumulative inflow and outflow of a merge cell where three distinct and time-shifted OD flows meet. A zoom on the beginning of the run is shown in figure 3.9 to bring out the gap between the cell inflow and the cell outflow for every OD flow. The inflow curves never intersect the associated outflow nor

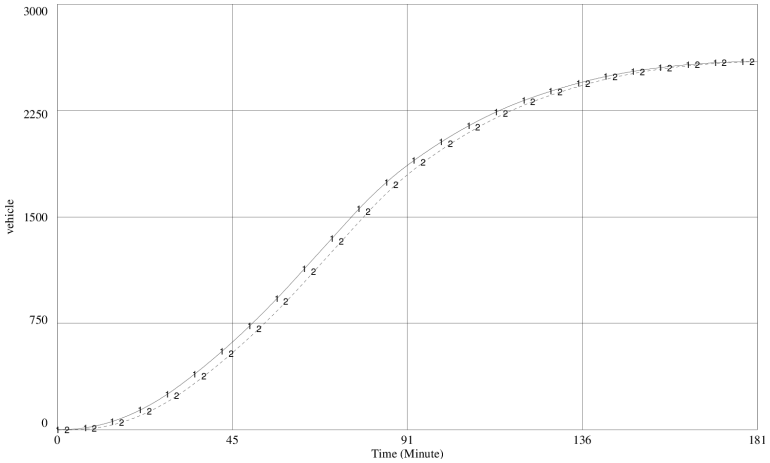


Figure 3.7: Cumulative inflow (plain curve, labeled with 1) and outflow (dashed curve, labeled with 2) of a road corridor over time in light traffic conditions.

other inflow curve between the beginning and the end of the run. It can be observed that the first flow leaving the system is the one the distance of which between its entrance point and the outlet is the shortest. Similarly, the OD flow that has the greatest distance to clear to exit the system is the last that reaches a constant value. As a consequence, the model correctly reproduces the FIFO. Based on all the previous results, the model is deemed valid in free flow conditions.

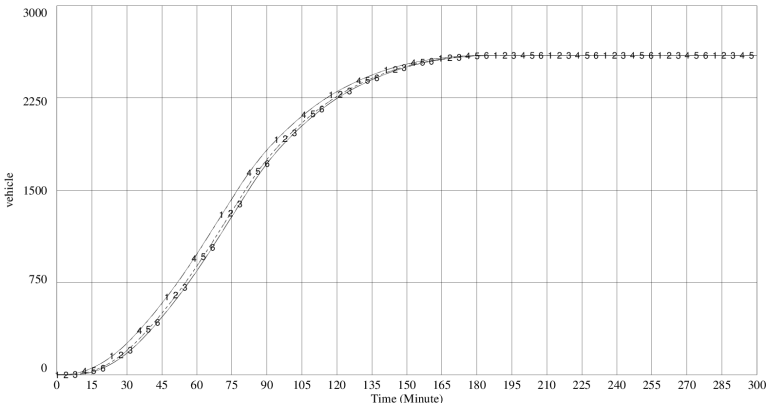


Figure 3.8: Cumulative inflows and outflows over time at the merge cell for each OD pair in light traffic conditions. The cumulative inflows associated with the OD flows 1, 2 and 3 are labeled respectively labeled with 1, 2 and 3. The cumulative outflows associated with the OD flows 1, 2 and 3 are labeled respectively labeled with 4,5 and 6. A zoom on the beginning of the run can be observed in figure 3.9

The outputs discussed in the previous paragraph show out a plausible behavior of the model across time. In order to complete it, scatter plots of the cell outflow with regard to the flow density of the same cells are created to explore and analyze the relationship between these two variables. Such plots are meant for validating the flowing dynamics. A plausible temporal behavior does not necessary means that the flow characteristics are properly related. In free flow conditions, the model built can be deemed valid if a plot of the total flow intensity with respect to the total density shows out a linear relationship. Indeed, as the figure 2.3 illustrates, the flow intensity should increase in relation to its density Since the total flow density of a cell is equal to the total number of vehicles it contains divided by its length, a similar relation should be visible between the total cell occupancy and the total flow intensity, only the slope should differ. The figures 3.10a and 3.10b present scatter plots of the total flow intensity with respect to the total count of vehicles within a cell. Two kind of cells are considered: a normal road cell and a merge cell. Both linear regression curves have coefficient of determination equal to 1. This means that the relation between the model outcomes is linear and its fit is perfect. The relation between the flow characteristics is therefore correct. Based on all the analyses detailed in this subsection, the model behavior can be considered as valid.

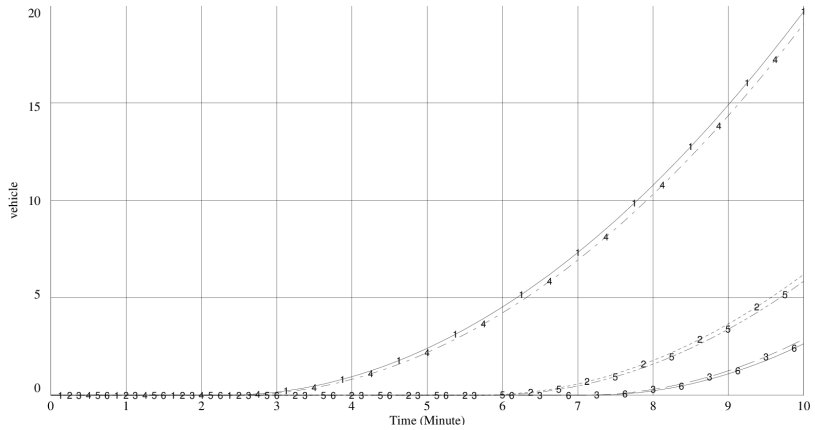
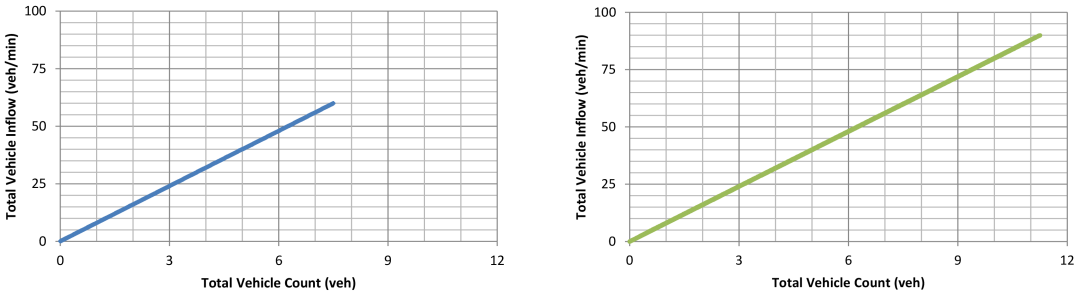


Figure 3.9: Zoom on the figure 3.8. The cumulative inflows associated with the OD flows 1, 2 and 3 are labeled respectively labeled with 1, 2 and 3. The cumulative outflows associated with the OD flows 1, 2 and 3 are labeled respectively labeled with 4,5 and 6.



(a) Road cell of the main carriageway. (b) Merge cell 1.

Figure 3.10: Plots of cell outflow intensity with respect its occupancy for light traffic conditions.

3.4.2. Congested Conditions

As explained in the introduction, congestion occur when the actual road capacity C cannot handle the total demand crossing it D. In other words, congestion occurs when $C < D$. For light traffic conditions, congestion may arise when the road capacity temporary reduces owing to an accident for instance. A similar situation takes place when the total flow that has to cross a section exceeds its nominal capacity. Any of these situation leads to the generation of shock waves due to sudden changes in flow characteristics. As a result thereof, the flowing dynamics are impacted. These situations are investigated thanks to the three following examples:

- a temporary bottleneck—60 % of the nominal capacity—for light traffic conditions,
- the initial blocking of a cell followed a recovery to its nominal capacity, for light traffic conditions,
- no issue on the network, for heavy traffic condition.

All these three examples are tested on the section featuring a merge and a diverge so that their behavior can be assessed as well. The bottleneck conditions are applied at the system outlet located at the end of the section. Even though the outlet does not feature a cell, its capacity can vary and thereby simulate a bottleneck. A simplified model of the section is presented in the figure 3.11. Similarly to free-flow case, the behavior of the model for each case is described in two times: first its temporal behavior, and second the relation between flow and density.

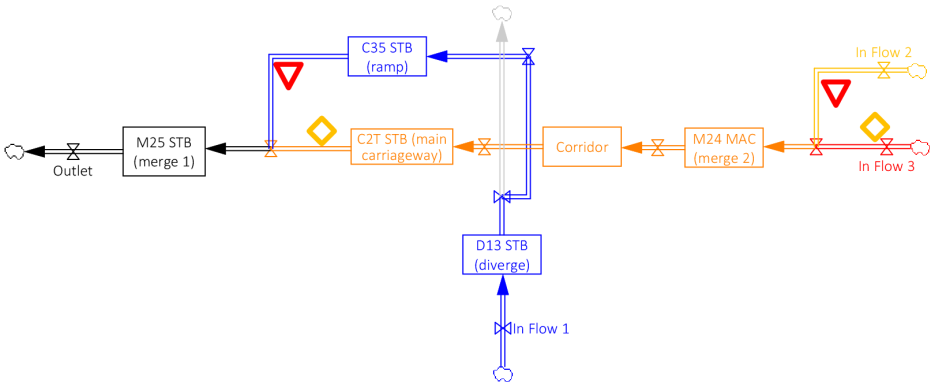


Figure 3.11: Schematic representation of the section where the validation tests in congested conditions are carried out. Diamonds represent cells that have the right-of-way, triangles the one where flow yields.

Temporary Bottleneck at the Outlet

From a quantitative point of view, the same observations as for free flow conditions can be made about the model behavior. All disaggregated and, as a result thereof, aggregated flows are non-negative and never exceeds the road capacity. The count of vehicles per OD within all the cells is always positive or nil; the only negative values taken have an order of magnitude being equal to 10^{-7} at most. They can thus be reasonably rounded to 0. Qualitatively, the crowding out of the flow arriving from the ramp can be observed. The figure 3.12 depicts the evolution of the instantaneous outflow of the merge cell 1 and of the system outlet across time. The lowest value reached by capacity of the system outlet due to the bottleneck is equal to 65 vehicles per minute. As the figure 3.6 indicates, the highest instantaneous inflow into the system is equal to 30 vehicles per minute. The highest instantaneous flow leaving the merge is thus equal to 90 vehicles per minute. However, this peak takes place when the bottleneck capacity has reached its lowest value. Fewer vehicles are then expected to leave then the merge cell; they should therefore start to queue inside it until the merge inflow is equal to its outflow. As a consequence, the composition of the merge inflow should change.

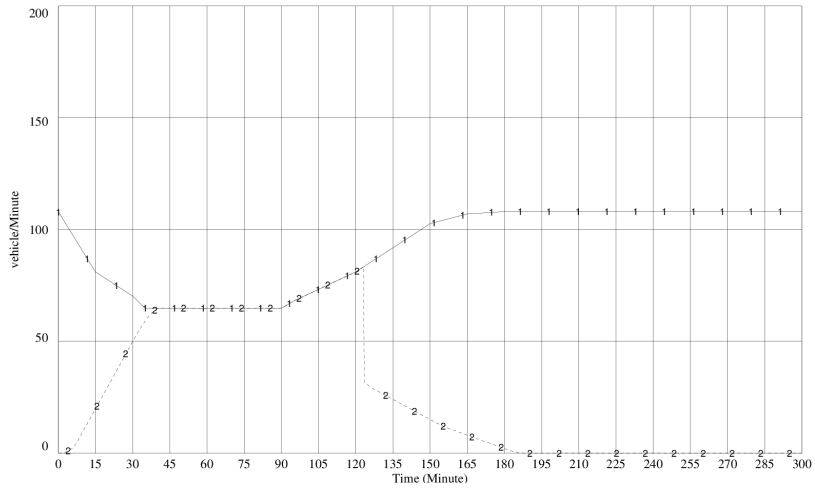


Figure 3.12: Evolution of the total instantaneous outflow of the merge 1 (dashed, labeled with 2) compared to the system outlet capacity (plain, labeled with 1) when this latter is a bottleneck.

In the figure 3.13, the cumulative inflow arriving from the ramp (labeled with 1) reveals a singular behavior compared to the two other OD flows. It can be observed that the slope, that is the flow intensity leaving the ramp, decreases. After this, a stiffer increase of the same flow, compared to the two other flows, can be observed as well. This is actually in line with the expectations. Indeed, due to the right-of-way regime at the merge, vehicles arriving from the main carriageway are allocated first to the available capacity. Remaining capacity is then allocated to vehicles from the ramp. Since the total

Table 3.3: Legend of figure 3.14. The higher the cell ID, the closer to the merge the cell is.

Cell ID	Line Style	Label	Cell ID	Line Style	Label
1	plain	1	9	dash-dot	9
2	dash	2	10	dash-double dot	A
3	em-dash	3	11	plain	B
4	dash-dot	4	12	dash	C
5	dash-double dot	5	13	em-dash	1
6	plain	6	14	dash-dot	2
7	dash	7	15	dash-double dot	3
8	em-dash	8	16	plain	4

inflow exceeds the actual outlet capacity, the ramp outflow decreases down to the remaining capacity value. As long as the outlet capacity remains bounded, queue appears and gradually spills back across the ramp. Once the road has recovered enough, the inflow of vehicles from the ramp into the merge cell increases. This is actually a consequence of queuing. Since the available capacity is fully allocated, the ramp outflow takes higher values compared to the initial profile. Finally, when the number of vehicles encompassed by a cell has become low enough, the outflow starts to follow the initial flow pattern. It can be inferred from these observations that the model correctly crowds out the flow that must yield at the merge.

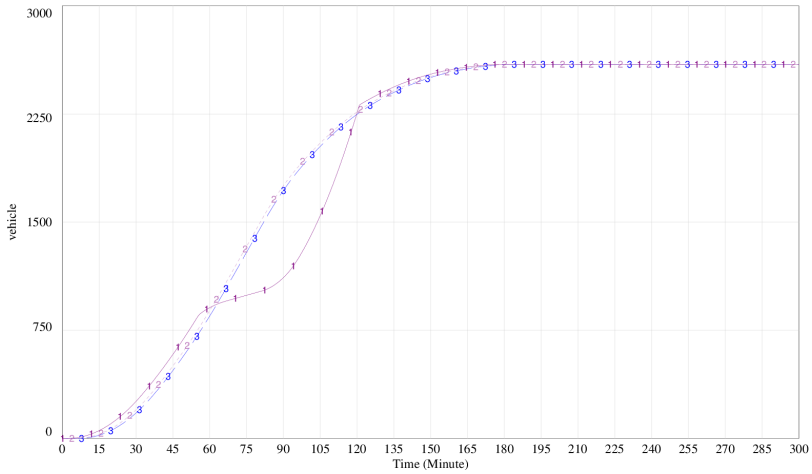


Figure 3.13: Cumulative inflows over time at the merge cell for each OD pair when a bottleneck appears in light traffic conditions. The cumulative inflow arriving from the ramp is labeled with 1. The cumulative inflows leaving the main carriageway are labeled with 2 and 3.

Because of the ramp flow crowding out, sudden variations of the intensity take place. As a result thereof, shock waves are bound to be generated and to travel backwards across the ramp. In the figure 3.14 are represented the cumulative inflows of each ramp cell where crowding out occurs. Two crucial points can be pointed up on this figure. First, the first cell stricken by the capacity reduction is the one with the highest ID, that is the cell 16. The cell ID can be retrieved from the table 3.3, which acts as a legend of figure 3.14. According to this table, the cell 16 is the ramp cell that is directly bound to the merge cell. The next cells impacted are, in this order, the cells 15, 14, 13, and so forth until the cell 1. This figure depicts then the proper spilling back of congestion backwards. Since this ramp is connected to a merge cell, this figure illustrates both backward and mixed causality regimes presented by Daganzo [17]. Indeed, the dynamics of flows having the right-of-way remains unchanged: their dynamics are still driven by conditions upstream of it. On the other hand, the characteristics of the flow that must yield evolve during the run because of the bottleneck: they are then impacted by changes that happened downstream of it.

Once the bottleneck has disappeared, the flow characteristics evolve until they match the initial

profile. The second remark that can be made on this graph is related to the average travel time. Given a vehicle count, the average travel time to clear the ramp can be approximated by computing the difference between the inflow of the first cell and the inflow of the last cell. When congestion starts to spill back, it can be seen that the travel time starts to increase due to the limited capacity allocated to the flow arriving from the ramp. The gap between the first cell inflow and the last cell inflow widens. When the bottleneck start to disappear, the gap progressively narrows down to reach its initial value. When traffic disturbance is over, the rate at which available room grows is equal to $\frac{w}{v}$, which is smaller than one. Traffic recovery is thus slower: the time required to clear the ramp does not go back to its initial value instantaneously. Based on these observations, the temporal behavior of the model may be deemed plausible.

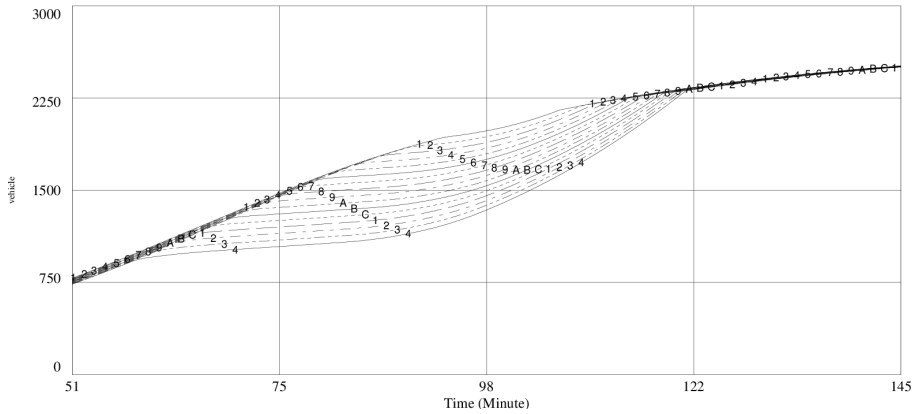
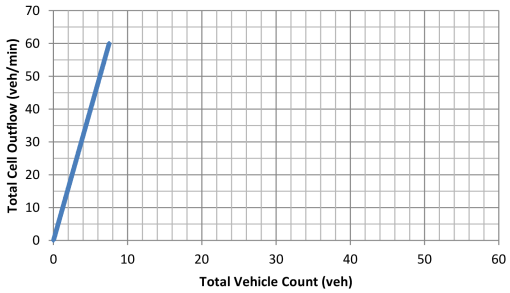


Figure 3.14: Cumulative inflow across time of each ramp cell when a bottleneck appears in light traffic conditions. The legend of this plot is detailed in the table 3.3.

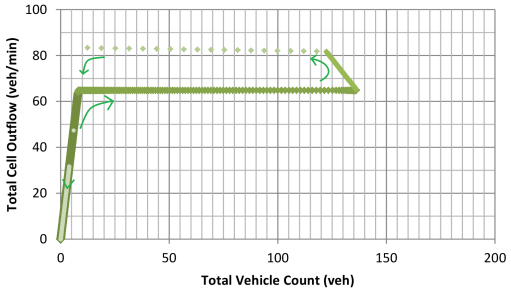
In order to validate the behavior of the model in the case of a temporary capacity decreases the scatter plots of the total outflow with respect to the total occupancy are built for three cells: the merge cell 1, located upstream of the bottleneck, one cell from the ramp and one cell from the main carriageway. The figure 3.15, shows out the resulting plots. The plot 3.15a is similar to the plots shown in the figure 3.10, to wit a perfectly fit linear relation between the intensity and the cell occupancy. This result is in line with the expectations since the flow traveling along the main carriageway is not impacted by the perturbation at the outlet. Regarding the merge outflow, the plot associated to which is 3.15b, a more complex, non-functional relation can be observed. It is possible to divide this plot into five different, functional sub-plots:

1. A linear increase, similar to the figure 3.15a;
2. A plateau, the value of which is equal to the minimal bottleneck capacity.
3. An increase of the outflow intensity which empties the cell;
4. A plateau, the value of which is equal to the flow that actually leaves the merge;
5. A linear decrease when the last flows leave the network, similar to the figure 3.15a.

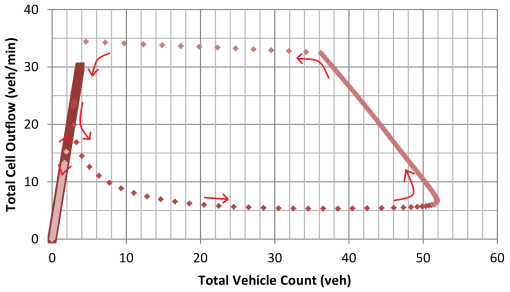
The first sub-plot matches the time period during which the network, and hence the cell, is loading. However, the outlet capacity is smaller than the merge capacity: the former thus bounds the merge outflow. When the outlet capacity reaches its minimum, the total flow leaving the merge cell no longer increases. Since the available capacity is always allocated, the merge cell outflow takes steady values as well as leads to queue formation. This is what the sub-plot 2 shows out. The sub-plot 3 indicates a outflow increase in relation to a decrease in occupancy. A careful analysis of this sub-plot shows that this sub-plot is actually belonging to the MFD associated with this flow. In the sub-plot 4, the cell unloads at a steady rate, the value of which is lower than the outlet capacity. This plateau appears because progressive recovery of the bottleneck capacity to its initial value, combined with the progressive decrease of the inflow arriving from the merge carriageway. The fifth sub-plot shows that the cell



(a) Road cell from the main carriageway.



(b) Merge cell 1. Each hue identifies an analyzed sub-plot.



(c) Road cell from the ramp. Each hue identifies an analyzed sub-plot.

Figure 3.15: Plots displaying the evolution of the total cell outflow with respect to its total occupancy for light traffic conditions and a bottleneck at the system outlet. Arrows indicate the reading direction of the plots.

unloads according to the MFD associated with its outflow. Based on all these observations, it can be concluded that the merge outflow behaves as expected.

The last plot, associated with a cell from the ramp and displayed in figure 3.15b, can be divided into four distinct sub-plots as well:

1. A linear increase, similar to the figure 3.15a;
2. A two-step decrease of the outflow.
3. A two-step increase of the outflow;
4. A linear decrease when the last flows leave the network, similar to the figure 3.15a.

The first sub-plot shows the cell loading and the associated and expected increase of the cell density. The second sub-plot is singular because of the stiff decrease that can be observed. This decrease is actually related to the crowding out of the ramp outflow. The first and second parts of the third sub-plot are actually identical to the third and fourth ones of the merge cell. The same observations as for the sub-plot associated with the merge cell can be made on this one, to wit:

- the point where the sub-plot 3 intercepts the sub-plot 2 is the one predicted by the MFD 2.3,
- the first part of the sub-plot belongs to the same MFD,
- the slight increase observed in the second part of the sub-plot is caused by the temporal evolution of the capacity available for the outflow arriving from the ramp,
- the outflow never exceeds the cell capacity.

Based on all these observations, the ramp cell behavior can be deemed valid. As a consequence of all the previous analyses, the model properly models congestion caused by a bottleneck for light traffic conditions.

Closed Outlet and Recovering

For this second case, an initial gridlock is generated from the outlet: no vehicle can leave the system during two hours. After this, the capacity recovers to its nominal value after 30 minutes. Similar qualitative observations can be made regarding the model: all the OD flows are positive or nil; the total flow entering a cell never exceeds its capacity; and the lowest value taken by cell occupancy are around -10^{-7} and can thus be rounded to 0. From a qualitative point of view, the model behavior is analyzed by means of two same plots as before: time-based, and density-intensity plots. The figure 3.16, depicts the cumulative inflows arriving at the merge 1. Three large plateaus can be observed at the beginning of the run. Since the plots are cumulative inflows, a plateau indicates that the merge inflow is equal to 0. It can then be inferred that no more vehicles enter the cell once it is full, and the queue that appeared in the cell spills back upstream on both ramp and main carriageway, and finally throughout the network.

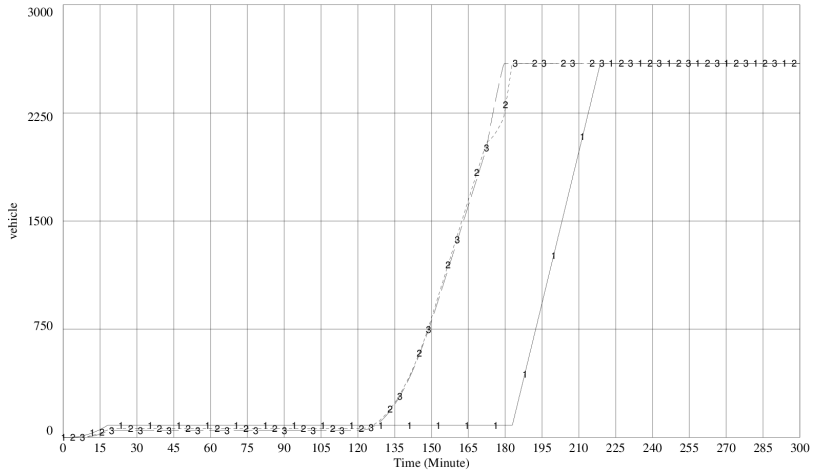


Figure 3.16: Cumulative inflows over time at the merge cell 1 for each OD pair when gridlock takes place in light traffic conditions. The cumulative inflow arriving from the ramp is labeled with 1. The two cumulative inflows leaving the main carriageway are labeled with 2 and 3.

A notable difference between the cumulative inflow arriving from the ramp and the two coming from the main carriageway can be observed. Indeed, the first flow remains still longer than the two other ones. This illustrates then the complete crowding out of the flow arriving from the ramp due to the right-of-way regime at the merge. Indeed, queue has spilled back through both ramp and main carriageway because of the closed outlet. When this recovers to its nominal capacity, each cell tend to send the maximal number of vehicles possible. Because of the right-of-way rule, capacity is, as expected, allocated first to the flow arriving from the main carriageway. As a consequence, vehicle flow coming from the ramp leaves the system later, once sufficient capacity is available at the merge. A second, less intense, crowding out can be observed between the flows labeled 2 and 3. Because of congestion spill back, the queue reaches the merge cell 2, where flows 2 and 3 are combined. The figure 3.17 present the cumulative inflows of these two flows at merge 2. The right-of-way configuration of which is the same as the merge cell 1, as shown in the figure 3.11. The flow 2, arriving from the ramp , must yield to vehicles from flow 3. Since the merge 2 is quite distant from the merge 1, the crowding out is less intense at the former merge. These two crowding out thereby reveal that allocation process therefore works fine. Regarding the FIFO logic, it can be observed that the first vehicles leaving the system are the one from flow 3, which have the right-of-way all along the road section. Because of the lesser crowding out at merge 2, vehicles from flow 2 leave the system after vehicles from flow 3. Finally, because of its total crowding out, vehicles from flow 1 are the last to exit the merge and the system. The leaving sequence is thus correct.

Similar results can be observed on the cumulative inflow of all the cells of the ramp that must yield at the merge, displayed in the figure 3.18. None of flows cross each other except at the beginning and the end of the run: the FIFO rule is well respected throughout the ramp. Besides this, perturbation caused by the flow crowding out properly occurs first at the cells that are the closest to the merge and then propagates backwards. Moreover, it should be outlined that this ramp is actually connected to a

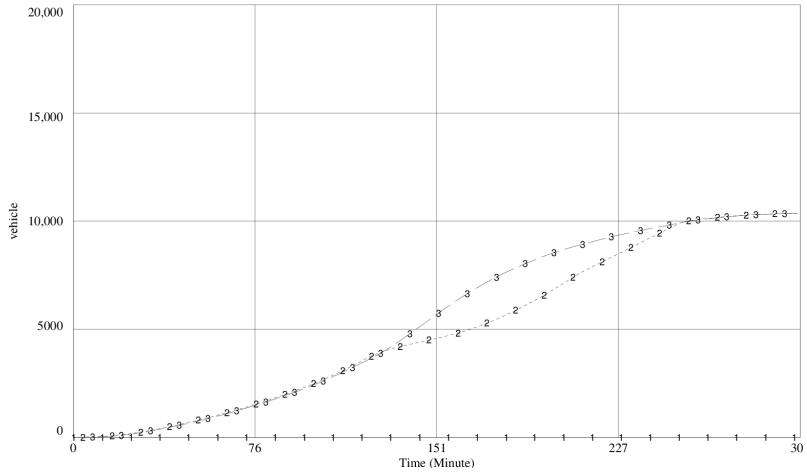


Figure 3.17: Cumulative inflows over time at the merge cell 2 for each OD pair when gridlock takes place in light traffic conditions. The cumulative inflow arriving from the ramp is labeled with 2. The cumulative inflow leaving the main carriageway are labeled with 3.

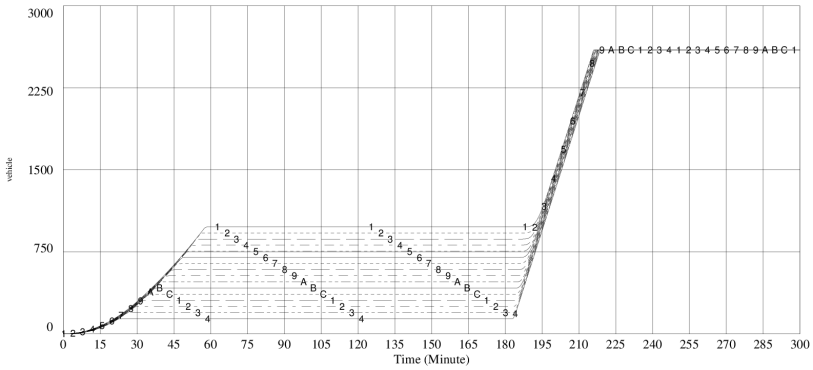


Figure 3.18: Cumulative inflow across time of each ramp cell when a gridlock takes place in light traffic conditions. The legend of this plot is detailed in the table 3.3.

diverge cell where two distinct flows are separated. Because of the congestion spill back, the diverge cell should be congested as well and prevent any flow from leaving it. The figure 3.19 presents the cumulative outflows of the diverge cell connected to the ramp. It can then be seen that none of the flows leave the cell actually leaves it when gridlock occurs. This means that no vehicle leaves the diverge cell when one of its branches is blocked. This behavior is actually expected since it is a key building hypothesis of the diverge cell described by Daganzo [17]. As a consequence of these different points, the temporal behavior of the model can be considered as plausible.

To conclude over the correct behavior of the model, the scatter plot of the three same cells as the one chosen for the first case of congestion are drawn and represented in the figures 3.20a to 3.20c. The plots 3.20a and 3.20c present a similar shape and can be defined as the combination of two sub-plots:

1. A sub-plot describing the evolution of the outflow when the outlet is blocked.

2. A sub-plot showing the evolution of the outflow from the time instant at which the outlet start to recover.

The plots 3.20a and 3.20c have the same layout. The following analysis is carried out for the main carriageway cell, but holds true for the ramp cell as well. The first sub-plot depicts the exact MFD associated to the cell outflow. The plateau value is actually equal to the maximal intensity that enters each cell. Since traffic load on the system is light, the maximal flow intensity is equal to 60 (30 for the ramp cell) vehicles per minute, as presented in the figure 3.6. As long as traffic can leave the cell, the flow intensity never exceeds 60 vehicles per minute for the ramp cell. When congestion spill back has

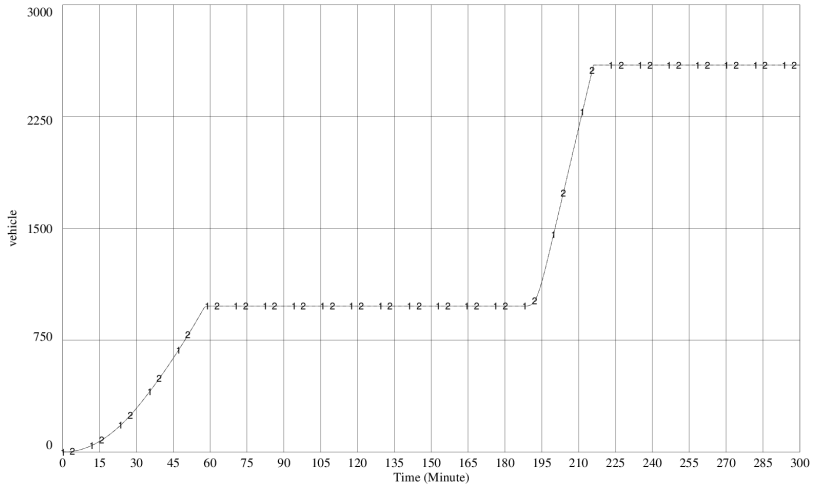


Figure 3.19: Cumulative outflow across time of the diverge cell connected to the ramp when a gridlock in light traffic conditions. The flow entering the ramp is labeled with 2. The flow labeled with 1 arrives from the same inlet as flow 2 but takes the other branch of the diverge cell.

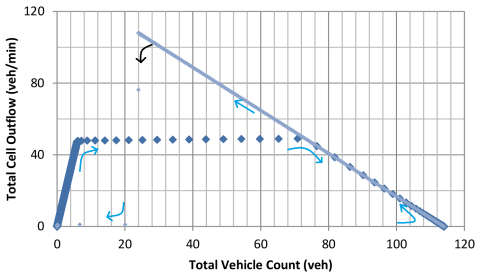
reached the first cell downstream of the cell analyzed, less capacity becomes available for outbound vehicles. The cell outflow is therefore equal to the flow the cell downstream can receive, which decreases in relation to its occupancy as expected. The second sub-plot follows again the embedded MFD, but does not follow exactly the first sub-plot. The smooth evolution is caused by the progressive recovery of the bottleneck. The increase beyond the plateau value of the first sub-plot is expected since queue has spilled back in the cell and available capacity in the next cell downstream is always fully allocated. As a consequence, the outflow overshoots the plateau of the first sub-plot. The highest value reached is close to 108 (70 for the ramp cell) vehicles per minute, which is equal to the lowest capacity value. Some isolated points can be observed and may have been caused by numerical errors.

For the plot 3.20b, the analysis is even more straightforward. The first sub-plot is actually matching the x-axis. It is correct since the merge 1 is directly connected to the system outlet. As a result thereof, no vehicle leave the merge cell and vehicles start to queue into the cell. It can be observed that the number of vehicles does not exceed 190, which is equal to the cell size. The second sub-plot looks like a neat MFD, similar to the ones depicted by the first sub-plots of figures 3.20a and 3.20c. It should be underlined though that the outlet is not a cell. The shape observed on the sub-plot 2 stems hence from the progressive recovery of the outlet capacity. For a stiffer capacity recovery, indicated in the figure 3.21 this gradual increase is not shown out. Whichever the type of recovery, it can be concluded that available capacity is well fully allocated to the outflow. Based on all the observations and analyses led in this subsection that the model behavior is valid when it reproduces an initial gridlock and its recovery.

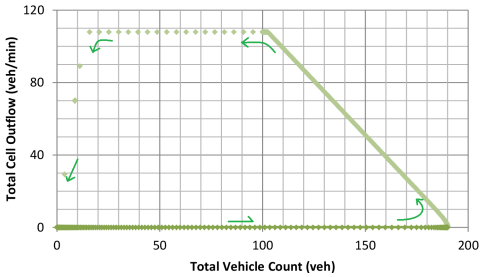
Important Traffic Load

The last case where congestion arises is when traffic crossing the network is quite intense and no disruption takes place on the network. The demand pattern at the system inlets is the one labeled with 2 in the figure 3.6. The pattern is identical, but is more spread across time, and the traffic peak is equal to 80 vehicles per minute. In such situation, the total traffic load may not be supported by the network and thus the road cells. Similarly to the previous cases, the different flow between cells are always positive or nil. The lowest values recorded for cell occupancy are about 10^{-8} and may be then reasonably rounded to 0. Else, the occupancy values are always greater or equal to 0. The flow propagates then properly across the network.

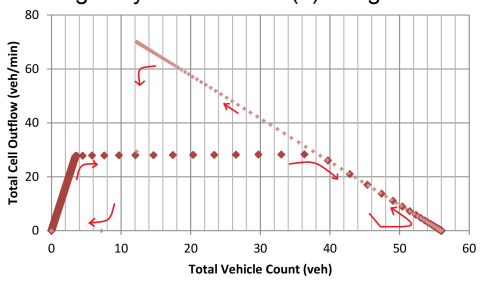
From a qualitative point of view, the same conclusions as before can be drawn regarding the temporal behavior of the model. First, as the figure 3.22 shows, the cumulative inflows per OD pair at the same merge cell present a similar pattern as the figures 3.13 and 3.16. The flow 1 arriving from the



(a) Road cell from the main carriageway.



(b) Merge cell 1.



(c) Road cell from the ramp.

Figure 3.20: Plots displaying the evolution of the total cell outflow with respect to its total occupancy for light traffic conditions and a gridlock at a system outlet. For all the figures, the first sub-plot evoked in the analysis is represented with a dark hue. The second sub-plot is depicted by means of a clearer hue. Arrows indicate the reading direction.

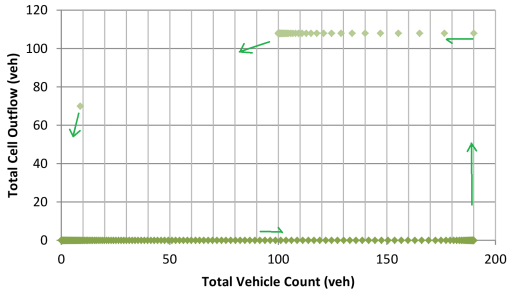


Figure 3.21: Plots displaying the evolution of the total merge 1 outflow with respect to its total occupancy for light traffic conditions, a gridlock outlet at the beginning of the run and a direct recovery to its initial capacity. The first sub-plot evoked in the analysis is represented with a dark hue. The second sub-plot is depicted by means of a clearer hue.

ramp at the merge 1 is properly crowded out by flows 2 and 3 at the merge. Similarly, the flow 2 is crowded out by the flow 3 at the merge 2. However, this one is less intense than the crowding out at merge one because of the temporal pattern of heavy demand. At merge 2, capacity available for vehicles arriving from the ramp is roughly equal to 25 vehicles per minute when the flow intensity associated to OD flow 3 peaks at 80 vehicles per minute. The resulting flow intensity is then equal to 105 vehicles per minutes, that is to say the lowest capacity of the road section. When the combined flow reaches the merge cell 1, capacity available for the flow arriving from the ramp is therefore smaller. As a result thereof, the crowding out of te ramp outflow is almost total. Regarding the cumulative inflow of the ramps cells, similar points can be outlined on the figure 3.23. Perturbations strike first the cells with the highest ID, that are the ones closest to the merge cell and two distinct plots never intersect during the run. FIFO rule is hence respected and the perturbations propagate well backwards. The temporal behavior of the system is therefore correct.

Similarly to the three previous traffic situations, the density-intensity plots of the same cells are graphed and shown on the figures 3.24 and 3.25. In the figure 3.24 are represented the plots for a normal road cell from the main carriageway. For these two plots, the relation displayed is functional and expected. The plateau observed on the figure 3.24b of the merge cell is equal to the outlet capacity. For these cells, the model behavior can be deemed valid.

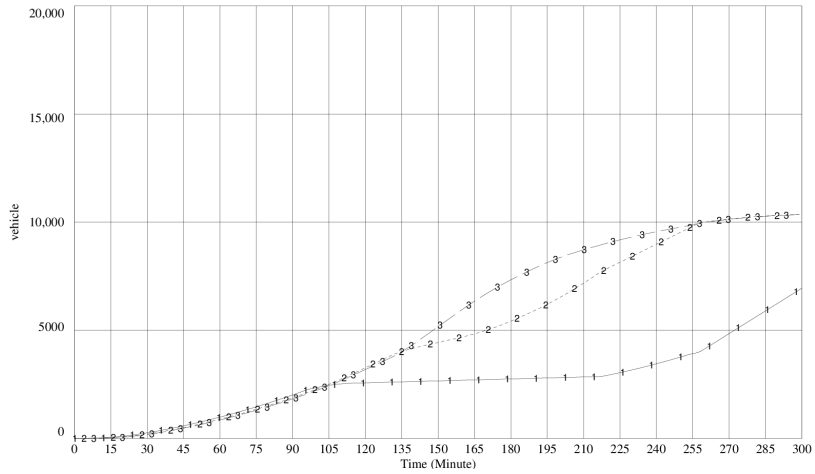


Figure 3.22: Cumulative inflows over time at the merge cell 1 for each OD pair and for dense traffic loads. The cumulative inflow arriving from the ramp is labeled with 1. The two cumulative flow coming from the main carriageway are labeled with 2 and 3.

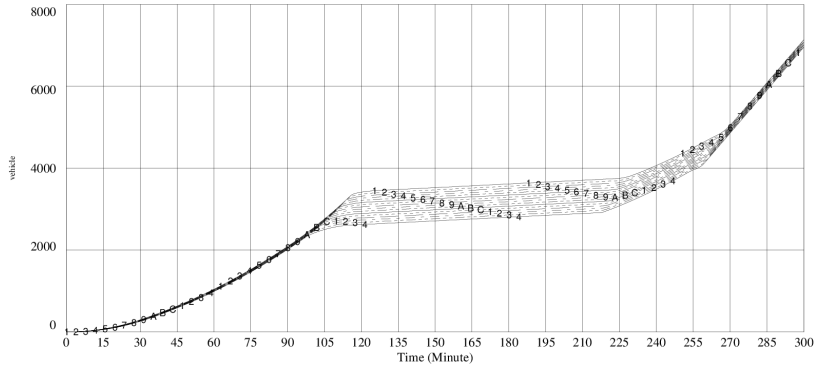
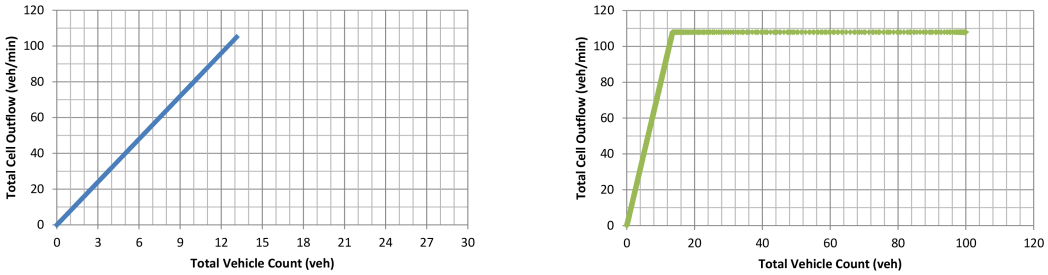


Figure 3.23: Cumulative inflow across time of each ramp cell for heavy traffic conditions. The legend of this plot is detailed in the table 3.3.

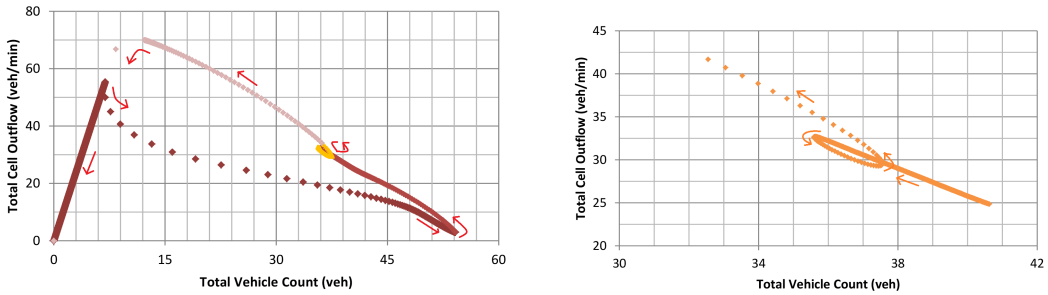
On the other hand, the plot associated with the ramp cell, shown in figure 3.25a, presents a more notable pattern. It globally looks like the figure 3.15c. The crowding out of the flow is well depicted, and the total outflow never exceeds the ramp capacity, which is equal to 70 vehicles per minute. For a high occupancy, the behavior shown is sharper than on figure 3.15c. This is actually a consequence of the high traffic flows that are going through the network. Since no perturbation takes place on the infrastructure, the global shape of the plot is a result of the progressive evolution of the flow intensity at the inlets. The only notable difference comes from the sub-plot indicated in orange. A zoom on this is presented in figure 3.25b. This pattern seems to indicate that traffic hysteresis is reproduced by the model. The hysteresis in traffic can be described as the delay that exist between the drivers' reaction and the actual state of traffic [47]. In other words, for a given flow density, a discrepancy may exist between the flow measured when network loads and the one measured when the same network unloads.

Hysteresis in traffic flow is well documented in recent literatures [20; 32; 33; 41; 47; 54; 60]. In Knoop et al. [48, p. 238], hysteresis is a "result of macroscopic queueing and spillback processes". Observing such behavior in the plot density-intensity of the ramp cell sounds plausible. However, hysteretic behavior is not accounted for in the LWR model. As a consequence, the loop observed on the figure 3.25a is likely to have been caused by numerical errors while computing the ramp cell outflow. In spite of this small part of the plot, it can be concluded that the model behavior gotten for heavy traffic conditions is valid. However, some investigation needs to be made to understand the reason why this loop appears.



(a) Road cell from the main carriageway. (b) Merge cell 1.

Figure 3.24: Plots displaying the evolution of the total cell outflow with respect to its total occupancy for heavy traffic conditions.



(a) Complete run. (b) Zoom on the sub-plot indicated in orange.

Figure 3.25: Plots displaying the evolution of the total outflow of a ramp cell with respect to its total occupancy for heavy traffic conditions. Arrows indicate the reading direction of each plot.

3.5. Influence of Uncertainty

In the previous section, model and cell parameters have been assumed as constant, which may not be true in reality. For instance, the actual road capacity may differ from its theoretical value because of weather conditions, an accident or its wear and tear caused by traffic. The sensitivity of the model for small variations—$\pm 10\%$ of the initial value—of each parameter needs then to be assessed *ceteris paribus*. As explained in the section 3.3, the value of the time step δt cannot be changed since it determines the number of cells of the model and hence its whole structure. Besides cell capacity, the model sensitivity is explored for the shock wave speed and the cell size. Since the later depends on the jam density, the sensitivity of the model to small variations of the jam density can be determined by testing the model for small changes in the cell size. Finally, the last parameter that can be of influence for the system is the traffic level. Due to the high number of cells and corridors in the model, the sensitivity and uncertainty analysis is carried out on another part of the model. The effect on system variables of small variations of these different parameters are recorded for the cell and corridor inflows and outflows represented in the figure 3.26. Sensitivity outcomes differ from the previous ones as their plot may have a variable thickness. Thanks to this representation, it is possible to determine confidence intervals that indicate the area where a given percentage of runs fits in it. Given a model parameter, the wider this area, the more sensitive to this parameter the model is. Based on the sensitivity outcomes, potential policy leverages and critical factors can be highlighted.

Unlike the previous section, the different graphs that are to be presented are instantaneous graphs. Cumulative plots cannot be used for displaying the results of sensitivity runs. The traffic loads entering the system follow the second demand pattern plotted in the figure 3.6. The reference run to which sensitivity results are compared to is described in the figure 3.27. The behavior shown is correct since the flow 3 actually yields at the merge cell. Because of the heavy traffic levels, queue builds up in the ramp. When it reaches the diverge cell, the two other flows that take the main carriageway are bounded as well. The three flows have the same intensity since they arrive from the same inlet and therefore are not delayed between each other.

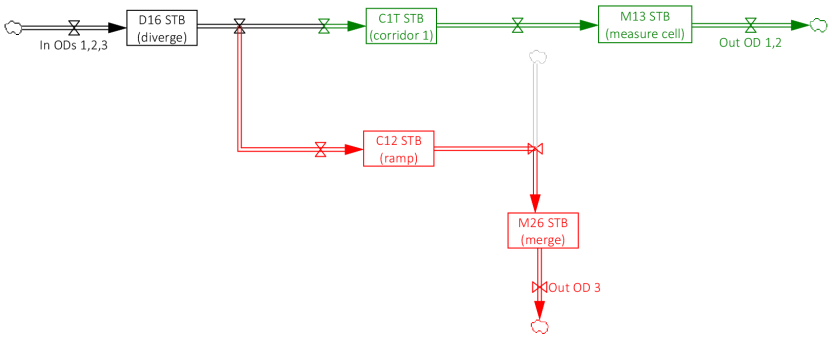


Figure 3.26: Schematic representation of the section where the sensitivity and uncertainty tests are carried out.

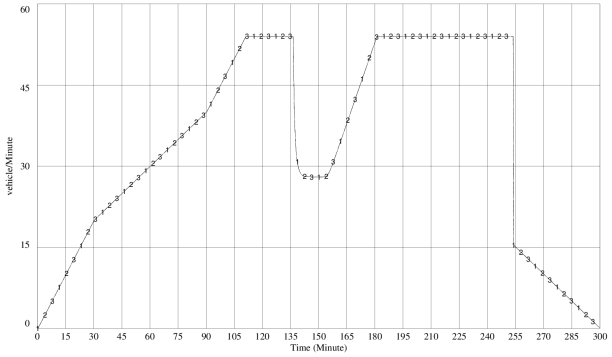


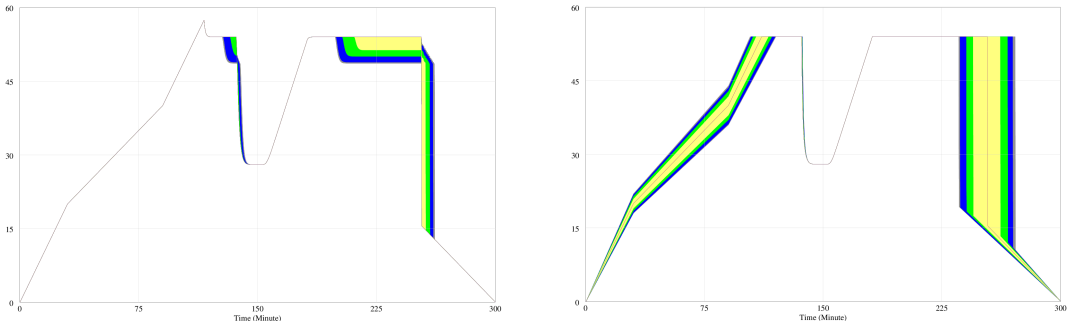
Figure 3.27: Temporal evolution of the diverge outflow for heavy traffic congestion. The flows staying on the main carriageway are labeled with 1 and 2. The flow taking the off-ramp at the diverge is labeled with 3. This plot is the reference run for sensitivity and uncertainty analyses.

Among these parameters, three are found to have some influence on the model: the cell capacity, whichever type, the level of demand and the shock wave speed. This can be seen on the figures 3.28a, 3.28b and 3.29. More precisely, the model is numerically sensitive to these variables. The colored bands surrounding each plot indicates the confidence bounds of the sensitivity runs. It can be read as follows:

- The yellow bands indicates the bandwidth wherein 50 % of the runs fall into;
- The green bands indicates the maximal values between which 75 % of the runs are encompassed
- The green bands indicates the maximal values between which 95 % of the runs are encompassed
- The grey bands indicates the interval to which belong all the runs.

The wider the bands, the more sensitive the model is to this variable. The sensitivity of the model is the greatest for the cell capacity and the demand level. For the shock wave speed, the sensitivity is lesser, but can be deemed as significant, especially when network unloads. The two other ones, the free flow speed and the cell size, are found to have a very limited and localized influence on the model.

The sensitivity of the model to the capacity is actually a consequence of its structure: the cell capacity indeed bounds the flows that it can either sent or receive. Smaller values therefore impacts the flows that can be received or sent by a cell. This parameter is actually ambivalent. On the one hand, it can be used as a policy leverage. Increasing the capacity of a road can be done by building an extra lane on the carriageway. this would enable higher traffic loads on this section. On the other hand though, road capacity is also influenced by external parameters such as weather or wear. Even though maintenance can mitigate the impact of wear, the effects of climatic conditions cannot be easily dealt with. The level of demand entering the network is, from a policy-maker point of view, another potential policy leverage.



(a) Sensitivity to cell capacity variations.

(b) Sensitivity to system inflow variation.

Figure 3.28: Impact of small variations of model parameters on the model behavior. The width of colored band brings out the sensitivity of the model to these small variations.

The current level of demand for an OD pair depends not only on travelers' preferences, but also on the transportation offer. This would then be influenced by policies influencing the public transportation system. But, as explained in the previous paragraph, the model is only numerically sensitive to these parameters. For all the parameters to which the model is sensitive, the qualitative behavior of the model remain unchanged. Using these variables as adequate policy leverages may not be relevant then.

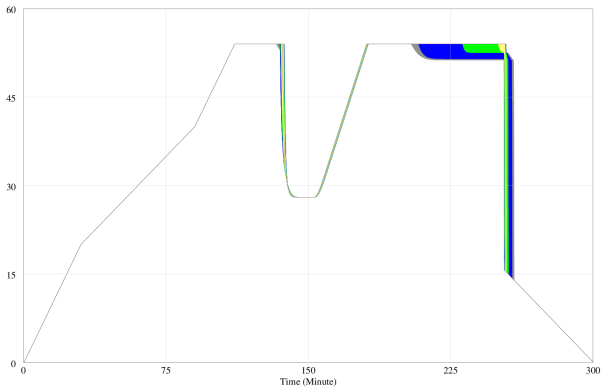


Figure 3.29: Impact of small variations of the shock wave speed on the model behavior. The width of colored band brings out the sensitivity of the model to these small variations.

The shock wave speed has been proven to be a sensitive parameter for the model. It is analyzed apart from the two other parameters because of the uncertainty of this value. As explained in the section 3.3, the shock wave speed that has been chosen in the model was set up to 18 km/h, or 0.3 km/min [25]. The actual value for shock wave speeds may actually widely differ from the one implemented. As a result thereof, a deeper analysis of the variable is carried out. Its range is equal to $[0, v_0]$, as the shock waves are either not existing or exist, but cannot travel at faster speeds than the free flow speed [16]. The figure 3.29 shows out the effect of small changes of the shock wave speed on the model behavior. It stems from these observation that this speed is influential in the model: the width of the range possible for the outcomes is quite broad. This influence is actually important regarding the network unloading—right-hand side of the figure. The figure 3.30 describes the theoretical influence of the shock wave speed on the MFD of a cell. The quantity $\frac{k_j}{\frac{1}{v}+\frac{1}{w}}$ represents the ratio of the jam density divided by the harmonic average of the free flow speed v and the shock wave speed w.

Two cases are distinguished: shock wave speeds greater than 0.3 km/min, and shock wave speeds smaller than 0.3 km/min. The section on which the analysis is performed is the one introduced at the beginning of this section in the figure 3.26. For high shock wave speeds (green curve), it can be seen that the density from which the cell outflow start to decline is higher. Besides this, the shape of the MFD remains the same. It can then be inferred that the general behavior of the model would not be

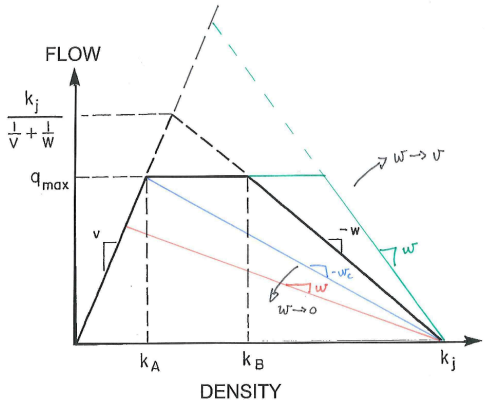


Figure 3.30: Theoretical impact of the shock wave speed on the MFD of the CTM. The figure is taken from Daganzo [16]

Table 3.4: Value of w_c for the different cells of the model. The jam density k_j is equal to 150 vehicles per km per lane.

C (veh/(km.lane))	v_0 (km/min)	2	1.5	1
33		x	x	0.28
35		x	0.28	x
36		0.27	x	x
38		x	0.30	x
40		0.31	x	x

impacted by higher values of w. The figure 3.31a presents total inflow of a road cell. Based on this graph, it can be seen that the global model behavior remains the same: the three plots showing the cumulative total outflow of the diverge cell. The three plots are almost coincident. This result is thus in line with theoretical expectations.

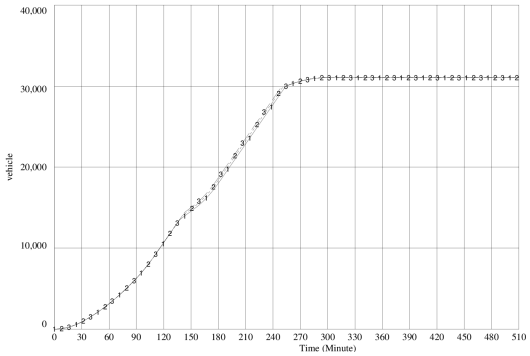
For lower shock waves speeds two cases occur: the case where the quantity $\frac{k_j}{\frac{1}{v}+\frac{1}{w}}$ is equal to the cell capacity—blue curve on the figure 3.30—and the case where this quantity is lower than the capacity—red curve on the figure 3.30. In the former case, the flow properties directly change when the flow density reaches its critical value. Let w_c be the critical value from which the MFD of a cell changes, its expression is the following[4]

$$w_c = \frac{C \cdot v_0}{k_j \cdot v_0 - C} \tag{3.1}$$

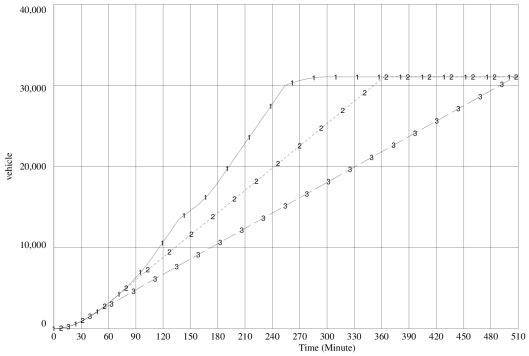
The table 3.4 presents the critical values for the different cells parameters of the model. It can be seen that the value chosen for w is equal to the critical value of the merge and diverge cells with a free flow speed equal to 120 km/h, and for the road cells limited to 90 km/h. When the shock wave speed is even lower, the maximal flow intensity decreases and is reached for even lower densities. In the meantime, the intensity decreases slower when the density increases. Since the shock waves propagates slower, the downward slope of the MFD tends to become flatter, which means that the total flow intensity is bound to be almost steady whatever the value of the flow density, but at a rate below the cell capacity.

The figure 3.31b shows out the impact of lower shock wave speeds on the total outflow of the same diverge cell. It can be seen that lower shock wave speeds actually impacts the behavior of the model. The cumulative outflow of the diverge cell becomes linear. Lower shock wave speeds are therefore leading to steadier flow across time. However, the time required to empty the network becomes longer for lower shock wave speeds. Even though out of the section chosen for exploring the sensitivity of the model, a last word is to be made on the impact of the changes on the merge 1 of the figure 3.11. Indeed, as it was presented in the section 3.4, a significant crowding out takes place there when traffic

[4]See Appendix C for the proof.



(a) Higher values of the shock wave speed. The curve associated with the reference case (w = 0.3 km/min) is labeled with 1. Curves labeled with 2 and 3 are gotten for respective values of w equal to 0.5 km/min and 1 km/min



(b) Lower values of the shock wave speed. The curve associated with the reference case (w = 0.3 km/min) is labeled with 1. Curves labeled with 2 and 3 are gotten for respective values of w equal to 0.15 km/min and 0.1 km/min

Figure 3.31: Analysis of the impact of the shock wave speed on the cumulative outflow of the diverge cell from section 3.26 across time, for heavy traffic conditions.

is heavy. It is then deemed appropriate to see what are the effect of lower shock wave speeds on the flow crowding out.

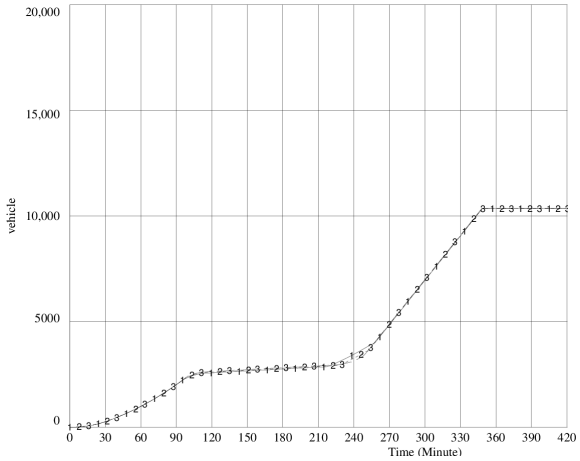
On the figure 3.32a, the same conclusions as the ones drawn from figure 3.31a: the system behavior is insensitive to higher values of the shock wave speed, crowding out still persists. On the other hand, interesting results can be observed on the figure 3.32a. Lower values for the shock wave speed prevent the flow arriving from the ramp to crowd out. However, too low values leads to a longer time required to empty the network. Based on these observations, it can be concluded that behavior of the model is sensitive to low values of w. These results are actually crucial for policy-making. As the equation 2.4, the shock wave speed depends on the ratio of the sudden change in intensity over the change in density. These two variables are related thanks to the fundamental diagram, it can thus be inferred that the shock wave speed depends only on the flow density. A potential policy would consist in avoiding the apparition of discontinuities in the flow density so that shock waves may be prevented from being generated. In this sense, changing speed limitations may be an appealing policy around critical sections. When the total flow at a bottleneck reaches a predefined threshold over a specific network, speed limitation may be automatically reduced upstream of it so as to guarantee a continuous and steady flow intensity, at a cost of a longer travel time. If a dynamic speed limitation cannot be set up, the free flow speed upstream of and at the bottleneck can be definitively be lowered.

3.6. Policy Analysis

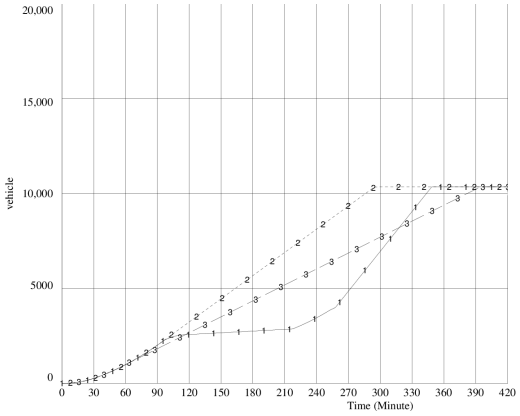
In the previous sections, the model has been shown to be valid and realistic, and policy leverages identified. In this last section, a basic demonstration of how policy analysis can be carried out with the model is to be displayed. The range of traffic-related policies available for policy-makers is wide. It is possible to distinguish two different, but non-exhaustive categories of transport policies: A first category encompasses capacity-based policies, the objective of which consists in increasing the capacity of road sections in order to increase their vehicle throughput. Two sub-categories can be distinguished

- definitive increase, for instance by adding extra lanes or by upgrading existing infrastructure, at it was done for the southern section of the A4 in the Netherlands, between the Belgian border and the A29.
- temporary increase, for instance during rush hours. An example of such policy is the use of the emergency stopping lane as a normal lane on the A13 in the Netherlands along Delft.

Besides these exist speed-based policies. Unlike capacity-based, these policies aims at reducing the flow speed and therefore prevent the creation of traffic shock waves when an accident or queuing



(a) Higher values of the shock wave speed. The curve associated with the reference case (w = 0.3 km/min) is labeled with 1. Curves labeled with 2 and 3 are gotten for respective values of w equal to 0.5 km/min and 1 km/min



(b) Lower values of the shock wave speed. The curve associated with the reference case (w = 0.3 km/min) is labeled with 1. Curves labeled with 2 and 3 are gotten for respective values of w equal to 0.15 km/min and 0.1 km/min

Figure 3.32: Analysis of the impact of the shock wave speed on the cumulative inflow arriving from the ramp at merge cell 1 from figure 3.11 across time, for heavy traffic conditions.

appears at an off-ramp. Again, these policies can be divided into two categories:

- definitive decrease, as it was done for the Boulevard Périphérique around Paris. The speed was lowered from 80 km/h to 70 km/h in 2014.
- dynamic decrease, for instance around Rotterdam or Antwerp ring roads. During peak hours, the speed is lowered and increase to its initial value once traffic situation has become lighter.

Any policy that falls into one of these categories tries to change the capacity of the transportation system.

Instead of changing the capacity of the system, transportation policies can aim at optimizing its use, that is to say promoting the use of different routes or different modes. Imposed route choice can be a first potential solution to cope with congestion over arterials by rerouting traffic upstream of it. Two types of rerouting can be distinguished:

- static routing, in order to steer clear from a bottleneck. For instance, traffic arriving from Belgium and going to Amsterdam tends to be rerouted via Utrecht in order to limit traffic over the A13 or the ring of Rotterdam. These two roadways are actually important bottlenecks of the Dutch highway network.
- dynamic routing, in case of an extreme event had occurred, such as an accident, or if traffic on a given route tends to be quite dense. In the Netherlands, this is done by indicating real-time travel time to an interchange for two—or several—alternative routes.

Even though useful for preventing dire congestion, it may not be sufficient to reduce enough the traffic loads on the road network. Incentivizing alternative modes can be then a relevant alternative to divert road-based traffic. This can be done by two methods:

- subsidizing alternatives, such as carpooling, by diminishing taxes for drivers and passengers; or public transports, by diminishing subscriptions for specific users. Off-peak discounts that are proposed by the Dutch railways service is an example of a potential policy that incites travelers to adapt their departure time.
- increasing the cost of road-based traffic so as to make it less attractive. This can be achieved by developing deterring parking costs or setting up a urban toll inside a specific area. Urban toll

policies were recently implemented in Beijing or London in order to deal with the increase of traffic that was caused by the Olympic games.

In order to determine which policy or combination of policies may yield interesting results in the long run, tests are carried out on traffic models. Recommendations for policy-makers are drawn from the analysis of the model outcomes. With the current model though, the range of testable policies is quite narrow. First, the model only reproduces the physical propagation of traffic flows for predefined OD pairs for which one single route has been modeled. As a result thereof, routing or economic policies cannot be tested. In the case of the pair Brussels-Antwerp though, two routes were designed. However, the conclusions that can be drawn are somewhat straightforward. A rough glance at the current configuration indicates that the most interesting policy consists of rerouting the traffic between Brussels and Antwerp through Strombeek-Bever because the flow crossing this interchange need not yield while crossing the network. Regarding the pairs Antwerp-Brussels, conclusions may be irrelevant since the sections that are bound to be congested are too short to properly assess the efficiency of a choice over the other. As a consequence, no optimizing—influencing the route choice—policy can be tested with the current model. The only remaining policies are hence infrastructure-based policies.

Because of the model structure, any capacity-based policy can be easily tested. Whatever its temporal character—definitive or temporary—capacity of a cell or a corridor can be adapted by changing the number of lanes, or directly the capacity in the case of an outlet. Definitive change of speed limit can be straightforward to include as well. It can be done by increasing the number of cells of a corridor for instance, but this may impact its total length. This only holds true if the policy is an increase of the free flow speed. In the case of a speed reduction, changing the number of cells needs not be done. Indeed, if the distance cleared by a cell is shorter than the cell length, then flow characteristics within the cell become heterogeneous and leads to a smoother behavior [16]. However, the seminal works from Daganzo do not explain how to model changes of the free flow speed. As a consequence, speed-based policies are discarded from this study. The policy proposed is hence an increase of the infrastructure capacity around a bottleneck. This is then executed on the same section where validation tests have been carried out, showed in the figure 3.11.

The objective of this policy is to add an extra lane at the merge 1 and the system outlet, so that more vehicles can leave the system. However, several ways of adding this extra lane exist, and would lead to different merging dynamics. Indeed, the priority factor of a branch at the merge depends on its relative capacity. Adding an extra cell might lead to a more intense crowding out of the ramp cell if the lane is added to the main carriageway. As a consequence, the two policies tested are the following:

1. An increase of the merge, the outlet and the last cell of the main carriageway capacities. The outcomes are labeled with 2 in the figures thereafter.

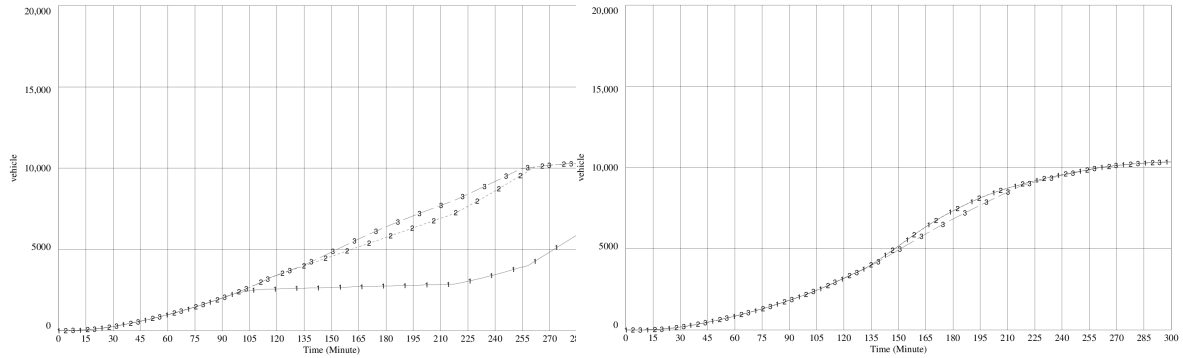
2. An increase of the merge, the outlet and the last cell of the ramp capacities. The outcomes are labeled with 3 in the figures thereafter.

The impact on the cumulative inflows of the merge cell are represented in the figures 3.33a for the flow arriving from the ramp, and on figure 3.33b for the flow arriving from the main carriageway.

The results of each policy is compared to the base case, which is represented by the plain line labeled 1. It can be seen from these graphs that adding a new lane around the merge cell is an efficient policy in order to reduce the impact of congestion. This can be seen especially on the flow arriving from the ramp: thanks to both policies, no more plateau can be observed on the cumulative inflow. Allocating an extra lane to the ramp is actually to most efficient policy to reduce the effect of crowding out on the ramp. Indeed, allocating more capacity to the ramp yields a evener allocation of the capacity between the two flows.

3.7. Reflection on the Model

Throughout the previous sections, it has been shown that the model gotten with this method is valid. The temporal behavior is plausible, and the relations between the cell occupancy and its outflow are



(a) Flow arriving from the ramp

(b) Flow arriving from the main carriageway.

Figure 3.33: Effects of the addition of a new lane on the cumulative flows arriving at the merge cell 1 of figure 3.11. The curves labeled with 1 represent the reference case. The curves labeled with 2 represent the situation where an extra lane added to the main carriageway. The curves labeled with 3 represent the situation where the extra lane is added to the last ramp cell.

correct. A sensitivity analysis of the model has revealed that it is numerically sensitive to variables that can be considered as policy leverages. These variables are the cell capacity, the shock wave speed and the level of demand entering the system. Besides this, a deeper analysis of the shock wave speed has shown that the model the model behavior is impacted when this parameter takes lower values. A lower shock wave speed means that the sudden variations of density tend to be limited in amplitude. However, this reduction should not be too important, otherwise the potential benefits of the speed reduction may vanish. Based on all these observations, the use of SD for traffic-related policy analysis seems very promising.

However, several criticisms must be formulated regarding the model. The first limitation is methodological. The model has built according to the seminal CTM developed by Daganzo [16]. This model is a first-order Godunov scheme of the LWR equations [15; 39; 44; 65] from which criticisms can be formulated. On the one hand, numerous improvements of these models have been made and can be found in the literature. Herrera & Bayen [39] give two examples of modifications made in order to create more accurate dynamics: the switching-mode model, which embeds the modeling of discrete events; and the asymmetric CTM, wherein the merging dynamics are reconsidered. Another example of improvement is the stochastic CTM developed by Sumalee et al. [81]. This model accounts for the variations of density over segments in the case of stochastic supply and demand and its propagation through the network. On the other hand, as Spiliopoulou et al. [77] underline, the behaviors first-order models can reproduce is limited. Indeed, these models cannot reproduce capacity drop, hysteresis or stop-and-go wave that occurs when congestion sets in because of a bottleneck. All these phenomena have been observed in real traffic flows, but are not part of the seminal LWR model and CTM. The crowding out that is observed is in line with Daganzo [17] works, but cannot be considered as an actual capacity drop. As a consequence, aforementioned CTMs, or second-order models such as the lagged CTM proposed by Daganzo [18] and enhanced by Szeto [82], should be preferred to increase the accuracy and the range of behaviors that can be simulated.

The second and third limitations that can be raised about this model are related to the computational efficiency of the model. As explained in the chapter 2, the CTM computes, at every time step, the evolution of the number of cars held by all the cells of the network. The complexity of the model increases thus in relation to the number of cells in the network and may become a burden if the time step of the simulation becomes too small or if the network is too extended. In comparison for a given network and level of accuracy, the link-transmission model (LTM) developed by Yperman et al. [99] and 2007 is more efficient computationally speaking. As a consequence, the approach presented in this section seems to be suitable if the network that has to be modeled remains limited in size. The second limitation is related to the FIFO discipline implemented. Even though a rule similar to the level 2 defined by Carey et al. [10], violations can still take place on the network. The only ways of ensuring that FIFO is respected throughout the network is to choose short time steps or to set up transition rule based on the entrance time of the vehicles in all of the previous cells upstream. Choosing one of these

approaches would then lead to a burdening computational time for the model.

The last criticism about the modeling approach deals with the use of the function ALLOCATION BY PRIORITY presented in the section 2.2. The different graphs presented and analyzed in the previous sections show at first sight that the allocation process seems to work fine. And yet, a careful investigation of the outcomes reveals that the allocation function is actually a source of numerical instability. The first type of instability comes from the allocation process *per se*. As the figure 3.34 displays, the temporal evolution of each OD flow is somewhat jerky: the graph shows sudden peaks that seems to have been caused by the function. This may then explain small hysteretic plot of the figure 3.17. Removing these dots leads to a smoother behavior.

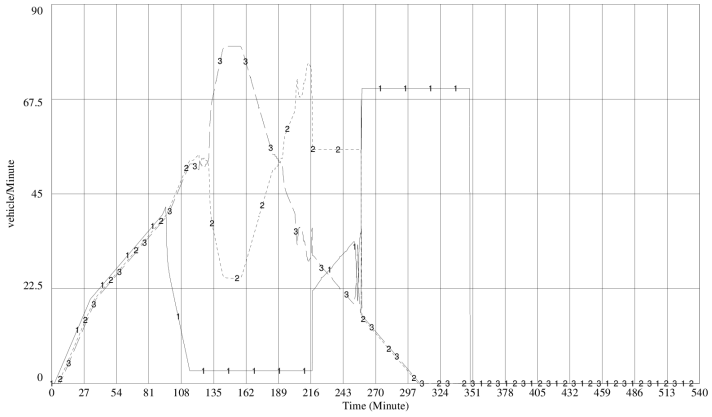


Figure 3.34: Instantaneous inflow intensity per OD pair across time at the merge cell 1 of section 3.11. The flow arriving from the ramp of merge cell 1 is labeled with 1. The flow arriving from the ramp of merge cell 2 is labeled with 2. The flow having the right-of-way at both merge cells is labeled with 3. The different peaks observed reveal the instability of the allocation function.

The second source of instability is the value of the width parameter, defined in the section 2.2. The instability only arises when the allocation must comply with the FIFO rule. In the process, the width can be interpreted as the number of time steps spent by a vehicle in the outbound cell that would guarantee it to leave the cell first. For low values of width—strict FIFO rule—static-like phenomenon appear, as the figure 3.35 indicates. The amplitude of the perturbations increases when the width decreases, however the global behavior of the model remain the same: the cumulative flows, for different values of the width, coincide. The FIFO rule seems then to be respected even if the width value is quite large. For the allocation of the outflow of a merge, the process, based on the actual priority regime, no similar perturbation can be observed. Since the behavior of the model is not impacted by the width parameter, a high value was hence chosen so that the instantaneous value of the OD flows can be retrieved if required. Based on the two last points, it can be concluded that the ALLOCATE BY PRIORITY function, even though convenient to use, is not fully satisfactory. Further information about how to deal with it in future research is motivated in the chapter 5.

Finally, a last point should be risen regarding the limited extent of policies that can be tested with the current approach. The current range of policies has been proven to be quite narrow. It is actually reduced to the sole capacity-based policies. The relevance of this method for policy analysis should therefore be challenged. However, it should be kept in mind that the development of a flow propagation model with SD has not been carried out yet. The work presented should then be seen as a preliminary investigation to see if SD is suitable for modeling traffic flows. The different results have shown that the model is valid since it reproduces the traffic dynamics as detailed in the CTM. Even though real data about the traffic flows is missing, the approach has been shown to be promising for policy analysis. The policy leverages are the one expected and a basic analysis of a capacity increase yields plausible results. A deeper reflection about the relevance of SD is to be carried out in the following chapter.

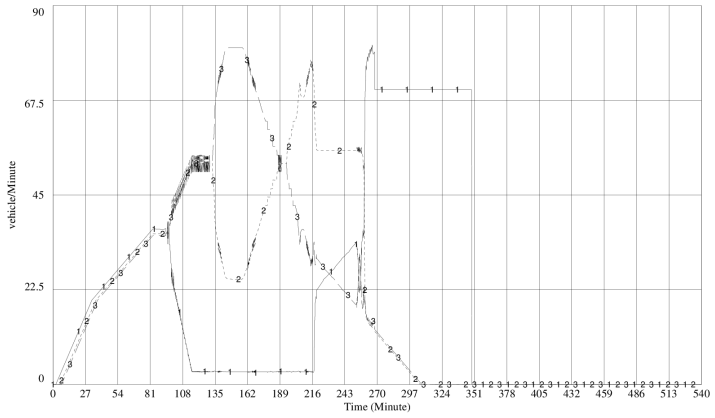


Figure 3.35: Numerical instability caused by the width parameter. The value chosen for the width is smaller. The labels on the plots have the same meaning as the one from figure 3.34. The instability can be observed on plot 2 with the static-like pattern.

4

Discussion

In the previous parts of this thesis, it has been shown that SD is a promising for building traffic propagation models. The elements developed are based on the CTM developed by Daganzo [16] and Daganzo [17], which approximates the LWR model. These elements can then be combined together in order to form larger road elements such as a corridor or an interchange. A small section of the ring of Brussels was built using these elements as an example and showed a promising behavior. In this section, the added value brought by SD models is to be discussed. Indeed, models based on the CTM are generally built and simulated with MATLAB [6; 54; 78] since the equations are already known. As a example, a ready-to-use package to reproduce traffic flows for MATLAB can be found on internet [65].

The first striking difference between the models introduced in the previous paragraph and SD is their external interface. SD models exhibits a clear structure: all its elements are related by means of flows or causal links. It can be inferred from this that this graphical feature is the added value of SD. However, there is no intrinsic difference between SD and MATLAB models for instance. A stock-flow structure is strictly equivalent to a first-order differential equation, as explained in the chapter 2. Moreover, as explained in the chapter 3, the computational complexity of the CTM, and hence of the model built, is high. Based on these points, using SD for traffic modeling is clearly superfluous and may be seen as tricky. And yet, this way of building model may be of interest to develop transportation models reproducing traffic propagation. Three comparative advantages can be listed from SD modeling and can be used to appraise the usefulness of SD over other methods. These points can be finally used to draw conclusion over the added value of SD for traffic modeling .

The first is related to the holistic character of SD. A holistic approach consists of considering a system as a whole. As a consequence, its behavior cannot be derived from the behavior of its subcomponents taken separately. This notion of holism can be derived from the ‘land-use transport feedback structure’ developed by Wegener [95] and presented in the figure 4.1. From this figure, it can be inferred from it that land-use cannot be thought separately from the transportation system as they mutually influence each other. Studying the transportation system in isolation from land-use would then limits its understanding. As a consequence, a transportation system should be thought as a complex system, namely a system where “ “you can’t do just one thing” and “everything is connected to everything else”. ” [80, p. 10]. Four-step model, defined by Ortúzar & Willumsen [69] as the classic transport model, lacks this holistic point of view. Indeed, the relation between transportation system and traffic flows is unidirectional, so is the one between activities and traffic flows [67]. In reality, too high traffic loads are bound to impact the state of infrastructure because of a faster wear. Reciprocal relations seems then to be more correct. Moreover, traffic creates economic externalities, that is to say elements that everybody must cope with once emitted. The main traffic externality is pollution, whichever its type. As a result thereof, traffic is likely to impact the traffic levels in the long run. On the other hand, because of its orientation towards system thinking, SD can be of interest when it comes to deal with complex systems where feedback plays a key role [79].

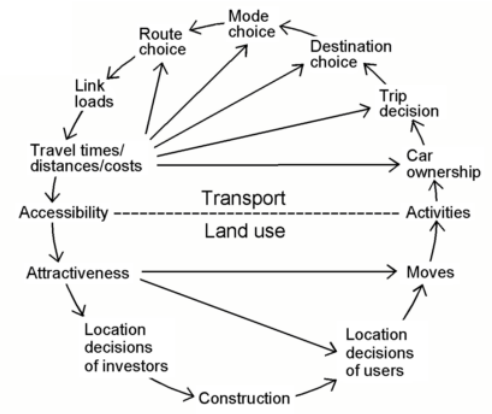


Figure 4.1: Feedback structure between land-use and transportation [95]

This holistic character of SD is interesting when it comes to model building. Because of the equivalence between differential equations and stock-flow, models with a large scope can be built. This point has already been arisen by Abbas [1]. Bringing out the model structure rather than the differential equations governing the model behavior is convenient for expanding the scope of the model. This is especially true when it comes to include fields where the notion of differential equation does not exist, or where no global model is available. Social or behavioral science are examples of fields where differential equation would make no sense. SD can be then considered as a potential framework or platform which would enable cross-disciplinary model building. Models developed in very different fields can be translated into plain, clean modeling elements. Presenting the model as a set of feedback loops and stocks is very advantageous when it comes to model conceptualization. SD models are powerful to draw mental maps from which more complex models can be built. Because of the emphasis on the structure, models can be easily modified and rearranged throughout the building process. Finally, the notion of feedback loop is comfortable to explain the relations between elements and therefore the effects that take place in reality. SD may be therefore an interesting tool to develop even more realistic models.

A second advantage of SD is the possibility to cope with temporal effects. As Maerivoet [59] explains, four-step models tend to remain static models, in spite of computational improvements. Policies are then tested for a given period of time, under the assumption that all the trips that are generated must take place during the planning period. The effect of a time-varying parking scheme such as the one developed by Fosgerau & de Palma [30] may not be tested. Indeed, their pricing schemes aims at deterring trips during peak hours and incentivize trips undertaken before them. Another example of temporal effect are delays in traffic information. Because of its dynamic character, congestion can quickly propagate through a road network. Information about the traffic state are broadcast on a regular basis to drivers, either as radio bulletins, travel time between interchanges or as areas to avoid. If the refreshing time of traffic information is too slow compared to congestion propagation speed, provided travel time may delude drivers in their route choice. As a consequence, congestion may turn direr. Compared to four-step models, SD can address these effects because of its dynamic character. It can generate them thanks to specific function or, as Sterman [79] explains, by means of stock-flow structures dynamically generate delays within the model and therefore introduce disequilibrium. All these different effects may be then be of interest to introduce complex temporal behavior in the model.

Because of their static character, four-step models are used for determining a traffic equilibrium. Cascetta [11, p. 396] defines a traffic equilibrium as “the relevant state of the system as that in which average demand and costs are mutually consistent.” In traffic modeling, equilibrium matches the notion of travel cost minimization. Based on this notion, two types of equilibrium can be defined:

- the user equilibrium, wherein the travel cost of every individual trip undertaken during the planning period has been minimized. The equilibrium state yielded by the model may vary if stochasticity or congestion must be taken into account.

- the system optimum, wherein the total travel cost throughout the network had been minimized. Unlike the user equilibrium, the social optimum does not guarantee the minimization of all the individual costs: some travelers may be worse-off compared to the user-equilibrium situation.

The main criticism that can be formulated regarding static equilibria is their ideal character. They assume that any traveler knows perfectly the detailed state of the system and therefore always choose the optimal route. In reality, such situation barely happens. Human mind has limited capacities [76] and cannot know the exact state of the system at a given time instant. Decisions tend then to rely more on heuristics [38]. However, heuristics is never entirely reliable, and thus may mislead drivers in their decision-making [79]. As a consequence, and as Cascetta [11] underlines, traffic tends to be more often in a non-equilibrium state, but may tend towards an equilibrium in the long-run.

The last advantage of SD is related to uncertainty in modeling. Four-step models aims at comparing different traffic policies and give recommendations about their efficiency on future traffic loads. However, as Ortúzar & Willumsen [69, p.534] outline

> We consider here the role of models in forecasting, but recognise that models alone are not good enough to provide sufficient evidence of future revenues to support the significant risks usually associated to these projects.

Besides the evolution of demand, uncertainty exists on the actual efficiency of policy instruments. For instance, Wang et al. [92] show that the limited efficiency of a driving restriction set up in Beijing: about one out of two drivers does not comply with the policy, especially if this driver dwells far from Beijing city center. Moreover, this restriction have led to the development of a black market for registration plates in order to get round the ban. This example illustrate the concept of policy resistance of Sterman [79]. Another example of uncertainty on policy efficiency has been arisen by Proost & Sen [70] and is about the impact of governance complexity. Their key finding is the undermining effect of several level of governance on the efficiency of economic policies. As de Jong et al. [21, p. 64] explains that "the degree of uncertainty and ignorance ought to affect the approach to decisionmaking." As a consequence, Ortúzar & Willumsen [69] explicitly propose to use other modeling approaches before drawing recommendations for future.

From these three points, it can be concluded that SD seems to be a suitable technique to develop comprehensive models with finer dynamics. In order to illustrate this, two examples of improvement that can be brought to the model developed for this thesis are presented. The first example is related to the road capacity. It has been shown in section 3.5 that the model is sensitive to small changes in road section capacity and is a potential policy leverage since road capacity can be increased by building new lanes. However, capacity is sensitive to exogenous factors, such as the weather or aging, the impact of which may be intensified by traffic loads, as indicated by Tan et al. [83]. Furthermore, as Gonzalez & Winch [34] show, increasing the capacity leads to an increase of the traffic loads and thereby to a faster aging. Since four-step models tend to be static in spite of the enhancement of computational capacities [59], impact of wear and its consequences are not accounted for. With SD on the other hand, modeling the wear of road and its impact can be done by using a stock-flow structure similar to the one presented in the figure 4.2. In this example of model, three feedback loops can be outlined: two balancing ones, B1 and B2, representing respectively the normal and the traffic-induced wear of the infrastructure, and one reinforcing one, R, representing the counter-balancing effect of the maintenance budget on the wear. Such model is then able to represent more complex propagation dynamics.

Because of its cross-disciplinary character, SD may be of interest for the development of complex choice models. As the figure 4.1 displays, choices are a key component of transportation system. Traffic loads are the result of a succession of choices regarding the destination, the mode and the departure time. In four-step modeling, discrete choice models (DCM) are widely used for determining, among others, the number of tours undertaken per area, the modal split, the route choice or the departure choice. A complete overview of these models can be found in Bonnel [7] and Ortúzar & Willumsen [69]. Let be an individual who can choose between several transportation modes or routes to reach her destination. According to the utilitarian theory, this individual has a perfect information about all the existing modes or routes and carries out a rational choice: she chooses the mode or route that maximizes her utility. In transportation, the notion of disutility is more common [12], since traveling is often associated with the

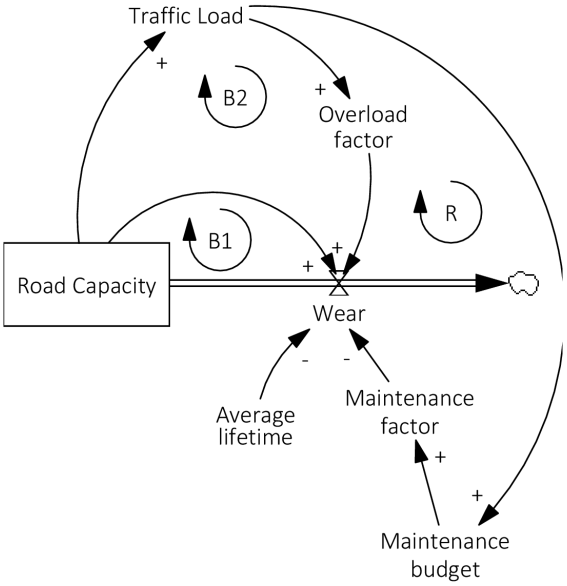


Figure 4.2: Example of an advanced function for the road capacity using SD

notion of cost expressed in units of time or in currency. As a consequence, the individual chooses the alternative which has the smallest travel cost. A detailed overview of the different ways of deriving a DCM is presented by Ortúzar & Willumsen [69]. In the mainlines, the determination of a DCMs consists in deriving a utility function from available data about individual preferences. The share of each alternative is finally determined by using probabilistic distributions such as the extreme-value distribution.

Several criticisms can be made on these models, the first being their data intensive character. In order to determine a utility function, large datasets are mandatory in order to identify the most relevant alternatives and to find out which variables should be included into the utility function. The second criticism, related to it, is the limited extent of a model. As Bonnel [7] and Ortúzar & Willumsen [69] explain, the value of the different parameters of a DCMs depend on the dataset from which it has been derived. Applying them to a different case may not yield correct results. As a consequence of these two criticisms, developing a DCM for a specific case requires a large amount of data in order to build a robust model. The third criticism is based on the paradigm of utility maximization, which assumes that individuals have complete information regarding all the alternative available. As a result thereof, their choice is purely rational since the alternative chosen is the one maximizing their utility. In reality though, travel time over a route may vary with respect to the traffic state in it. The accuracy of information provided is of influence regarding route choice Ben-Elia et al. [5]. Besides this lack of information, human mind faces cognitive limitations. As a result thereof, the rationality of an individual is bounded [76]: the choices this individual makes may not maximize her utility. Finally, these models do not address for temporal effects such as learning, habit or experience. As Cascetta [11] points out, these different parameters are of interest when it comes to route choice. [61] explains that route choice of person may be influenced by his own experience and information he received from information systems.

SD has already been used for developing choice models [68] including day-to-day dynamics. In such model, the decisions taken by an individual depend not only on travel costs, but also on experience [11]. In this paragraph, a conceptual model is being developed and related to the three assets of SD, presented in the figure 4.3. For the sake of simplicity, individuals are assumed to choose between 2 distinct routes. The key idea of this model is to base changes in route choice on experience. The run is set up so that it reproduces a long time span (several weeks or months). The left-hand side of the model show the route choice dynamics. Four different stocks partitioning the total demand are distinguished:

- drivers sticking strictly to route 1,

- drivers dissatisfied from route 1 who decide to test route 2,
- drivers sticking strictly to route 2,
- drivers dissatisfied from route 2 who decide to test route 1,

The objective of the second and fourth stock is to account for ditherer drivers. These two stocks are fed by dissatisfied drivers, namely drivers for whom the cumulative extra travel time spent on congestion has exceeded a given threshold. As a result thereof, drivers falling into these stocks decide to take the other route in order to see whether they are better-off or worse-off.

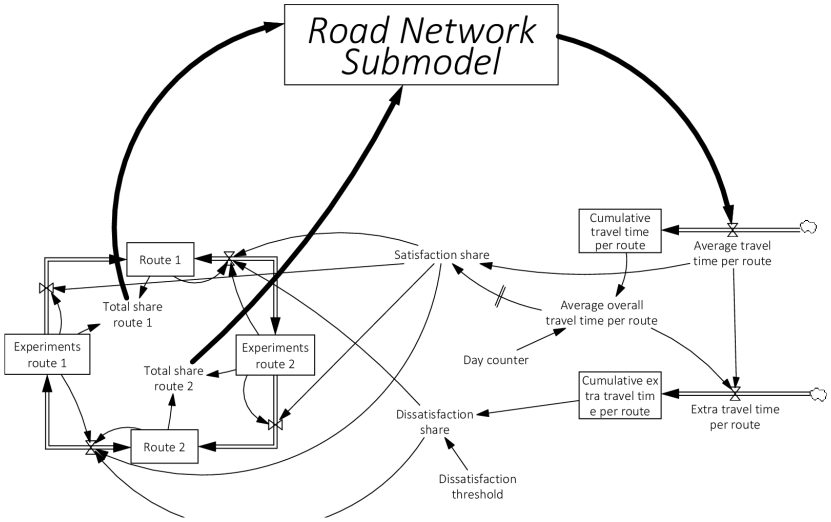


Figure 4.3: Example of a realistic choice model using SD

The right-hand side of the model exhibits the choice parameters, that are:

- the cumulative travel time per route, which tallies up the total time spent by vehicles on a given route,
- the cumulative extra travel time per route, which sums up the difference, if greater than 0, between the average route travel time on a specific day compared to the overall average travel time over the run.

The latter stock is used for generating the dissatisfaction dynamics: travelers are willing to change their route if the cumulative extra travel time exceeds a certain threshold. The former stock on the other hand is used for creating drivers‘ experience: the overall average travel time spent by drivers on a route is derived from it. Moreover, it is then utilized as a reference by drivers willing to change their route whether they have been better-off by taking the other route. These variable influence finally the transition dynamics between the different route shares.

All the different elements listed and discussed in the previous paragraph indicate that SD is, methodologically speaking, suitable to develop transportation models that include realistic traffic dynamics. It is important to underline that none of these are intrinsically innovative though. SD has been developed in the 1960s [29] and its relevance for transportation was discussed by Abbas [1] in the 1990s. Many transportation models [3; 4; 34; 37] were developed with SD in the 2000s. Traffic and its effects were already accounted for, even though remaining global. As a consequence, the added value of SD that stems from the results of the model developed is narrow. However, SD tools are evolving. The tools

that are under development are likely to have a higher added value that the current ones.

The first tool is exploration modeling based on SD, named ESDMA—Exploratory SD Modeling and Analysis. This approach, developed by Kwakkel & Pruyt [51, 52], is an assessing tool for policy robustness. The method consists in identifying the main modes of behavior a model can generate from a qualitative point of view. The model analyzed is run for a wide range of parameters and can therefore reproduce diverse scenarios, including the most uncertain ones. Because of the focus of SD on qualitative behavior [1; 79], the trends drawn by the outcomes matter more than their numerical value. By doing so, it is possible to determine the robustness of policies and desirable behaviors. Even though models investigated are not based on the most recent software developments—EBSD—this method is valuable when it comes to deal with highly uncertain situations. An example of such situation is the influence of climate change on traffic flows. As explained in the introduction, transportation generates almost a quarter of the total emissions of greenhouse gases. Traffic flows are therefore bound to affect climate change as well. In the same time, as pointed out by Koetse & Rietveld [49], climate change is bound to impact, among others, traffic flows, infrastructure disruptions, road safety and reliability of travel time forecast. Even though correlations exist, the exact effects on the long-run of climate change may be difficult to assess. Thanks to ESDMA, it may be possible to investigate how major and uncertain changes are bound to influence traffic flows, and therefore assess the robustness of different policies.

The second promising tool is entity-based SD (EBSD). In the chapter 2, it has been explained that the model was developed by means of the sixth release of VENSIM. This version, even though being the most recent of VENSIM, is not the most up-to-date SD software development. Recently, Yeager et al. [96] introduce EBSD. This advanced version of SD aims at combining its strength with agent-based modeling. Its key objective is to develop modular building blocks, named entities, as SD models. The first conclusion of this thesis is that SD is methodologically adapted to model traffic flow propagation. As a consequence, flow propagation models can be developed with EBSD. The main difference comes from the fact that the different modeling elements are defined as entities that need not be redefined later on. The modeling of large networks is then less tedious than the method used in this thesis. Interchanges need to be modeled and set up once for all. Since EBSD is SD modeling, models developed with this new technique have the same advantages and strengths as current SD models. Another strength comes from the ability to create entities directly from big databases. Model building could then become very straightforward.

5

Conclusion

In the previous chapters, it has been shown possible to build a macroscopic traffic-propagating model by means of SD. The cornerstone of this approach is the CTM, which discretizes the seminal LWR model for traffic flow. Thanks to this model, it is possible to develop elementary building blocks for road networks. These elements can be combined to create more complex elements such as complete road interchanges. These elements were used for developing a model of the northern section of the ring of Brussels. This modeled network was tested in order to see whether the flowing dynamics are correctly replicated. Several traffic situations were tested and analyzed. They included free flow conditions and several congestion sources. Based on the different outcomes, it has been presented that the model behavior is correct for both light and heavy traffic conditions. In light traffic conditions, the outcomes indicate that the model can generate a correct behavior when several traffic flow are proceeding through the network. The exiting sequence is respected: vehicles arriving the first at an outlet are the ones that are located to closest to it. Moreover, the relation between the cell density and its outflow is linear, as it is expected.

Three potential causes of congestion have been investigated: a bottleneck, a gridlock, and intense traffic. Both first cases were tested for light traffic conditions. For all these cases, disruptions on traffic propagation can be observed. For all these cases, right-of-way-regime is well modeled: flow that must yield are properly crowded out. The recovery of traffic flow is shown as progressive and slower, as it is expected from the MFD associated to the flow between two cells. Sensitivity and uncertainty analyses reveal that variables that were fond influential for model behavior are the usual policy leverages for traffic management. It is then possible to influence the system behavior from a numerical point of view by increasing infrastructure capacity or reducing the inflows of vehicle at its outlet. Besides this, the shock wave speed is found to change the model behavior. This means that adaptive speed policies may be very appealing when it comes to limit the impact of congestion. A basic policy analysis indicated the importance of allocating strategically extra capacity to limit the impact of congestion. When an extra lane should be added around a on-ramp, it should preferably be allocated to the ramp. This may be of interest to reduce the crowding out of the flow that arrive from the ramp and that must yield. Based on all these observations, it is possible to answer the first research question. SD is thereby a suitable method to reproduce the propagation of traffic flow at it is predicted by the LWR model.

However, a careful investigation of the model outcomes reveals that the model and the method are not entirely satisfying. The allocation process is unstable and therefore undermines the quality of the outcomes. Even though the qualitative behavior of the model matters more in SD, this instability indicates that the quality of numerical outcomes tends to be unsatisfying. Besides this, the CTM implemented is the seminal one; it is not the most up-to-date development of it. The range of behaviors the model can reproduce then remains limited. A model based on the original CTM may quickly become a computational burden if the time step is too low or the network modeled is too long. A deeper reflection about the modeling approach questions the relevance of SD as a modeling approach for traffic. Intrinsically, there are no difference between existing models and SD. Stock-flows are equivalent to differential equations, and the other way round. SD models for the CTM are thereby identical to ex-

isting model. Using SD does not seem very pertinent since other equivalent methods exist. SD owns neat advantages when it comes to scope broadening or dealing with uncertainty and temporal effects. These are not entirely new, as transportation models based on SD can be found in literature.

And yet, upcoming developments of SD may soon bring an added value to the traffic modeling. Indeed, SD is suitable for exploratory analysis. It is then possible to analyze, for instance long-term consequences of climate change over traffic flows. This can be of interest for long-term urban planning. Including such uncertain effects can be relevant to design robust traffic policies. Besides exploration purpose, the development of EBSD bears promising opportunities for traffic models. By taking the best of SD and agent-based modeling, it is possible to easily create large and computationally efficient traffic models that can be connected to real-time databases. Furthermore, it also embeds the technical advantages of SD since entities are SD models. Traffic models can then be quickly developed and run by policy makers. Based on these observations, the second research question can be answered. The added value of SD does not come from the way of modeling a system. However handier it is compared to MATLAB programming, the underlying equations remain the same. The added value actually stems from exploratory analysis and EBSD. On the one hand, it is adapted to draw recommendation on the long-run regarding traffic policies under high uncertainty. On the other hand, the development of traffic model may become even simpler and more accurate. EBSD permits easy replication of SD structures and handling of real data within the model.

Exploratory Modeling and EBSD tend to bring out the relevance of choosing SD for traffic flow modeling. However, further developments need to be carried out before applying this method. A first investigation that can be made is about the choice of a more adapted numerical scheme. The seminal CTM is, as explained in the section 3.7, is not the most up-to-date version of the CTM. On the one hand, the range of policies that can be tested tested with it is limited. Adaptive speed policies, aiming at diminishing the shock wave speed across traffic flows, were proven to have a strong influence on model behavior. And yet, there is no way to easily test them. In the section 2.1, it was explained that a corrective term in w/v_0 was added in the expression of the flow that can be received by a cell so as to take into account shock waves generated by sudden variations of density. Regarding the flow that a cell can sent, this factor does not exist since the flow is assumed to proceed at its free flow speed. A naive approach would consist of changing the size of a cell, but this would impact the length of road elements. By analogy to the factor w/v_0, a potential idea would consists in introducing a term equal to $v/v_0 \leq 1$ into the expression of the flow a cell can send. Since the flow speed is lower than v_0, the flow needs more than a time step to leave a cell. The second improvement is related to the choice of the numerical scheme to build the model. Since the seminal CTM was implemented in the model built from this thesis, the behavior that can be generated remain limited. As listed in the section 3.7, many developments of this model have been done, such as the stochastic and the delayed CTM. These are then able to reproduce more advanced behavior than the original CTM [18]. However, they would suffer from the same computational inefficiency as the seminal CTM. As a consequence, it should be investigated the extent to which another numerical scheme, such as the link-transmission model can be implemented in EBSD modeling for instance. Indeed, this approach has been proven to be computationally more efficient than the CTM [99]. One of the further research consists then in determining an appropriate scheme for traffic modeling thanks to SD.

As underlined at the end of section 3.7, the ALLOCATE BY PRIORITY function is actually not satisfactory. The use of this function was motivated by its simplicity and its adequacy to the desired task. However, it introduces numeric instability and therefore undermines the model accuracy. It is therefore recommended to avoid the use of this function in further research. Other allocation functions exist in VENSIM, but are likely to reproduce the same instabilities. The best solution would then consist in developing a complete algorithm from scratch. The objective of this algorithm is to allocate the flow leaving a cell to the available capacity of the receiving cell by respecting the FIFO rule. The oldest vehicles within a cell should then be allocated in priority. The paper of Carey et al. [10], or the Wood algorithm on which the allocation functions of VENSIM are built [88] can be used as starting points. Once the algorithm developed and tested, it can be integrated as a macro into the model. Finally, a last word is to be made regarding the model outcomes. In this demonstration model, only the length congested and the expected travel time per cell and per corridor were computed. These outcomes,

although straightforward, are not sufficient to carry out policy analysis with the model. Other relevant outputs can be the average flow speed crossing a cell or a corridor and the total travel time per OD pairs. These would be of interest to assess policy performances. But these outcomes remain limited to the sole transportation system. Taking decisions based on these sole variables may result in the selection of inappropriate policy instruments. An example of larger outcome is the total level of greenhouse gases emissions. On the one hand, it can be used for assessing or selecting traffic policies. Policies can be discarded if the level of emission does not comply with specified threshold for instance. On the other hand, this may be useful to include the impact of greenhouse gases on climate change. As a consequence, it would enable the generation of more complex dynamics into the model.

A

Overview of Models used in Transportation Issues

***Foreword**: In this appendix, a detailed, albeit not exhaustive, presentation of existing transportation models is given. It is intended for readers that are not familiar or do not have a background in transportation engineering, so that they can contextualize the research topic.*

Because of its importance in both developing and developed countries, transportation requires specific attention when it comes to planning. The recent developments of ICT and of computational power have enabled the diffusion and the use of numerical models. Such models can then be used by planners as a supporting tool for decision-making: outcomes of a model are inputs helping decision makers to map the one which fulfills the most given requirements or objectives [69]. Modeling in transport-related research is common and covers a wide range of applications and methods. Maerivoet [59] carried out an exhaustive inventory of the different models existing for transport-related issues. In his review, two main categories of models are distinguished: transport planning models and traffic flow models. The figure below summarizes this classification. For the sake of clarity, his work is implicitly referenced in the two first sections thereafter. Only relevant quotations and works from other authors are explicitly referenced.

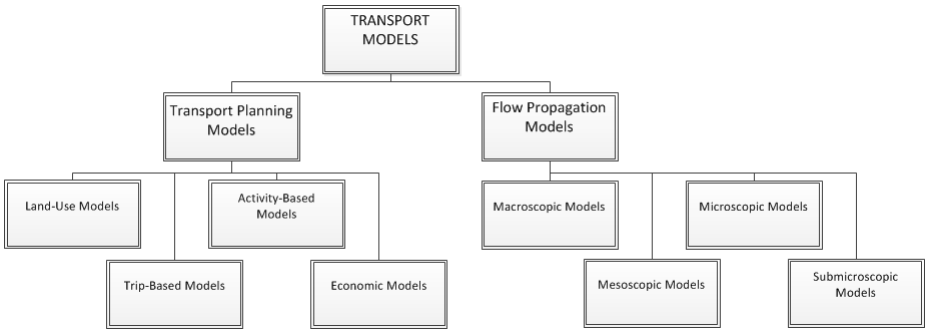


Figure A.1: Classification of transport models from Maerivoet [59]

A.1. Planning Models

The first category of models consists of models for **transport planning**. According to the Transportation Planning Capacity Building Program [84, p. 3], transport planning is “a cooperative process designed to foster involvement by all the users of the system (...) through a proactive public participation process”. Through this process, decision-makers seek for sustaining transportation system. This includes not only monitoring of the current system, but also development forecasts and policy proposals for further improvements of the system. Models may be then of interest as support for decision-making. The focus of planning models is on the highest level of transportation system. Planners can thereby assess the impact of large measures such as an increase of infrastructure capacity.

A.1.1. Land-use Models

Transport planning models include first *land-use models*, the focus of which is about spatial development of human activities and therefore of transportation infrastructure. The first land-use models has been developed in the nineteenth century by von Thünen and the first half of the twentieth century. They focused on the development of some US cities and the way available land is used by activities. This was of importance since land use feeds back into the transportation system that impacts the land use in return [95]. This structure has already be displayed in the section 4. On the one hand, the land use determines where human activities—work, living among others—take place. These places may be located in different areas that must be connected. A transport network is hence developed so that the inhabitants can reach these different locations. These locations may differ with respect to their purpose, such as dwelling, commercial activities, industries and so on. The accessibility of an area stands for the potential level of interactions enabled by the transport system. If the accessibility of an area is important for a given activity—e.g. living—then this can lead to new land use.

A first example of land-use model is the Hansen's model [36]. Let be a set of areas wherein the available space, the number of jobs and the travel cost between all the areas are known. The Hansen model distributes an increase of population and/or of available jobs over the different areas, given their available space. Its main assumption is that people would rather live in an area that can be easily accessed. The increase of population (resp. number of jobs) within an area depends on its accessibility that varies with respect to the available space (resp. number of inhabitants) and of the travel cost between all the other areas. However, this rise is determined once and does not lay on the aforementioned feedback structure. Another land-use model is the one developed by Lowry [57] in 'A Model of Metropolis'. Unlike Hansen, this model is iterative and distinguishes two categories of job: location-bound jobs, and service jobs, which depends on the population count of the area, such as educational jobs. This model lays on two assumptions: for all the areas, the ratios of population versus jobs and of service jobs versus population are given and fixed. Moreover, the travel costs between the different areas are assumed to be symmetrical—the travel cost between A and B is equal to the travel cost between B and A—and fully known. Because of these assumptions, the Lowry model presents a feedback structure: the model yields its outcome after several iterations. The most recent models developed are usually simulation-based, twenty of them are listed by Wegener [95]. In general, the transport network is actually used in such models as an input for determining the travel costs.

Two main criticisms may be formulated regarding these models. The first is their simplicity: seminal models were based on sole observations of the urban sprawl of cities, thus they were bound to omit potential key factors explaining it. The level of income has been shown to influence the land-use, but cannot explain the complete phenomenon. The expansion of a city should actually be seen as a multi-agent system: the population is made of a high number of agents that interacts with other agents. The second limitation is the limited validity of the models since the studies were mainly about American cities. Highlighted pattern may not hold true in another country. In the United States, wealthy people usually dwell far from the urban centers; which does not hold true in Paris for instance. However, the main objective of these model was more about providing interesting insights regarding the sprawling pattern of cities than forecasting land use in the long run.

A.1.2. Trip- and Activity-Based Models

A second category of planning models groups the *trip-based models*. The models are actually based on a seminal model known as the four-step model, which is the practical application of a framework initially developed by Manheim [62] and Florian et al. [28]. In the four-step model, McNally [67] distinguishes two systems and four procedures encompassed in a two-looped feedback structure. Its structure is presented in the figure A.2. The two systems are the transportation and activity systems, that is to say any element that is not related to the transport system, such as the features of land-use. These two systems are then used as inputs to determine the performance and demand by means of procedures. The outcomes of these procedures are then balanced in order to determine the different flows over the network. The actual model structure is presented on the figure A.3, as well as the influence of transportation and activity systems. Equilibration and dashed arrows points out a feedback structure: this model is therefore iterative. The four different steps are the trip generation, the trip distribution,

the mode choice, and the route choice or route assignment. Each of these steps actually matches decisions that are taken during the transportation step of Wegener's feedback structure presented in the previous section. The table A.1 presents each steps with the matching decision.

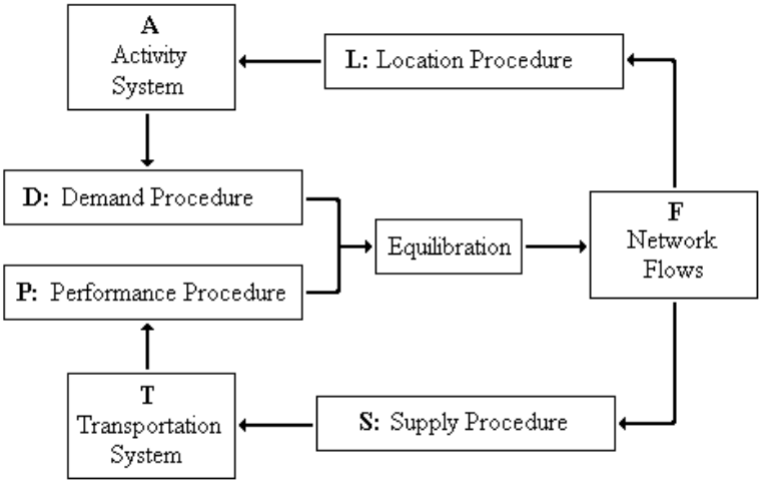


Figure A.2: The conceptual framework of the 4-stage model [67]

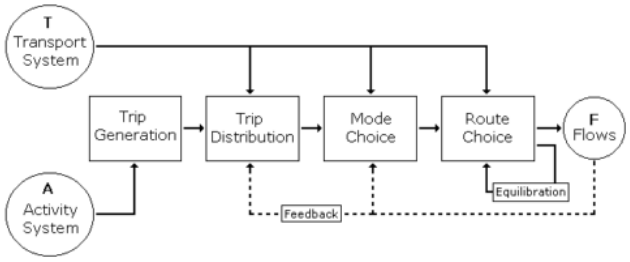


Figure A.3: The 4-stage model [67]

Table A.1: Equivalence of decisions and steps in the four-step model

Step	Decision
Trip Generation	Trip Decision
Trip Distribution	Destination Choice
Mode Choice	Mode Choice
Route Assignment	Route Choice

The base unit of this model is the trip. A trip is defined as the concrete outcome of the 4 different decisions presented in the table. A trip is hence related to the activity this individual would like to execute and therefore features a time-and-space dimension. However, in the four-step model, the underlying activity matters less than the trip *per se*. In this framework, the time dimension of a trip vanishes because the trip is assumed to be executed during the modeled period. Besides this, individual trips are aggregated into bundles of trips generated between two large areas, in order to reduce the computational complexity of the model. As a consequence of this double aggregation, the trips are assumed to take place between central points of the areas, during the period of interest.

The first step is the trip generation and aims at expressing the number of trips that an area generates and attracts. These number of trips are determined with respect to the activity, for instance trips from home to workplace. The second step is the trip distribution. Its goal is to determine the quantity trips

that takes place between two areas, based on the network, the total number of trips from/to each area and the deterrence function of travel. The latter input quantifies the extent to which a traveler is willing to trip while he knows its cost. At the end of these two steps the amount of trips within and between each origin and destination is determined. The results are often condensed and presented as a matrix known as the Origin-Destination Matrix.

After these two steps, the total number of trips per mode of transportation available in the current transportation system is usually determined. Usual modes include car driving, public transport, walking or cycling. Some models, such as the LMS—Dutch regional model— includes also a mode "car passenger" that stands for carpooling [21]. The modal split used to be executed at the same time as the trip generation; but, as Maerivoet [59] points out that household data are not the only reason for choosing a specific mode. For instance, a user may rather use public transportation if there is no parking infrastructure close to its workplace; regardless of its cost. Modal split may take place during the trip distribution step, if the deterrence functions for all the modes are known. In that case then, modal split models are often based on discrete choice theory. In the main lines, a discrete choice model (DSM) aims at determining the proportion of each mode given a utility function and a set of alternatives assumed as independent. The preferred alternative is then the one with the highest level of utility. The usual distribution is the extreme value distribution, which is close to the maximization function [7; 69]. If some modes are interrelated—first half of a trip by car, second half by train from a P+R facility—nested models are better alternatives to prevent overlaps.

Finally, once the total number of travelers per mode and per destination is known, the trips can be assigned on the network. Wardrop [93, p. 345] was the first to define the choice of a route by defining the notion of user equilibrium:

1. The journey times on all the routes actually used are equal, and less than those which would be experienced by a single vehicle on any unused route.
2. The average journey time is a minimum.

This equilibrium can be reformulated as follows: **an individual tends to choose the shortest route to reach his destination, whatever the choice of other travelers may be. Choosing another route would not make him better-off.** This choice, rational and egoistic, is deterministic: the travel time between two points of the network is constant for all the available alternatives. Another potential equilibrium is known as the social optimum, for which the total travel time is minimized. However, this equilibrium has a cost: some users may become worse-off compared to an user equilibrium. A key trade-off must then be made: which travel cost should be minimized: individual or collective? Both situations are idealistic though. In reality, choices tend to be based on heuristics and habits [11].

The assignment of traffic loads on the network can be either static or dynamic. Static assignment seeks for a traffic equilibrium that minimizes the travel time knowing the travel capacity provided by the transportation system and the travel demand. Conditions are added in order to assign properly the flows, two notable examples of which are stochasticity and congestion. The minimal found can be either a user equilibrium, which matches Wardrop's first principle; or a social equilibrium, wherein the overall travel time has been minimized. However, this kind of assignment neglects the temporal character of traffic flow and congestion, and leads to paradoxical situations. Since congestion cannot be modeled properly with this type of assignment, dynamic policies or effects cannot be modeled. In dynamic assignment instead, temporal dimension of traffic is accounted for. The trips are turned into traffic flows that are generated across time and are loaded through the network. This assignment technique yields more realistic results. However, it may become a computational burden because more computational power is required to estimate all the shortest paths. Shorter networks are hence preferred for this kind of assignment.

As explained at the beginning of this subsection, trip-based model are based on aggregated data where temporal dimension has been removed. And yet, this latter characteristic is fundamental in transportation planning, especially regarding policy design. For instance, a pricing policy that aims at shifting the departure of commuters out of the peak periods may lead to trip departures out of the

planning period. It may be deemed more relevant to define a trip as an individual's decision made in order to carry out one or several activities. Instead of focusing on trips, the sequence of trips made by an individual during a given period can be set up as the basic element for a model. The resulting chain of trips, called a journey or a tour, is the cornerstone of *activity-based models*. Similarly to trip-based models, activity-based models feature an activity-generation component or choice models to select an activity or a transportation mode. But these models also enable the choice of a time profile for the tour: departure times, stages and return time.

The most convenient way of building such a model is to use a multi-agent approach: individuals are modeled as independent agents taking their own decisions and performing consequently. The activity patterns specify then the time-and-space evolution of the agents. Besides the activity pattern, the agents feature choice models for modal split and route. Propagation models ensure their physical evolution through the transportation system. Two criticisms can be made about activity-based models though. First, the amount of data required to run the model is substantial: since trips are no longer aggregated, data about trips has to be highly accurate and exhaustive, such as a "*travel diar[y]*" [59, p. 86] describing the exact trip pattern across time and space. The recent boom of smartphones and the democratization of embedded GPS devices into cars have made data acquisition easier. Second, the sequence of choices made by individuals may not be structured around a clear causal chain. In that case, agents may not be able to adapt their route if disruptions on the network appear.

A.1.3. Economic Models

The last category of planning model gathers models the theoretical background of which is economics. It is indeed possible to define a transportation system as a market between transportation supply—the capacity provided by infrastructure and services such as public transports—and transportation demand, that is the trips that individuals want to undertake in order to carry out their activities. In that configuration, congestion can be interpreted as the imbalance between transportation supply and a too high transportation demand. The setting of economic models can be plotted as cost/demand functions with respect to the number of trips made. The demand function is assumed as decreasing, since users would be less willing to travel when the number of trips is too high and congestion is likely to occur on the network. Instead, the supply function is rather represented as an average cost function that adds up any cost related to transport. By plotting these two functions—average cost and total demand—it is possible to map the equilibrium points, which are the intersection points of these two curves. Recently, a family of model named TRENEN has been developed with the support of the European Commission to address the development of economic-based transport policy based on this notion of equilibrium between supply and demand. De Borger et al. [19] and Proost & Sen [70] include this framework and analyze its outcomes.

Economic models may be of interest for dealing with the trade-off between user-equilibrium and system optimum that was introduced in section A.1.2. Average cost of transportation is usually split into two components:

- The private average costs that a user "charges" while traveling, such as tolls or fuel consumption;
- The external average costs, or externalities, that are charged by other users, such as carbon dioxide emissions.

In the economic setting, an individual behaves rationally and therefore seeks for minimizing its own private cost, which leads to an user equilibrium. All individual travel costs were reduced regardless of the consequences on other users. Because of this egoistic choice, they have to deal with the negative externalities of traffic that are congestion and pollution. The user equilibrium is then totally different from the system optimum for which the overall travel time is the lowest. This can be done for instance by internalizing external costs into private costs [19]. The table below presents different policies aiming at that purpose. A toll is a charge that is directly paid by the users to a public or private company, whereas a tax is indirectly paid to the government.

Economic models are actually efficient tools to design pricing policies. Their theoretical impact on transportation is significant compared to other policies. The bottleneck model developed byVickrey [90]

Table A.2: List of policies that an economic model can investigate

Measure	Articles	Remarks
Tolls (Direct Pricing)	Vickrey [90] De Borger et al. [19] Proost & Sen [70] Hensher & Puckett [38] Kilani et al. [46]	Road-specific Time-varying; Space-specific: – urban – suburban...
Taxes (Indirect Pricing)	De Borger et al. [19] Proost & Sen [70] Börjesson & Kristoffersson [8] van Essen et al. [87] Fosgerau & de Palma [30] Delhaye et al. [23]	Mode-specific: – car ownership – public transport fare... Time-varying; Fuel price; Parking price
Subsidies	De Borger et al. [19] van Essen et al. [87]	Tax exemptions; Premia

shows that they can influence the behavior of morning commuters who must clear a section with a limited capacity. In this model, a varying pricing scheme applied to a road section with a limited capacity is more efficient than a capacity increase of this bottleneck. The former solution is actually bound to incite more commuters to adapt their departure time if going through the bottleneck during peak hours become costly. A similar idea of time-varying price can be found in Fosgerau & de Palma [30]. They point out that a parking price that varies with respect to time and congestion level may give people the "incentive to reduce the length of time spent at work" 2013. However, as Proost & Sen [70] outlines, the efficiency of pricing policies may be reduced if at least two levels of governance are involved in policy application. A lack of cooperation between these two level of governance may undermine the benefits of a policy. However, economic models have to cope with two problems, the first being the extent to which internal cost should be internalized. Internalizing more externalities may lead to policies with higher efficiency, but a lower acceptance: users may be reluctant to accept a pricing policy seen as an unfair burden for low-income users. The second issue is related to the redistribution of the benefits granted by such actions. The public acceptance may be higher if collected money is actually useful, that is to say that earned revenues are actually and efficiently spent somewhere else in the economy, for instance as subsidies.

A.2. Flow Propagation Models

The second category of models outlined by Maerivoet [59] consists of any model the focus of which is made on the propagation of traffic across the transportation system. Since traffic study is quite recent, many different models have been developed to gain insights about the way traffic behaves. Besides this, flow propagation models may be embedded as sub-models into planning models in order to include flowing dynamics or variables related to it. However, there exist many different models and approaches to describe it. Hoogendoorn & Bovy [40][1] established a thorough list of existing models for flow propagation models and five different ways of classifying them:

- The level of details of the flow, which ranges from the individual vehicles to a continuum;
- The scale of independent variables: models can be either continuous or discrete;
- The representation of the process: the process can be modeled either as a deterministic or as a stochastic phenomenon;
- The operationalization: the model is either analytical or numerical;
- The scale of application: the conditions under which the model can be used.

[1] For the sake of clarity, this paper is to be implicitly referenced in this section as well.

In this section, the same classification as Hoogendoorn & Bovy [40] and Maerivoet [59] is chosen: the flow propagation models are to be sorted with respect to their level of details. The classification consists of four distinct categories that are, from the highest level of details lowest:

- Submicroscopic: traffic flow is modeled as individual vehicles with their own behavior that interact with other vehicles on the network. Besides this, the vehicle is modeled as a system with its own internal dynamics.
- Microscopic: same as submicroscopic but without the internal dynamics of vehicles. In this section, the distinction is collapsed.
- Mesoscopic: traffic flow is modeled as vehicles for which only the behavioral rules with other vehicles are explicitly detailed.
- Macroscopic: traffic flow is perceived as a continuum where individual vehicles cannot be distinguished. Historically, this approach is the cornerstone of the first flow models developed [56].

It is deemed important to outline that categories of models are actually related [24; 40] and may be combined in order to build more efficient models. Manley et al. [63] gives the example of a microscopic traffic model using an agent-based approach of traffic with an embedded macroscopic model, the BPR formula. Including the latter model results in lower computational times compared to pure agent-based approaches. Similar results have been found by McCrea & Moutari [66], who built a macroscopic flow model that includes probabilistic models.

The two first types of model, microscopic and submicroscopic, were developed during the 1960s and are initially based on the following behavior of individual vehicles in a flow or in a platoon. In the latter situation, the following vehicles can either stay behind the leading one at a *safety distance*, or *reproduce its behavior* with a small delay. Since each vehicle is individually modeled, the response to a change of the behavior of the leading one varies. These straightforward models are the cornerstone of a microscopic model known as the General Motors non-linear model. Similarly to these *follow-the-leader* model have been developed *optimal velocity models*, wherein a vehicle adapts its speed with regard to both leading vehicle and the headway in between. The boom of computational power has enabled the development of numerical schemes such as the *Cellular Automata*. In this model, vehicles proceed through cells of a specific length that can contain either one or no vehicle, and behave according to definite transition rules. Computationally speaking, this model has been proven more efficient than other existing simulators.

In the third category, that is the mesoscopic level, the focus remains on vehicles. But, unlike the microscopic level, the vehicles are no longer differentiated and thoroughly described; only behavioral rules of vehicles remain detailed. Probability distributions are then introduces to model ‘differences’ between the vehicles. There exist three main paradigms for mesoscopic models. The first, known as *headway distribution*, consists of creating distributions for the headway, that is the time between the clearing of a fixed point by two consecutive vehicles assumed as identical. In the second, vehicles are dynamically gathered in *clusters* with regard to a shared traffic property such as their average speed. Once created, the internal dynamics of a cluster becomes of lesser importance: the flow is then made of proceeding clusters of vehicles that change over time. The third paradigm is based on gas kinetics. In these models is described “the dynamics of the velocity distribution functions of vehicles in the traffic flow” [40, p. 290]. According to Maerivoet [59, p. 116], this approach aims at “bridg[ing] the gap between microscopic driver behaviour and the aggregated macroscopic modelling approach.” Several formulations have been made from the seminal model in order to correct critical formulations or to include new dynamics such as lane changing. However, the formulation of these models remain similar: they are written as a set differential equations. Numerical schemes must be therefore derived from them.

Macroscopic flow models were historically the first models investigated to model flow propagation. A thorough overview of these models, as well as an example of a numerical scheme reproducing it have been presented in the section 2.1.

A.3. Use of System Dynamics in Transportation-related Issues

As explained in the introduction, wicked problems are bound to occur within a transportation system because of its structural complexity. As Wegener's circle presented in figure 4.1 shows, a transport system can be seen as a large feedback structure which influences the global behavior. Feedback is a typical notion in system dynamics (SD). Sterman [79] defines SD as a methodology that aims at modeling a human system as a set of quantifiable elements connected by causal links in order to gain understanding about it. A SD model can be seen as an extended mental model thanks to which feedback interactions are made visible and can be interpreted. The use of SD as a modeling method for transportation system was first evoked by Abbas [1]. In this seminal work, he lists several inputs that SD would be able to bring to transportation modeling. The added value of SD is discussed in the chapter 4.

Several papers about SD models used for transportation modeling have been reviewed: Heimgartner [37], Anh [3], Gonzalez & Winch [34], Wang et al. [91], Tan et al. [83] and Armah et al. [4]. The main objective of all but Heimgartner [37] paper is to carry out a policy analysis for the transportation system of interest in these papers. The figure A.4 presents a possible representation of a transportation system, in this case in Accra, Ghana. The policies investigated include, among others, development of public transportation [3; 4; 34]; increase of network capacity [3; 4], development of a freight program [83] or fees for car owners [4]. All these models would fall into the "Transportation Planning Models" category of Maerivoet classification presented at the beginning of this section. Heimgartner [37] is singular among all the papers investigated because it aims at creating a hybrid modeling approach between SD and agent-based modeling. But, as he explains, the long-term objective of such model is to develop a new modeling approach for policy analysis including accounting for sustainability in transportation. All these different models share a similar feature, which is a high level of aggregation. For instance, in Wang et al. [91], some features can be considered as 'black boxes', such as their congestion factor, which includes the phenomenon of congestion into their model. As a consequence, the validity of this variable may be challenged.

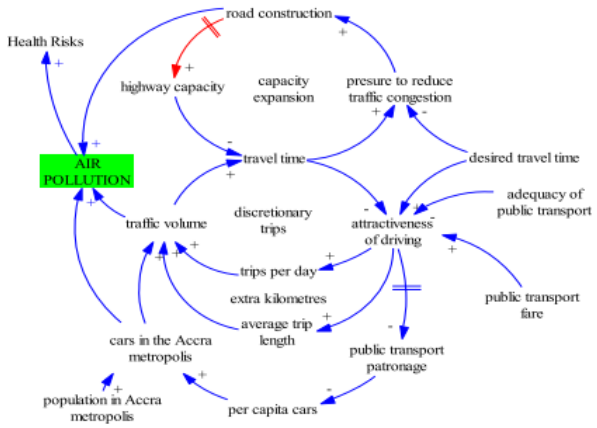


Figure A.4: Aggregated SD model of a transportation system [4]

B

Model Data

In this appendix are presented all the different data relative to the model.

This first table summarizes the values of the model design parameters. These are used for determining the parameter of every cell.

TIME STEP	0,125
Jam Density	150

Speed		Cell Length	Cell Size				
			Number of lanes				
km/h	km/min	km	1	2	3	4	5
120	2,0	0,250	38	75	113	150	188
110	1,8	0,23	34	69	103	138	172
100	1,7	0,21	31	63	94	125	156
90	1,5	0,19	28	56	84	113	141
80	1,3	0,17	25	50	75	100	125
70	1,2	0,15	22	44	66	88	109
60	1,0	0,125	19	38	56	75	94
50	0,8	0,10	16	31	47	63	78

Link Type	Capacity per lane {Source: HCM 2000}		Cell Capacity (veh/h)					Cell Capacity (veh/min)				
			Number of lanes					Number of lanes				
	veh/(h*ln)		1	2	3	4	5	1	2	3	4	5
Normal	120 km/h	2200	2200	4400	6600	8800	11000	36	73	110	146	183
	90 km/h	2100	2100	4200	6300	8400	10500	35	70	105	140	175
	50 -> 90 km/h	2000	2000	4000				33	66			
Merge	120 km/h	2400	2400	4800	7200	9600	12000	40	80	120	160	200
	90 km/h	2250	2250	4500	6750	9000	11250	37	75	112	150	187
Diverge	120 km/h	2400	2400	4800	7200	9600	12000	40	80	120	160	200
	90 km/h	2250	2250	4500	6750	9000	11250	37	75	112	150	187

This second table presents the values of cell and corridor characteristics. The section ID are used for mapping the different elements on the interchanges, and can be observed on the figures thereafter. The difference in values with the previous table comes from the rounding.

Interchange Name	Section ID	Free Flow Speed	# Cells	# Lanes	Capacity per Lane [1]		Capacity	Size per Lane	Total Size
		km/h	Cells	Lane	veh/(h*lane)	veh/(min*lane)	veh/min	veh/lane	veh
STB	C1T	120	11	3	2200	36	108	38	114
	C2T	120	11	3	2200	36	108	38	114
	C1C	120	4	3	2200	36	108	38	114
	C2C	120	4	3	2200	36	108	38	114
	D16	120	1	5	2400	40	200	38	190
	M26	120	1	5	2400	40	200	38	190
	D13	120	1	5	2400	40	200	38	190
	M13	120	1	3	2200	36	108	38	114
	D24	120	1	3	2200	36	108	38	114
	M14	120	1	3	2200	36	108	38	114
	D25	120	1	3	2200	36	108	38	114
	M25	120	1	5	2400	40	200	38	190
	C12	90	7	2	2100	35	70	28	56
	C35	90	16	2	2100	35	70	28	56
MAC	C1T	120	5	3	2200	36	108	38	114
	C2T	120	5	3	2200	36	108	38	114
	D13	90	1	5	2250	37	185	28	140
	M14	120	1	5	2400	40	200	38	190
	D23	120	1	5	2400	40	200	38	190
	M24	90	1	5	2250	37	185	28	140
	D24	90	1	4	2250	37	148	28	112
	M13	90	1	5	2250	37	185	28	140
	C13	90	7	2	2100	35	70	28	56
	C14	90	6	2	2100	35	70	28	56
	C23	90	4	2	2100	35	70	28	56
	C24	90	5	2	2100	35	70	28	56
ZAV	C1T	120	8	3	2200	36	108	38	114
	C2T	120	8	3	2200	36	108	38	114
	D15	120	1	5	2400	40	200	38	190
	M16	120	1	3	2400	40	120	38	114
	D25	120	1	3	2400	40	120	38	114
	M26	120	1	5	2400	40	200	38	190
	C15	90	5	2	2100	35	70	28	56
	C26	90	8	2	2100	35	70	28	56

The complete model documentation can be downloaded from the following folder: `https://goo.gl/6ouEkf`

This table lists all the notations used for variables in the model. A variable name can be divided in two components: its core name, which indicates what the variable describes; and a suffix, which indicates the road element to which the variable is related. For road links between interchanges, a prefix 'c' is indicated in order to indicate which elements belong to the carriageway on which traffic proceeds counter-clockwise.

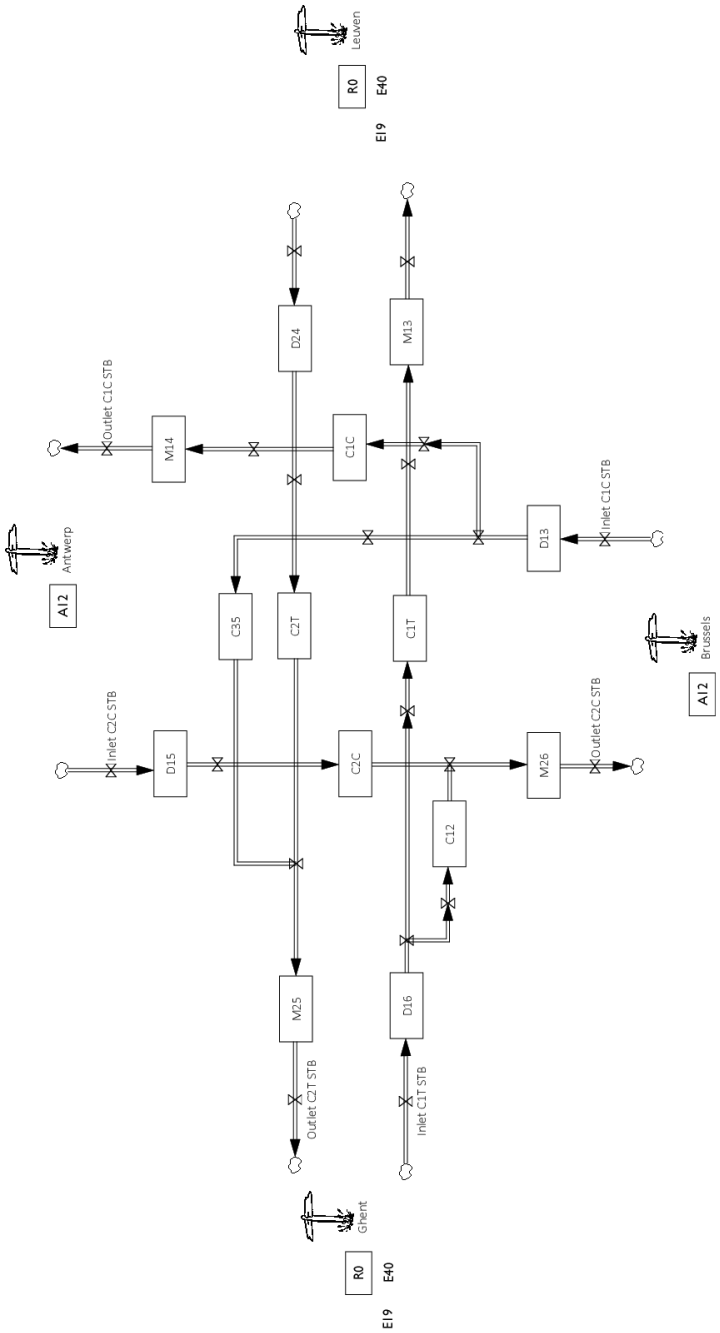
Variable core name	Meaning	Unit in model	Variable in formulae (if different)
C0	Nominal capacity per lane	veh/min/lane	N/A
C	Cell nominal capacity	veh/min	C
N0	Lane size	veh/lane	N/A
N	Cell size	veh	
Ln	Number of lanes of the cell	lane	
V0	Free flow speed	km/min	
Shockwave Speed	N/A	km/min	w
L	Cell length	km	N/A
Count	Number of vehicles per OD inside a cell	veh	n
r	Total flow that can be received	veh/min	
s	OD Flow that can be sent	veh/min	
s Ups	OD Flow that can be sent upstream	veh/min	
q	Cell inflow	veh/min	
In	Single cell or corridor inflow per OD	veh/min	q
P	Priority of leaving OD flow	Dimensionless	N/A
P Ups	Priority of leaving OD flow upstream	Dimensionless	N/A
L Sat	Total length saturated	km	N/A
Tot Count	Total number of vehicles inside a cell	veh	n
q out	Cell outflow per OD	veh/min	q
Tot q out	Total cell outflow	veh/min	q
t tr	Current cell travel time	min	t_{tr}
Tot t tr	Current corridor travel time	min	t_{tr}

In the three figures below are presented the cell structure of the three interchanges, that is to say the stock-flow structure without the different auxiliaries.

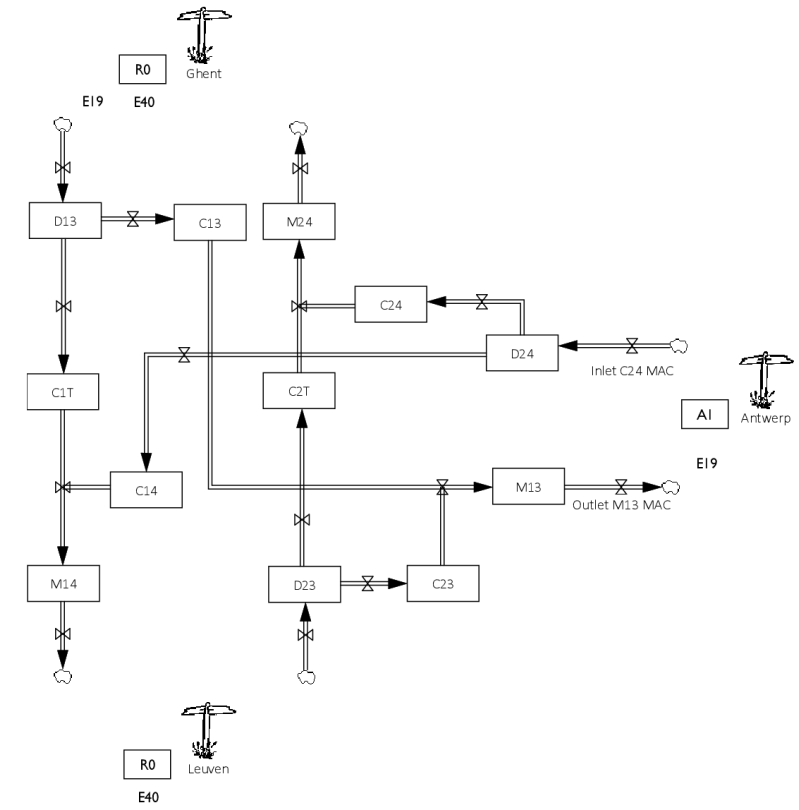
Some of these variables may be subscripted. Two ranges of subscripts are added: one for identifying vehicles with respect to their OD flows, and one for the cell position within a corridor. The variables that may be subscripted are indicated in the following table.

Variable	subscriped by cell	OD flow	Variable	subscriped by cell	OD flow
C0			C		
N0			N		
Ln			L		
V0			Shockwave Speed		
n	x	x	P	x	x
r	x		s	x	x
q	x	x	q out	x	x
Tot count	x		Tot q out		x
t tr	x		Tot t tr		
L sat					

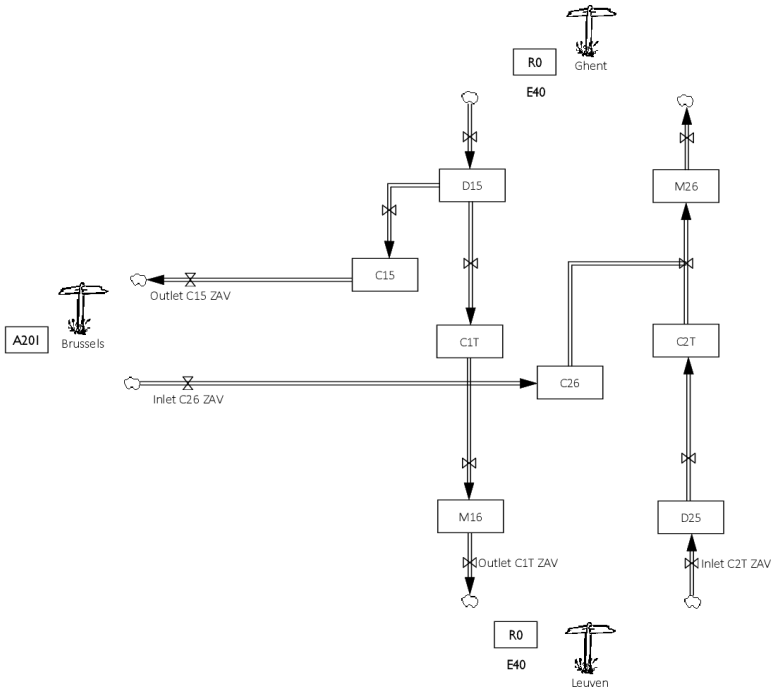
The first interchange is Strombeek-Bever. It connects the R0 to the A12 motorway, which connects Brussels Ring R21 to the ring of Antwerp. It runs parallel to the A1/E19 motorway. Since not all the ramps are used, the interchange modeled has been simplified.



The second interchange is Machelen. The A1/E19 motorway starts from this interchange, and connects the ring R0 to the ring of Antwerp.



The third and last interchange is Zaventem. It connects the R0 to the A201, a motorway that connects the east of Brussels to the International Airport of Brussels-Zaventem. Similarly to Strombeek-Bever, this interchange has been simplified. Branches that are not crossed by any flow are removed from the model.



C

Mathematical demonstrations

Cell travel time

The average travel time through a cell is a convenient indicator quantifying the strength of congestion. By definition of the CTM, the average travel time in free flow conditions is equal to one time step exactly. In congested situation, this average time ,noted t_i, is defined as the ratio of the cell length L_i versus the space-mean flow speed through this cell v_i:

$$t_i = \frac{L_i}{v_i}$$

Since the speed is the space-mean one, the equation of continuity 2.1 is valid, the equation then becomes:

$$t_i \cdot \frac{q_i}{k_i} = L_i$$

In this equation, the flow is equal to the cell outflow. Indeed, since congestion occurs on the network, the flow characteristics are driven by conditions at its leading edge. Applied to a cell, this means that flow intensity crossing it is equal to its outflow. In other words:

$$L_i = t_i \cdot \frac{q_{out,i}}{k_i}$$

Which can be written as:

$$t_i = \frac{L_i \cdot k_i}{q_{out,i}}$$

The quantity $L_i \cdot k_i$ is actually equal to the number of vehicles that is contained in the cell n_i. It hence stems from that:

$$t_i = \frac{n_i}{q_{i,out}}$$

Critical shock wave speed

The critical shock wave speed w_c is defined as highest speed for which the MFD associated with the CTM is triangular. In this case, the vertex height of the triangle is equal to the capacity of the cell, that is to say C. Based on the theoretical value of the vertex, w_C must checks:

$$\frac{k_j}{\frac{1}{v_0} + \frac{1}{w_C}} = C$$

Since the free flow speed v_0 is not nil, this equation becomes:

$$k_j \cdot \frac{v_0 \cdot w_C}{v_0 + w_C} = C$$

In other words:

$$k_j \cdot v_0 \cdot w_C = C \cdot (v_0 + w_C)$$

Thus

$$\left(k_j \cdot v_0 - C\right) \cdot w_C = C \cdot v_0\right)$$

As a consequence:

$$w_C = \frac{C \cdot v_0}{k_j \cdot v_0 - C}$$

Bibliography

[1] Abbas, K. A. (1990). The Use of System Dynamics in Modelling Transportation Systems With Respect to New Cities in Egypt.

[2] Ali, M. S., Adnan, M., Noman, S. M., & Baqueri, S. F. A. (2014). Estimation of Traffic Congestion Cost-A Case Study of a Major Arterial in Karachi. In *Fourth International Symposium on Infrastructure Engineering in Developing Countries*, volume 77 (pp. 37–44).: Elsevier B.V.

[3] Anh, T. T. (2003). System Dynamics Applied to Study the Urban Traffic Congestion of Hanoi. In *Eastern Asia Society for Transportation Studies* (pp. 1693–1697).

[4] Armah, F. A., Yawson, D. O., & Pappoe, A. A. N. M. (2010). A systems dynamics approach to explore traffic congestion and air pollution link in the city of Accra, Ghana. *Sustainability*, 2(1), 252–265.

[5] Ben-Elia, E., Di Pace, R., Bifulco, G. N., & Shiftan, Y. (2013). The impact of travel information's accuracy on route-choice. *Transportation Research Part C: Emerging Technologies*, 26, 146–159.

[6] Boel, R. & Mihaylova, L. (2006). A compositional stochastic model for real time freeway traffic simulation. *Transportation Research Part B: Methodological*.

[7] Bonnel, P. (2004). *Prévoir la Demande de Transport [In French: Forecasting Transport Demand]*. Paris: Presses de l'école nationale des Ponts et Chaussées.

[8] Börjesson, M. & Kristoffersson, I. (2012). Estimating welfare effects of congestion charges in real world settings. *Transportation Research Part E*, 70, 339–355.

[9] Bruxelles Mobilité (2012). Mise au point du modèle multimodal stratégique de déplacement [In French: Development of strategic multimodal traveling model].

[10] Carey, M., Bar-Gera, H., Watling, D., & Balijepalli, C. (2014). Implementing first-in-first-out in the cell transmission model for networks. *Transportation Research Part B: Methodological*, 65, 105–118.

[11] Cascetta, E. (2009). *TRANSPORTATION SYSTEMS Optimization and Its Applications*, volume 10.

[12] Cheu, R. L. & Kreinovich, V. (2007). Exponential Disutility Functions in Transportation Problems: A New Theoretical Justification.

[13] Conseil Economique et Social (2012). Cahier du Conseil économique et social de la Région de Bruxelles-Capitale: La Mobilité en Région de Bruxelles-Capitale.

[14] Corthout, R. (2012). *Intersection modelling and marginal simulation in macroscopic dynamic network loading*. Phd dissertation, Katholieke Universiteit Leuven.

[15] Costeseque, G. & Lebacque, J.-P. (2014). A variational formulation for higher order macroscopic traffic flow models: Numerical investigation. *Transportation Research Part B: Methodological*, 70, 112–133.

[16] Daganzo, C. F. (1993). The Cell Transmission Model. Part I: A Simple Dynamic Representation of Highway Traffic.

[17] Daganzo, C. F. (1995). The Cell Transmission Model. Part II: Network Traffic. *Transportation Research Part B: Methodological*, 29(2), 79–93.

[18] Daganzo, C. F. (1999). The Lagged Cell-Transmission Model. In *14th ISTTT Symposium,* Jerusalem, Israel.

[19] De Borger, B., Ochelen, S., Proost, S., & Swysen, D. (1997). Alternative transport pricing and regulation policies: A welfare analysis for Belgium in 2005. *Transportation Research Part D: Transport and Environment*, 2(3), 177–198.

[20] de Jong, D. (2012). *The Effect of Network Structure and Signal Settings on the Macroscopic Fundamental Diagram*. Master thesis, Delft University of Technology.

[21] de Jong, G., Pieters, M., Miller, S., Daly, A., Plasmeijer, R., Graafland, I., Lierens, A., Baak, J., & Walker, W. (2005). Uncertainty in Traffic Forecasts Literature Review and New Results for the Netherlands.

[22] De Schrijver, M. (2012). Irma et Osiris, pour mieux bouger [ONLINE. In French: Irma and Osiris, for a better mobility].

[23] Delhaye, E., De Ceuster, G., & Maerivoet, S. (2012). Internalisation of External Costs in Flanders. In *European Transport Conference 2012* (pp.16). Glasgow: Association for European Transport.

[24] Dolfin, M. (2012). From vehicle-driver behaviors to first order traffic flow macroscopic models. *Applied Mathematics Letters*, 25(12), 2162–2167.

[25] Fahkraeiroudsari, F. & Tampère, C. M. J. (2015). Benchmarking TRE Dynamic Traffic Assignment model : theoretical test cases.

[26] Fallah-Fini, S., Rahmandad, H., Chen, H. J., Xue, H., & Wang, Y. (2013). Connecting micro dynamics and population distributions in system dynamics models. *System Dynamics Review*, 29(4), 197–215.

[27] FHWA (2014). FHWA Operations - Operations Story.

[28] Florian, M., Gaudry, M., & Lardinois, C. (1988). A two-dimensional framework for the understanding of transportation planning models. *Transportation Research Part B: Methodological*, 22(6), 411–419.

[29] Forrester, J. W. (1961). *Industrial dynamics*. Collected Papers of Jay W. Forrester. Productivity Press.

[30] Fosgerau, M. & de Palma, A. (2013). The dynamics of urban traffic congestion and the price of parking. *Journal of Public Economics*, 105, 106–115.

[31] Gani, M. O., Hossain, M. M., & Andallah, L. S. (2011). A finite difference scheme for a fluid dynamic traffic flow model appended with two-point boundary condition. *GANIT: Journal of Bangladesh Mathematical Society*, 31, 43–52.

[32] Gayah, V. V. & Daganzo, C. F. (2011). Clockwise hysteresis loops in the Macroscopic Fundamental Diagram: An effect of network instability. *Transportation Research Part B: Methodological*, 45(4), 643–655.

[33] Geroliminis, N. & Sun, J. (2011). Hysteresis phenomena of a Macroscopic Fundamental Diagram in freeway networks. *Transportation Research Part A: Policy and Practice*, 45(9), 966–979.

[34] Gonzalez, J. & Winch, G. (2006). Coming To Terms With Traffic Congestion. In *The 24th International Conference of the System Dynamics Society* Nijmegen.

[35] Gordon, R. & Tighe, W. (2005). *Traffic Control Systems Handbook*. Technical Report October, Federal Highway Administration.

[36] Hansen, W. G. (1959). How Accessibility Shapes Land Use. *Journal of the American Institute of Planners*, 25(2), 73–76.

[37] Heimgartner, C. (2001). System Dynamic Modelling of Transport and Land use - A First Model Draft. In *1st Swiss Transport Research Conference* Monte Verità / Ascona (CH).

[38] Hensher, D. A. & Puckett, S. M. (2007). Congestion and variable user charging as an effective travel demand management instrument. *Transportation Research Part A: Policy and Practice*, 41(7), 615–626.

[39] Herrera, J. C. & Bayen, A. M. (2010). Incorporation of Lagrangian measurements in freeway traffic state estimation. *Transportation Research Part B: Methodological*, 44(4), 460–481.

[40] Hoogendoorn, S. P. & Bovy, P. H. L. (2001). State-of-the-art of Vehicular Traffic Flow Modelling. *Special Issue on Road Traffic Modelling and Control of the Journal of Systems and Control Engineering*, 215(4), 283–303.

[41] Hoogendoorn, S. P. & Knoop, V. (2013). Traffic flow theory and modelling. In *The Transport System and Transport Policy: An Introduction* chapter 7, (pp. 125–159).

[42] Hope, A. (2014). Air Unhealthy in Brussels and Antwerp; According to New Map [Online].

[43] INRIX (2014). Economic & Environmental Impact of Traffic Congestion in Europe & the US [Online].

[44] Jin, W. L., Gan, Q. J., & Gayah, V. V. (2013). A kinematic wave approach to traffic statics and dynamics in a double-ring network. *Transportation Research Part B: Methodological*, 57, 114–131.

[45] Kabir, M. H., Gani, M. O., & Andallah, L. S. (2010). Numerical Simulation of a Mathematical Traffic Flow Model Based on a Non-Linear Velocity-Density Function. *Journal of Bangladesh Academy of Sciences*, 34(1), 15–22.

[46] Kilani, M., Proost, S., & van der Loo, S. (2014). Road pricing and public transport pricing reform in Paris: complements or substitutes? *Economics of Transportation*, 3, 175–187.

[47] Knoop, V. L., Hoogendoorn, S. P., & Van Zuylen, H. (2010). Rerouting behaviour of travellers under exceptional traffic conditions - An empirical analysis of route choice. *Procedia Engineering*, 3, 113–128.

[48] Knoop, V. L., van Lint, H., & Hoogendoorn, S. P. (2015). Traffic dynamics: Its impact on the Macroscopic Fundamental Diagram. *Physica A: Statistical Mechanics and its Applications*, 438, 236–250.

[49] Koetse, M. J. & Rietveld, P. (2009). The impact of climate change and weather on transport: An overview of empirical findings. *Transportation Research Part D: Transport and Environment*, 14(3), 205–221.

[50] Kühne, R. D. (2011). Greenshields' Legacy: Highway Traffic. In *Greenshields 75 Symposium* (pp. 3–10). Woods Hole (MA).

[51] Kwakkel, J. H. & Pruyt, E. (2013). Exploratory Modeling and Analysis, an approach for model-based foresight under deep uncertainty. *Technological Forecasting and Social Change*, 80(3), 419–431.

[52] Kwakkel, J. H. & Pruyt, E. (2015). Using System Dynamics for Grand Challenges: The ESDMA Approach. *Systems Research and Behavioral Science*, 32(3), 358–375.

[53] Le Soir (2015). Les embouteillages coûtent 600.928 euros par jour [ONLINE, in French: Traffic Jam daily cost is equal to EUR 600,928].

[54] Li, H. (2014). Automatically Generating Empirical Speed-Flow Traffic Parameters from Archived Sensor Data. *Procedia - Social and Behavioral Sciences*, 138(138), 54–66.

[55] Liebens, J. & Vieren, P. (2014). Validatierapport basisresultaten provinciale verkeersmodellen versie 3.6.1 [In Dutch: Validation Report of Basic Results from the Provincial Traffic Models Version 3.6.1].

[56] Lighthill, M. & Whitham, G. (1955). A Theory of Traffic Flow on Long Crowded Routes. In *Proceedings of the Royal Society of London. Series A, Mathematical and Physical Sciences* (pp. 317–345).

[57] Lowry, I. S. (1964). A Model of Metropolis.

[58] Macharis, C. & Witte, A. D. (2012). The typical company car user does not exist: The case of flemish company car drivers. *Transport Policy*, 24, 91–98.

[59] Maerivoet, S. (2006). *Modelling Traffic on Motorways: State-of-the-Art, Numerical Data Analysis, and Dynamic Traffic Assignment*. PhD thesis, Katholieke Universiteit Leuven.

[60] Mahmassani, H. S., Saberi, M., & Zockaie, A. (2013). Urban network gridlock: Theory, characteristics, and dynamics. *Transportation Research Part C: Emerging Technologies*, 36, 480–497.

[61] Maio, M. L. D., Vitetta, A., & Watling, D. (2013). Influence of Experience on Users' Behaviour: A Day-to-Day Model for Route Choice Updating. *Procedia - Social and Behavioral Sciences*, 87, 60–74.

[62] Manheim, M. L. (1979). *Fundamental of Transportation Systems Analysis Vol. 1 Basic Concepts*. MIT Press.

[63] Manley, E., Cheng, T., Penn, A., & Emmonds, A. (2014). A framework for simulating large-scale complex urban traffic dynamics through hybrid agent-based modelling. *Computers, Environment and Urban Systems*, 44, 27–36.

[64] Massachussets Department of Transportation (2006). Interchanges. In *Project Development and Design Guide*, number January chapter 7. Boston, MA.

[65] Mazaré, P.-E., Dehwah, A. H., Claudel, C. G., & Bayen, A. M. (2011). Analytical and grid-free solutions to the Lighthill-Whitham-Richards traffic flow model. *Transportation Research Part B: Methodological*, 45(10), 1727–1748.

[66] McCrea, J. & Moutari, S. (2010). A hybrid macroscopic-based model for traffic flow in road networks. *European Journal of Operational Research*, 207(2), 676–684.

[67] McNally, M. G. (2007). The Four Step Model. *Transportation*, (UCI-ITS-AS-WP-00-51), 35–52.

[68] Meneguzzer, C. & Olivieri, A. (2013). Day-to-day traffic dynamics: laboratory-like experiment on route choice and route switching in a simple network with limited feedback information. *Procedia - Social and Behavioral Sciences*, 87, 44–59.

[69] Ortúzar, J. d. D. & Willumsen, L. G. (2011). *Modelling Transport*. John Wiley & Sons Ltd, 4 edition.

[70] Proost, S. & Sen, A. (2006). Urban transport pricing reform with two levels of government: A case study of Brussels. *Transport Policy*, 13(2), 127–139.

[71] Pruyt, E. (2013). *Small System Dynamics Models for Big Issues: Triple Jump towards Real-World Complexity*. Delft: TU Delft Library, 1 edition.

[72] Qian, X. (2009). *Application of Macroscopic Fundamental Diagrams to Dynamic Traffic Management*. Master thesis, Delft University of Technology.

[73] Région de Bruxelles-Capitale & ASBL (2013). Plan IRIS 2 [In French].

[74] Rittel, H. & Webber, M. (1973). Dilemnas in a general theory of planning. *Policy Sciences*, 4, 155–169.

[75] Ross, Z., Kheirbek, I., Clougherty, J. E., Ito, K., Matte, T., Markowitz, S., & Eisl, H. (2011). Noise, air pollutants and traffic: Continuous measurement and correlation at a high-traffic location in New York City. *Environmental Research*, 111(8), 1054–1063.

[76] Simon, H. A. (1997). *Administrative Behavior*. 4 edition.

[77] Spiliopoulou, a., Kontorinaki, M., Papageorgiou, M., & Kopelias, P. (2014). Macroscopic traffic flow model validation at congested freeway off-ramp areas. *Transportation Research Part C: Emerging Technologies*, 41, 18–29.

[78] Srivastava, A., Jin, W.-L., & Lebacque, J.-P. (2015). A modified Cell Transmission Model with realistic queue discharge features at signalized intersections. *Transportation Research Part B: Methodological*.

[79] Sterman, J. D. (2000). *Business Dynamics: Systems Thinking and Modeling for a Complex World*. Boston, MA, 1 edition.

[80] Sterman, J. D. (2001). System dynamics modeling: Tools for learning in a complex world. *California Management Review*, 43(4), 8–25.

[81] Sumalee, A., Zhong, R. X., Pan, T. L., & Szeto, W. Y. (2011). Stochastic cell transmission model (SCTM): A stochastic dynamic traffic model for traffic state surveillance and assignment. *Transportation Research Part B: Methodological*.

[82] Szeto, W. (2008). Enhanced Lagged Cell-Transmission Model for Dynamic Traffic Assignment. *Transportation Research Record: Journal of the Transportation Research Board*, 2085, 76–85.

[83] Tan, Z., Yang, H., & Guo, X. (2009). Maintenance, Built-operate-transfer Schemes for Road Franchising with Road Deterioration and Maintenance Effects. In W. H. K. Lam, S. C. Wong, & H. K. Lo (Eds.), *Transportation and Traffic Theory 2009: Golden Jubilee* chapter 12. Boston, MA: Springer US.

[84] Transportation Planning Capacity Building Program (2007). *The Transportation Planning Process: Key Issues*. Technical report.

[85] Transportation Research Board (2000). *Highway Capacity Manual*. Technical report, National Research Council.

[86] Treiterer, J. (1975). *Investigation of Traffic Dynamics by Aerial Photogrammetry Techniques*. Technical report, Ohio State University, Columbus.

[87] van Essen, H., Nelissen, D., Smit, M., van Grinsven, A., Aarnink, S., Breemersch, T., Martino, A., Rosa, C., Parolin, R., & Harmsen, J. (2012). *An inventory of measures for internalising external costs in transport*. Technical report, European Commission, Brussels.

[88] Ventana Systems, I. (2015). Vensim [ONLINE].

[89] Vermeersch, L. (2014). Five reasons Belgium has the worst traffic in Europe [Online].

[90] Vickrey, W. S. (1969). Congestion Theory and Transport Investment. *American Economic Review*, 59(2), 251–260.

[91] Wang, J., Lu, H., & Peng, H. (2008). System Dynamics Model of Urban Transportation System and Its Application.

[92] Wang, L., Xu, J., & Qin, P. (2014). Will a driving restriction policy reduce car trips ?— The case study of Beijing , China. *Transportation Research Part A*, 67, 279–290.

[93] Wardrop, J. G. (1952). Some Theoretical Aspects of Road Traffic Research. In *Road Engineering Division Meeting*, number 36 (pp. 325–362).

[94] Watts, J. (2010). Gridlock is a Way of Life for Chinese [Online].

[95] Wegener, M. (2004). Overview of land-use transport models. In D. A. Hensher & K. Button (Eds.), *Handbook of Transport Geography and Spatial Systems*, volume 5 chapter 9, (pp. 127–146). Kindlington (UK): Pergamon/Elsevier Science, 1 edition.

[96] Yeager, L., Fiddaman, & Peterson, D. (2014). A New Entity-Based System Dynamics Tool. In *Proceedings of the 30th International Conference of the System Dynamics Society* Delft: System Dynamics Society.

[97] Yousif, S. (2009). Partial elliptical two-regime speed-flow traffic model based on the highway capacity manual. (pp. 1–10).

[98] Yperman, I. (2007). *The Link Transmission Model for dynamic network loading*. Phd dissertation, Katholieke Universiteit Leuven.

[99] Yperman, I., Logghe, S., & Immers, B. (2005). The Link Transmission Model : an Efficient Implementation of the Kinematic Wave Theory in Traffic Networks. *Advanced OR and AI Methods in Transportation*.